

3-D Seismic Methods for Shallow Imaging Beneath Pavement

by

Brian Miller

M.S., Bowling Green State University, 1995

B.S., Eastern Michigan University, 1993

Submitted to the Department of Geology
and the Faculty of the Graduate School of The University of Kansas
in partial fulfillment of the requirements for the degree of
Doctor of Philosophy
2013

Advisory Committee:

George Tsoflias - Chair

Don W. Steeples

Michael H. Taylor

J.F. Devlin

Robert L. Parsons

Date Defended: 04/18/2013

The Dissertation Committee for Brian Miller certifies that this is the approved version of the following dissertation:

3-D Seismic Methods for Shallow Imaging Beneath Pavement

George Tsoflias - Chair

Date Approved: 04/23/2013

Abstract

The research presented in this dissertation focuses on survey design and acquisition of near-surface 3D seismic reflection and surface wave data on pavement. Increased efficiency for mapping simple subsurface interfaces through a combined use of modified land survey designs and a hydraulically driven acquisition device are demonstrated. Using these techniques subsurface reflectors can be quickly and efficiently imaged in the course of an afternoon.

The use of surface waves to analyze the upper several tens of meters of the subsurface has become an important technique for near-surface investigations. A new method for acquiring and visualizing surface wave information in three-dimensions is demonstrated. As will be shown, a volume of shear wave velocities can be created by acquiring surface waves along multiple, coincident lines. Using a series of computer algorithms the data can then be graphed in 2D or 3D space providing a method of visualization not previously available.

Acknowledgements

I would like to thank my parents and family for their support and encouragement. I also wish to thank my friends and the department of geology, all of whom have been generous during my time at The University of Kansas. I wish to thank my dissertation chair George Tsoflias for his direction and assistance throughout the course of my research and my committee members, Drs. Don Steeples, Rick Devlin, Robert Parsons and Michael Taylor for their assistance. Lastly I would like to thank the many graduate students who have helped me with field work.

Table of Contents

Chapter 1: Introduction to 3D Seismic Reflection	1
1.1 Introduction	2
1.2 Barriers to Near-Surface 3D Imaging	4
1.3 Historical background, seismic reflection	6
1.4 Historical background, near-surface 3D seismic reflection	10
Chapter 2: Land 3D Seismic Reflection Survey Design	13
2.1 Introduction	14
2.2 Land 3D Survey Geometries	16
2.2.1 Full-Fold	16
2.2.2 Swath	19
2.2.3 Orthogonal	21
2.2.4 Brick	23
2.2.5 Star	25
2.3 3D Survey Design	27
2.4 Design of a Near-surface 3D Reflection Survey	28
2.4.1 Receiver and Source Interval	29
2.4.2 Receiver and Source Line Interval	30
2.4.3 Migration Apron	30
2.4.4 Fold	31
2.5 Symmetrical Sampling	32
2.6 3D Survey Designs Applied to the Autojuggie	33
2.6.1 Conventional Methods	33
2.6.2 Survey Geometry	33
2.6.3 Fold	35
2.6.4 Offset and Azimuth Distribution	36
2.6.5 Trace Count	38
2.6.6 Redundancy	39
2.6.7 Symmetrical Sampling Method	41
2.6.8 Survey Geometry	41
2.6.9 Fold	43
2.6.10 Offset and Azimuth Distribution, Trace Count and Redundancy	44
2.7 Summary	48

Chapter 3: The Autojuggie	49
3.1 Introduction	50
3.2 Development of the Autojuggie	50
3.3 Prior Autojuggie Research	61
3.3.1 Early Autojuggie Application (Case Study 1)	61
3.3.2 Recent Autojuggie Application (Case Study 2)	62
3.3.3 Recent Autojuggie Application (Case Study 3)	63
3.4 Summary	68
Chapter 4: Development of Near-Surface Acquisition Designs	69
4.1 Introduction	70
4.2 Base Plate Development	72
4.3 Survey Design and Acquisition	75
4.4 Data Processing and Interpretation	83
4.4.1 Initial Data Processing	83
4.4.2 Secondary Data Processing	86
4.5 Base Plate Pitfalls	89
4.6 Summary	94
Chapter 5: Developing 3D Surface Wave Methods	97
5.1 Introduction	98
5.2 Historical background, near-surface surface wave methods	99
5.3 Autojuggie MASW	103
5.4 Psuedo-3D Surface Wave Profiles	107
5.4.1 Cross-line (vertical) Profiles	108
5.4.2 In-line (vertical) Profiles	110
5.4.3 Depth (horizontal) Profiles	112
5.5 Ground Penetrating Radar and Vs Comparisons	114
5.6 Summary	117
References	119
Appendix A - Example MASW Surface Wave Dispersion Curves	127

Appendix B - MASW Surface Wave 2D Vs Profiles	134
Appendix C - MASW Surface Wave Pseudo-3D Profiles	141
Appendix D - GPR and GPR/Surface Wave Combined Profiles	156
Appendix E - Driller Log	169

List of Figures

Figure 1. Full fold 3D survey geometry, source points (red) and receiver stations (blue). The station spacing is equal to line spacing and grids are offset by one bin size. A single bin is highlighted in yellow	17
Figure 2. Full fold survey bin offset; source points (red) and receiver stations (blue). Full fold surveys benefit from excellent offset distribution as illustrated by the blackened triangles within each bin	18
Figure 3. Full fold survey bin azimuth; source points (red) and receiver stations (blue) illustrating azimuth distribution as shown by the blackened squares within each bin	19
Figure 4. Swath survey geometry; source points (red) and receiver stations (blue). Source and receiver lines are parallel with source points positioned along the receiver line	20
Figure 5. Swath survey bin offset; source points (red) and receiver stations (blue). Offset distribution within a select offset range of bins is excellent however there is inadequate sampling in the cross-line direction	20
Figure 6. Swath survey bin azimuth; source points (red) and receiver stations (blue). The azimuth mix is narrow and depends on the number of live receiver lines and the line spacing	21
Figure 7. Orthogonal survey geometry; source points (red) and receiver positions (blue). The field layout is intuitive with the source and receivers simply orthogonal to one another	22
Figure 8. Orthogonal survey bin offset; source points (red) and receiver positions (blue). Inspection of the bin offset shows that not all offsets are sampled as illustrated by gaps within the blackened triangles within each bin	22
Figure 9. Orthogonal survey bin azimuth; source points (red) and receiver positions (blue). Inspection of the azimuth distribution within each bin reveals gaps	23
Figure 10. Brick survey geometry; source (red) and receiver (blue). Source lines are split and alternate in a brick like pattern	23
Figure 11. Brick survey bin offset; source points (red) and receiver stations (blue). The brick design offers an improved offset distribution over the orthogonal design	24
Figure 12. Brick survey bin azimuth; source points (red) and receiver stations (blue). The brick design offers a generally better azimuth distribution over the orthogonal design	25
Figure 13. Star survey geometry; source points (red) and receiver positions (blue). Source points are positioned along the receiver lines and the simplicity of the design makes it easy to acquire	25

Figure 14. Star survey bin offset; source points (red) and receiver positions (blue). Offset distribution is good near each source and receiver line however gaps appear between each source and receiver line	26
Figure 15. Star survey bin azimuth; source points (red) and receiver positions (blue). Azimuth distribution is generally good however there is an azimuthal bias within most bins	27
Figure 16. Autojuggie patch geometry, building sufficient fold over the target by rolling the receiver spread. The receiver spread is rolled half a spread length in both the in-line and cross-line directions	35
Figure 17. Autojuggie fold, building fold over the target of interest. Fold map of an area of 990 square meters with the highest fold reaching 30, covering an area of 324 square meters	36
Figure 18. Autojuggie offset distribution over a portion of the area of full fold. Good offset distribution is illustrated within the area of interest and surrounding areas	37
Figure 19. Autojuggie azimuth distribution. A portion of the target area is shown and the survey design leads to a narrow azimuth as result of the rectangular receiver grid	38
Figure 20. Autojuggie trace count vs. offset. Several thousand traces can be seen to illuminate the desired offset range of 8 to 25 meters	39
Figure 21. Autojuggie trace count vs. azimuth graph shows a large number of traces illuminating a narrow range of azimuth	39
Figure 22. Autojuggie bin offset distribution. The design leads to some offset redundancy however, the redundancy is at an acceptable level	40
Figure 23. Autojuggie bin azimuth distribution. The majority of bins are being illuminated while redundancy is kept to a minimum	41
Figure 24. Symmetrical sampling field geometry, full survey grid (left), close-up view (right). This geometry would require 25 source and receiver lines with 125 source and receivers per line	43
Figure 25. Symmetrical sampling fold. In comparison to the other survey designs fold becomes very high in a symmetrical sampling design	44
Figure 26. Symmetrical sampling offset distribution. There is a well sampled range of offset distribution within each bin as indicated by the blackened triangles within each bin	45
Figure 27. Symmetrical sampling azimuth distribution. Azimuth is well sampled within each bin as indicated by the blackened triangles within each bin	45

Figure 28. Symmetrical sampling trace count vs. offset. A large number of traces sample offsets ranging from approximately 5-45 meters	46
Figure 29. Symmetrical sampling trace count vs. azimuth. Traces are concentration within the 0-40 and 140-180 degree range	46
Figure 30. Symmetrical sampling bin offset redundancy plot. Bins are divided into colored blocks with the color indicating the number of times a particular offset was sampled	47
Figure 31. Symmetrical sampling bin azimuth distribution. The design leads to a number of redundant azimuths near the middle, however it is at an acceptable rate	47
Figure 32. Early Autojuggie development. Initial tests started by mounting geophones on a board (from Steeples et al., 1999a)	51
Figure 33. Early autojuggie development. Experiments continued by mounting geophones on lengths of channel iron (from Steeples et al., 1999b). As shown here the channel iron was adapted for deployment using farming equipment	52
Figure 34 Early autojuggie development. Geophones mounted on channel iron to demonstrate that rigidly attached geophones can accurately record common mid-point data (from Spikes et al., 2005). As shown here, the channel iron is being deployed using a series of hydraulic cylinders	54
Figure 35. Early autojuggie development. 2D geophone array that could be deployed simultaneously in a 3D survey mode (from Tsoflias et al., 2006). At this stage the geophones were entirely decoupled from the planting device	56
Figure 36. The Autojuggie in its current stage of development. The side wings are in an upright position allowing it to be towed on residential streets	57
Figure 37. Planting spiked geophones: Before planting begins (left), geophones being planted using the weight of the Autojuggie (middle), separation of the bars leaving geophones free-standing (right) (from Sloan et al., 2009)	59
Figure 38. Geophones mounted on base plates. The geophones have been deployed and are ready for data acquisition While deployed the geophones are not in contact with the Autojuggie and tension has been removed from the nylon strapping	60
Figure 39. The seismic equipment and cabling remain connected to the Autojuggie when moving the receiver grid to the next position. The seismographs, networking cables and batteries are housed at the rear of the Autojuggie	61
Figure 40. 3D image of the top of the water table from data acquired using a version of the Autojuggie during its developmental stage (from Czarnecki et al., 2006)	62

Figure 41. 3D diagram from data acquired using the Autojuggie in its current stage of development. Interpreted horizons: top of the saturated zone (blue), two stratigraphic boundaries (yellow and pink), and bedrock (green) (from Sloan et al., 2009)	63
Figure 42. Early base plate design (left) and seismic source (right). Early base plate designs used thin metal for the base with both vertical and Galperin geophones attached. A small sledge hammer is to strike the top of the metal rod	64
Figure 43. Free-fall seismic source. A heavy sledgehammer is connected at the end of a length of square iron which in turn is connected to the base of a Betsy Seisgun	65
Figure 44. Field file from a 2D survey conducted using geophones mounted to base plates. A 125 ms AGC window, 350-450 Hz Butterworth filter and 2dB pre-rasterization gain have been applied	66
Figure 45. Interpreted stacked section correlated to well log records from a 2D survey conducted using geophones mounted to base plates. A 125 ms AGC window, 350-450 Hz Butterworth filter and 2dB pre-rasterization gain have been applied	67
Figure 46. The Autojuggie deployed for marine streamer type acquisition	71
Figure 47. Geophone base plates and nylon strapping. The nylon strapping is secured to the Autojuggie using holes within the lower rung which house spiked geophones when performing surveys on soil	74
Figure 48. The Autojuggie as it was transported to the field site. Once at the field site only the seismographs, network cables and batteries need to be connected	75
Figure 49. The University of Kansas west campus Park-and-Ride parking lot. The site is located on university property within Lawrence, KS and the survey location is marked in red	76
Figure 50. Roll parameters and fold map for the marine streamer acquisition survey design. The receiver grid and source lines occupied a total of twenty positions (D). Several of these positions (A-C) are shown to illustrate how the survey progressed. The source positions are represented in red and receiver positions in blue. Moving the receiver grid results in geophone positions being occupied multiple times	77
Figure 51. Trace count vs. offset range for the survey. There is a narrow range of offsets with trace counts for offsets outside of 15.0-25.0 meters falling off quickly	78
Figure 52. Azimuth coverage for each shot within a patch (A-I) and total survey azimuth coverage (J). To capture a range of azimuth shots were moved along a path of forty-five degrees with a resulting coverage of ninety degrees of azimuth	79

Figure 53. Deploying geophone base plates (left), note the seismographs, cables and batteries on the far left of the image. Close-up view of the recording equipment contained within the Autojuggie during survey (right)	81
Figure 54. Source positions for each patch. To locate source positions each shot was placed within a Cartesian coordinate system for the source operator to follow	82
Figure 55. Field record filtered with a 125-350Hz Butterworth filter, 18db/octave rolloff slopes and a 125ms AGC window applied. The arrows indicate several reflectors	85
Figure 56. Frequency-amplitude spectra for a raw shot gather (left) and the same gather after applying a 60–350 Hz Butterworth filter (right)	85
Figure 57. Stack comparison from 2D lines extracted from the 3D volume. Data from the streamer survey (left), single-offset (middle) and common-offset (right)	86
Figure 58. Geometry (left) and fold map (right) for the single offset marine streamer design. A source point located 20.0m behind the receiver array and a 0.5m roll interval were used	87
Figure 59. 3D Chair diagram stack comparison. Data from the streamer survey (left), single-offset (middle) and common-offset (right)	88
Figure 60. Patch (left), complete survey geometry (middle) and fold (right). The receiver grid (blue) contains 10 receiver lines with 24 receivers for each line. For each patch 12 source lines with 12 source positions (red) for each source line were used	90
Figure 61. Trace count vs. offset (left) and trace count vs. azimuth (right). The majority of the traces fall between an offset range of 5.0-25.0 m with a concentration of traces within the 0-40 and 140-180 degree range	91
Figure 62. Bin offset redundancy plot. Bins are divided into colored blocks with the color indicating the number of times a particular offset was sampled	92
Figure 63. Surface wave receiver lines. Surface waves were acquired and processed individually for each receiver line	105
Figure 64. Dispersion curve for the first station of the first receiver line. Dispersion curves were picked for every shot position for each of the receiver lines	106
Figure 65. 2D Vs profile for line 2 of the survey. Depth of imaging is approximately 7.0 meters with shear wave velocities within the range of 200-600 m/s	107
Figure 66. 2D Vs cross-line profiles. Distances of 0.6, 1.6 and 2.6 meters are shown and a velocity inversion around 1.8m is evident (red arrows)	109

Figure 67. Pseudo 3D Vs cross-line profiles. Distances of 0.6, 1.6 and 2.6 meters are shown, however, profiles at 0.1 meter increments through the range of the survey area can be displayed	110
Figure 68. 2D Vs in-line profiles. The profiles shown span the entire length of the survey line at distances of 0.3, 1.3 and 2.3 meters in the crossline direction	111
Figure 69. Pseudo 3D Vs in-line profiles. Distances of 0.3, 1.3 and 2.3 meters are shown however, profiles at 0.1 meter increments through the range of the survey area can be displayed	112
Figure 70. 2D Vs horizontal (depth) profiles. Shown are depth plots from 1.061, 4.193 and 7.177 meters. The data shown within each plot spans the entire area of the survey	113
Figure 71. 2D Vs horizontal (depth) contoured profiles. The contoured profiles span the entire area of the survey and depths of 1.061, 4.193 and 7.177 meters are shown	114
Figure 72. GPR profile corresponding to the second receiver row. Data were acquired using 200 MHz antenna along each geophone receiver line	115
Figure 73. Superimposed Vs velocity field and GPR profile corresponding to the second geophone receiver row. Variation within the Vs velocity field can be seen to correlate with events imaged within the radar data	117

Chapter 1: Introduction to 3D Seismic Reflection

1.1 Introduction

While we're able to investigate the subsurface using two-dimensional (2D) seismic methods it's a three-dimensional (3D) world that we live within and to image the complexities of the subsurface, the move to 3D was a natural progression. The two main advantages of three-dimensional seismic reflection methods over 2D methods are an increase in spatial resolution and identification and correct positioning of out-of-plane reflections and diffractions (Kaiser et al., 2011; Hart, 1999; Cartwright and Huuse, 2005). Even in areas that may be considered geologically simple the subsurface can be complex. Three-dimensional seismic methods allow us to image this complexity with a high level of accuracy that is not possible with 2D methods. As an example, one of the main advantages of 3D methods is that they allow us to create laterally continuous seismic sections and to compensate for seismic energy arriving from regions outside of the vertical plane beneath the plane of incidence. These sections may then be combined with borehole data to provide a more complete image of the subsurface allowing us to make more informed decisions.

The case for 3D reflection surveying may be further emphasized if we consider a 2D seismic section in relation to a 3D data cube. The 2D section can be thought of as a cross-section, or single slice, of the 3D data volume. From this we can see that a 2D line provides a fraction of the information that is available from a 3D data cube.

Migration is also a consideration. Migration performs three distinct functions; 1) repositions reflections out-of-place because of dip, 2) focuses energy spread over the Fresnel zone and 3) collapses diffractions from points and edges. Migration of 3D data provides an adequate and detailed 3D image of the subsurface, leading to a more reliable interpretation. Two-dimensional seismic data contains signal from all directions, including out-of-plane,

although 2D migration generally assumes the entire signal is from the plane of the profile. Migration for the near-surface has not had as much importance placed upon it as exploration-scale surveys. However, the move from 2D to 3D for near-surface investigations will cause the need for migration to be considered more carefully.

Much of the move toward 3D seismic reflection has been driven by hydrocarbon exploration and acquisition of 3D seismic reflection data is the norm today within the exploration industry (Weiderhold, 2005). Hydrocarbons are often associated with complex geologic structures and stratigraphy and the ability to obtain accurate, high-resolution subsurface images is valuable. Because hydrocarbons are often associated with complex subsurface geology and the expense involved in identifying potential hydrocarbon traps, it is important to have the best possible subsurface information. Three-dimensional seismic reflection methods are one of the main tools providing these data. Even today much of the continued research driving seismic reflection methods is in an effort to better image complex geologic structures.

The fundamental physics governing 2D methods obey the same principles governing 3D seismology. However 3D methods offer an improvement over 2D by including an azimuthal component (Vermeer, 2002). It is not difficult to imagine a large 3D survey grid as a collection of multiple, closely spaced 2D lines. While interpolation between multiple 2D lines can be used to simulate a 3D survey the lack of an azimuthal component restricts it from being true 3D. In a simulated 3D survey, using multiple 2D lines, the source, receivers and subsequent generated seismic wave, all lie within the same plane because only a linear array of geophones are live for any given shot. When receiver and source orientations do not all fall within the same 2D plane the traces falling within a bin come from multiple azimuths,

sampling the subsurface from different orientations. It is the important contribution of variable azimuth raypaths added from a grid of live receivers and out-of-plane source positions that provide the necessary data to generate 3D reflection data volumes.

The ability to acquire and process 3D seismic data has largely been driven by advancements in computer technology (Dragoset, 2005). Only with the increase in computing power and storage capabilities, coupled with the dramatic decrease in cost, has the potential of being able to acquire data using the large channel counts necessary for 3D been realized. The technological explosion that started in the 1970's, and continues today, has reached a point that data acquired for large, near-surface 3D surveys can be processed on desktop personal computers.

1.2 Barriers to Near-Surface 3D Imaging

Three-dimensional imaging requires an increase in the effort of all aspects of seismic surveying compared to 2D. It requires more field personnel, more equipment, greater forethought and time spent on the survey design, more processing and more computer resources. Even on relatively small 3D surveys these requirements can add significant demands. The added difficulties may become pronounced for near-surface 3D surveys because of the limited resources of many near-surface research groups. The limited number of near-surface 3D papers in the peer-reviewed literature may illustrate this point. Although this may be the case results of some near-surface 3D surveys have been published and will be discussed in later sections.

One of the primary barriers to near-surface 3D investigations comes from having to emplace manually large numbers of geophones. To cover a sufficient area during a 3D

survey the geophones must be picked up and moved several times. Because geophones relay recorded information to a seismograph through a series of cables, moving them is no small task. To move the geophones they must be individually disconnected, picked up, repositioned and reconnected. Adding to the effort, when the geophones are moved they must be placed in very precise positions. For near-surface surveys this generally requires the time-consuming method of field personnel surveying the positions. In addition to moving geophones the seismographs and cabling must also be moved.

Wireless seismic systems are currently available which removes the need for cabling between geophones and the seismograph. Additionally, geophones with onboard GPS positioning are also available. Use of telemetry and GPS would reduce much of the manual labor involved in moving the receiver grid during 3D surveying. However, this equipment is expensive. Over time telemetered systems and GPS may become standard in near-surface surveying but it is likely to be many years before this change occurs.

Throughout a 3D survey the source also moves to different positions. As with geophone placement, the source placement needs to be accurate. This generally involves field crew members using a measuring tape to position the source locations. While there are source positioning concerns and equipment costs to consider, the effort involved in deploying the receiver grid and cabling can be a barrier for near-surface 3D investigations.

Part of the research presented here will be to demonstrate the functionality of automated geophone deployment instrumentation known as the Autojuggie. The Autojuggie is a hydraulically operated trailer that is capable of moving and emplacing large numbers of geophones simultaneously. This relieves a large amount of the effort involved and can reduce both the human and financial cost of performing a near-surface 3D survey. The Autojuggie

has been used in near-surface 3D reflection surveys which will be presented as evidence that it can dramatically increase the speed and accuracy at which a near-surface 3D survey can be performed.

While the ability to move large numbers of geophones simultaneously is an improvement the number of source points needed for a 3D survey also presents some barriers. A second objective of this research is to illustrate the additional efficiency that may be achieved when combining the Autojuggie and a survey design that minimizes source locations. These two in combination will help contribute to making it more economical to perform near-surface 3D surveys.

1.3 Historical background, seismic reflection

The earliest reported seismic testing was undertaken by Robert Mallet in 1851. Mallet was able to generate seismic waves using charges of gunpowder and time the resulting wave using a chronograph and an instrument known as a seismoscope. The chronograph would be started when the observer ignited the gunpowder electrically and stopped once the passing wave was indicated by the seismoscope. The distance between the shot and the seismoscope would have been carefully measured so the velocity could be calculated (Weatherby, 1948). In 1900 the first recording of seismic waves using a seismograph was performed by Hecker (Weatherby, 1948). Hecker used a mechanical seismograph to record seismic profiles as we know them today.

Refraction seismology preceded reflection seismology as the first method to be put to use in exploration. The refraction method was used to successfully locate several oil fields

throughout the 1920's and during this time it was put into regular use to find salt domes in locations such as Mexico and the Gulf Coast.

By the mid 1920's seismic reflection was starting to be used as an exploratory method (Allen, 1980). Although not as widely used as the seismic refraction method at this time, during this development stage seismic reflection had some limited use. By the end of the 1920's the seismic reflection method had been refined and in 1930 three oil fields were discovered with the assistance of seismic reflection (Weatherby, 1948). This established the value of seismic reflection as an exploratory tool. At the beginning of the 1930's there were 15 to 20 refraction crews in the field and possibly two to four reflection crews (Allen, 1980). This would soon change as the reflection method gained acceptance and soon become the method of choice.

Because large channel counts are generally required for 3D reflection surveys it is interesting to take a look at how channel counts increased over the years. As an example, in 1930 seismic crews were operating recording instruments with six recording channels. By 1980 some recording systems had more than 1,000 recording channels and by the 2000's channel counts exceeded 100,000.

Along with increasing channel counts an important advancement for exploration was the development of the magnetic tape recorder. In the early 1950's Mobil developed the magnetic recording tape capability based upon the Ampex commercial audio tape recorder. Magnetic recording was attractive because of its lack of optical and chemical problems, was rugged enough for field use and was able to generate reproducible seismograms (Loper and Pittman, 1954). Prior to the development of magnetic tape recording, data were recorded using a camera that could produce a visible seismic record on photosensitive paper (Loper

and Pittman, 1954). The benefits of recording on magnetic tape were such that by the end of the 1950s the industry had converted to analog magnetic tape recording.

In addition to advancements in equipment an important contribution to acquisition was documented by W. Harry Mayne (Mayne, 1962). Mayne published details documenting the common depth point (CDP) method of acquiring data which is still the foundation for reflection acquisition today. The importance of the CDP method is that information associated with a given reflection point, but recorded with a multiplicity of shot points and geophone locations, are added together. Thus, if the reflected signals received along the several paths are adjusted for coincidence, their resultant sum will be proportional to the number of signals (Mayne, 1962). Fold is a measure of how many times a subsurface point has been sampled and the result of the summation is an improvement of signal-to-noise which approximates the square root of fold. Although the CDP method was developed and patented in the mid-1950's it wasn't until the 1960's that the method gained widespread use.

Walton (1971, 1972), of Esso Production Research Company, detailed a practical approach that could work with the limited number of channels available at that time and gets credit for developing the first method of acquiring 3D reflection data. In his technique the source and receivers are laid out in what Walton referred to as an X spread, known today as a cross-spread. This method uses a single source and single receiver line orthogonal to one another with equal source and receiver intervals. This produces single-fold subsurface coverage equal to half of the receiver and source-line lengths. Shooting in this fashion allowed data to be viewed as trace gathers or time slices using a custom made viewer (Walton, 1972).

During the 1960's, with the advent of Conoco's Vibroseis, the components needed for 3D seismic exploration were coming together. The CDP method had been developed, Vibroseis was deployed as an efficient source, computing power was steadily increasing and channel counts were on the rise. Technologies had advanced to the point that almost all of the tools needed to perform 3D were available in the 1960's. The ability to record large numbers of channels was the last function needed and this advancement came in the 1970's when channel capacity increased dramatically. As an example of increasing channel counts Bourgoise and Jones of Shell Oil Company described a 200 channel acquisition system in 1972, Sercel announced a model capable of up to 500 channels (Convert et al, 1976) and in 1978 Geophysical Systems Corporation introduced its 1,024 channel system (Allen, 1980).

With all of the converging technologies the ability to perform 3D seismic surveys was established during the 1970's. Although the first attempts were limited by the channel counts available at the time, Geophysical Service Incorporated (GSI) was able to perform what is probably the industry's first true 3D field survey in Lea County, New Mexico, in August, 1973. For this survey they used two 48 channel systems while moving vibrators at right angles across the geophone lines (Allen, 1980), what is known today as an orthogonal geometry.

While seismic exploration has a long history the technological advancements of the last 30 years has opened the possibility of performing 3D seismic reflection surveys. Today 3D surveys are being acquired using systems with a capacity of greater than 100,000 channels and 3D acquisition has become established as practical, and often necessary.

1.4 Historical background, near-surface 3D seismic reflection

There are numerous publications within the refereed literature pertaining to exploration scale 3D seismic reflection. However, the number of publications in regards to near-surface 3D seismic reflection is limited. One of the first near-surface 3D reflection papers was published in 1988 by Corsmit, et al. This paper discusses a survey conducted on a tidal flat in the Netherlands which covered an area of 22 x 36 meters. Other near-surface 3D reflection papers were published in the latter half of the 1990's and the early 2000's. Among these includes works by Barnes and Mereu (1996) who discuss a 3D survey acquired near London, Ontario. The geology of their survey area consisted of unconsolidated glaciolacustrine and till sediments overlying bedrock. They used a coarse bin size of 3 x 6 meters which led to images of the shallow reflectors that were not as good as images created using 2D methods. This was a result of the coarse bin size and poor offset distributions.

Interesting publications by Green et al. (1995) and Lanz et al. (1996) compare 2D and 3D reflection data over glacial sediments at a landfill site in Switzerland. The nature of the landfill material led to multiple diffractions and out of plane reflections. Because of this it was determined that 3D data, which could be properly migrated, was necessary to image the reflectors.

One of the most comprehensive near-surface 3D surveys is reported by Büker et al. (1998, 2000). For their research they conducted a survey in the Suhre Valley, Switzerland covering an area of 357 x 432 meters. Their results showed that high fold with well sampled offset and azimuth distributions, along with near offset traces are necessary when imaging shallow reflectors. While this was a comprehensive near-surface 3D survey a considerable

amount of work was required. The authors state that it took a crew of 5–7 people 85 days to permit, survey, and acquire the data.

Van der Veen et al. (2001) describe a pseudo-3D reflection simulation that could be achieved using a towed land streamer. Their simulation was based upon a subset of data acquired by Bükler et al. (1998, 2000). As described by the authors there were several limitations with this simulation. Specifically more source points would be necessary with the towed streamer to have both adequate subsurface and azimuthal coverage. However their simulation indicates that the streamer would have significantly reduced the effort involved in acquisition. In comparison of the simulated land streamer to the field work of Bükler et al., the land streamer could have reduced the effort of acquiring data by reducing the number of field personnel by two and the total number of man hours by 608 hours. Using a land streamer, the same area could have been surveyed with 7% the effort required by Bükler et al.'s field crew (van der Veen, 2001), but with a loss of high-frequency content.

Additional examples of reported near-surface 3D reflection surveys can be found by House et al. (1996), Villella et al. (1997), Spitzer et al. (2003), Miller et al. (2004), and Schmelzbach et al. (2007).

While there have been few publications in the refereed literature in regards to near-surface 3D seismic reflection surveys there have been even fewer detailing attempts to construct an acquisition device that allow geophones to be moved and planted en-masse. The earliest paper describing such a device comes from Bachrach and Mukerji (2001, 2004). The authors describe a non-rigid portable 2D geophone mount made of inelastic material. The array consisted of 72 geophones arranged in eight rows of nine geophones with a geophone spacing of 0.25 meters.

Recent examples of acquiring near-surface 3D data using an acquisition system come from Sloan (2009) and Miller (2009). Sloan successfully used the Autojuggie in the investigation of a shallow water table and lithology while Miller adapted the Autojuggie with the ability to deploy geophones mounted to metal plates for conducting reflection investigations on pavement systems.

One of the common factors between the early 3D near-surface reflection investigations was the amount of effort required to survey relatively small areas. Given the amount of effort and equipment required the initial near-surface 3D reflection publications were ambitious in their scope and design. While the number of publications in regards to near-surface 3D acquisition is limited recent publications have shown that the amount of effort and time required for performing 3D near-surface reflection surveys may be significantly reduced by improved acquisition equipment.

Chapter 2: Land 3D Seismic Reflection Survey Design

2.1 Introduction

The main objective when designing a seismic reflection survey should be to image the target economically and efficiently. While this may seem intuitive this author's experience has found that there may be a tendency to expand the scope of a survey. This generally comes through acquiring additional equipment, adding more source points and/or adding more roll positions. While there may be benefits to increasing the size of a survey care must be taken because additional management and potential problems come as part of the price of a larger survey. If increasing the size of a survey is necessary to meet the objective then that is part of the project, if not then increasing the survey size should be carefully considered before proceeding.

There are many considerations that must be addressed when designing a 3D seismic reflection survey. Among these are the depths of the shallowest and deepest horizons, size of the target, resolution requirements, frequency content, velocities, signal to noise requirements, land access and ease of mobility within the survey area, to name a few. Because 3D surveys utilize multiple source and receiver lines the parameters that defined the traditional 2D line must now be extended to include the possibility of multiple survey geometries. The availability of multiple geometries adds complexity and the 3D geometry that will best suit the survey must be considered.

When designing a 2D survey the design centers on the subsurface coverage in the form of common-mid points (CMP). For 3D surveys, the CMP becomes two-dimensional and is termed a bin. Bins take on the shape of a square or rectangular and define the spatial extent of the data sampling. During stacking all of the traces within the same bin will be added and contribute to the fold of that bin. One of the first steps in designing a 3D survey is

to determine the bin size. As with a 2D survey, fold is also a concern when designing a 3D survey. However, a departure from 2D survey design that must be taken into account for a 3D survey design is the addition of azimuth. If structure is complex, then good azimuthal range becomes important and the range of azimuths within each bin is a consideration.

Another change in the process of survey design when creating a 3D survey is the use of computers and specialized software to aid in the design process. The multiple source and receiver lines, the difficulty in visualizing fold, azimuth distribution and offset ranges within bins make the use of a survey design program almost a necessity.

Imaging shallow and deep target horizons still requires a range of source and receiver offsets. With the geometries of 3D surveys we need to recognize that offsets may be measured at an angle and the depth is that of a plane rather than a line.

Performing 3D reflection surveys requires that a significant amount of equipment be deployed at any given time. This includes geophones, cables, seismographs and source generators which will be moved several times over the course of the survey. During this time a field crew must be able to keep track of all the source and receiver positions. Therefore it is best to try and keep field geometries simple while still being able to meet the survey objectives. It should also be taken into account that it is difficult to change acquisition strategy after starting a 3D survey. Because of this it is important to carefully consider all aspects of a 3D survey design before beginning acquisition.

2.2 Land 3D Survey Geometries

While a few 3D survey geometries may be favored, numerous designs have been developed for land 3D surveying. Important features in the area of the survey, such as ease of access, space available and terrain must be considered to select the best design option. The geometry of the survey is not independent of the target so the location, direction, and length of the lines are important considerations in the design process. In 3D reflection surveying there are always tradeoffs that come in the form of offset distribution, azimuth distribution and fold when changing the number and/or position of the sources and receivers. While many designs are available the following descriptions of several 3D survey geometries and accompanying figures (Cordsen et al., 2000) will give the reader an introduction to some of the more common designs and illustrate how offset, azimuth and fold change with acquisition design.

2.2.1 Full-Fold

A full fold 3D survey (Figure 1) is one where source points and receiver stations are distributed on an even two-dimensional grid with station spacing equal to line spacing and grids offset by one bin size (Cordsen et al., 2000). It can be seen that a full-fold 3D survey requires many source and receiver positions, which is one of the main detractors of this

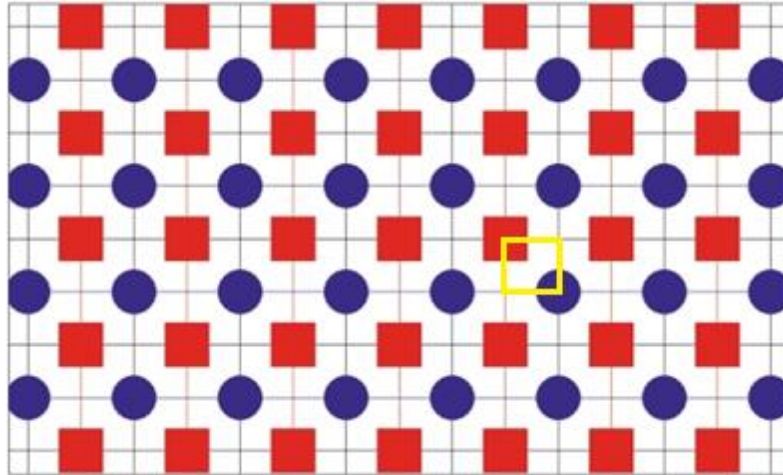


Figure 1. Full fold 3D survey geometry, source points (red) and receiver stations (blue). The station spacing is equal to line spacing and grids are offset by one bin size. A single bin is highlighted in yellow

layout. Full-fold 3D surveys are essentially the optimal survey design. However, the amount of work, equipment and time required to perform this survey would likely be uneconomical. Even so the design is a good starting point from which to develop other designs that will ultimately have tradeoffs between offset and azimuth distribution in favor of time and economy.

Full-fold 3D surveys have the benefit of excellent offset distribution (Figure 2) and azimuth distribution (Figure 3). Offset distribution, as illustrated by the black triangles within each bin (Figure 2), is a collection of individual lines of varying length that create a completely filled triangle if all offsets are represented within a bin. The length of the black line is an indicator of the offset distance with the nearest offsets being represented by the shortest line, at the far left of each bin, with increasing offset represented by longer lines with the furthest offset represented at the far right of each bin. If particular offsets are missing there will be breaks within each triangle (i.e. white space).

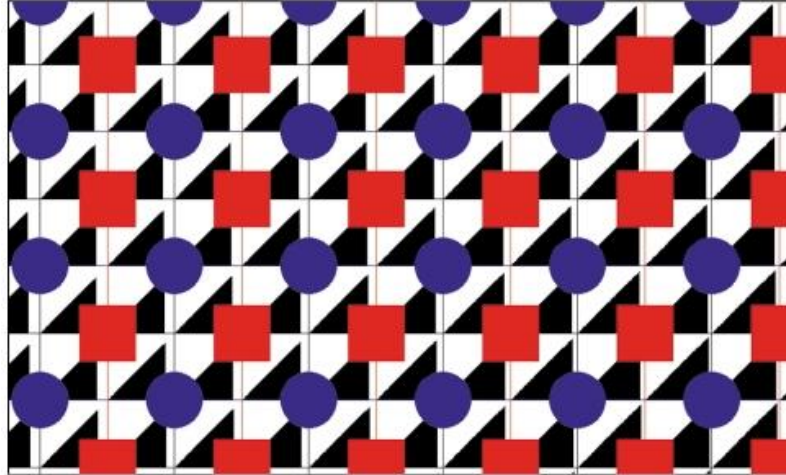


Figure 2. Full fold survey bin offset; source points (red) and receiver stations (blue). Full fold surveys benefit from excellent offset distribution as illustrated by the blackened triangles within each bin

Azimuth distribution is represented in a similar manner (Figure 3). Within each bin individual black lines are used to represent azimuth distribution. A completely blackened square within a bin indicates that all azimuths have been sampled. While complete offset and azimuth distribution is highly desirable they come at the cost of a high density of source and receiver positions.

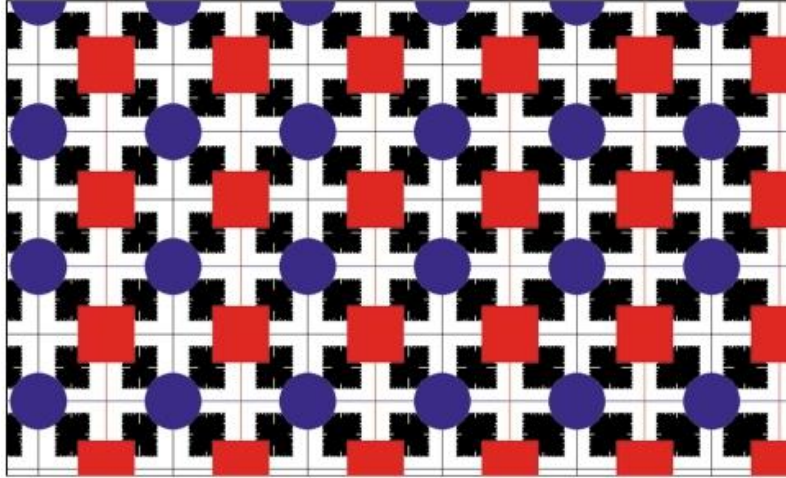


Figure 3. Full fold survey bin azimuth; source points (red) and receiver stations (blue) illustrating azimuth distribution as shown by the blackened squares within each bin

2.2.2 Swath

The swath design, and essentially all other designs, are simply subsets of the full-fold design. Because it would be cost prohibitive to acquire data using the full-fold design other geometries such as swath have been developed. The swath method was one of the earliest 3D designs and in this geometry source and receiver lines are parallel with source points positioned along the receiver line (Figure 4). The offset distribution (Figure 5) within a select offset range of bins is excellent however inadequate sampling in the cross-line direction makes this design a “poor man’s 3-D”, because many bins are empty (Cordsen et al., 2000). The azimuth (Figure 6) mix is narrow and depends on the number of live receiver lines in the recording patch and the line spacing.

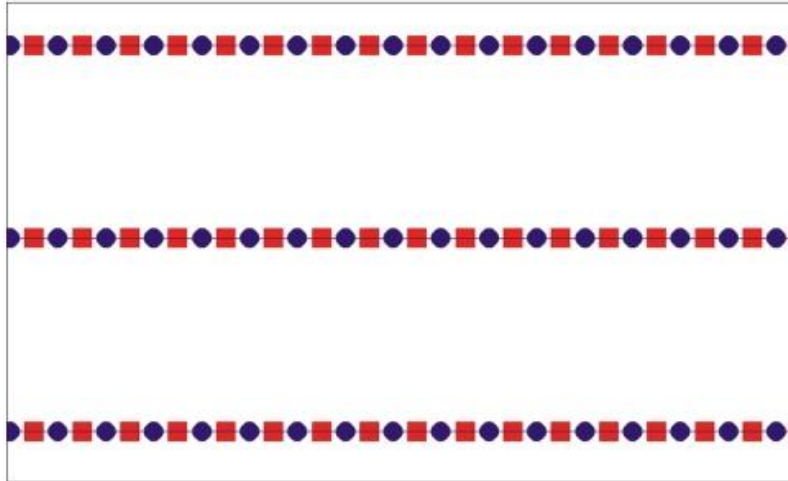


Figure 4. Swath survey geometry; source points (red) and receiver stations (blue). Source and receiver lines are parallel with source points positioned along the receiver line

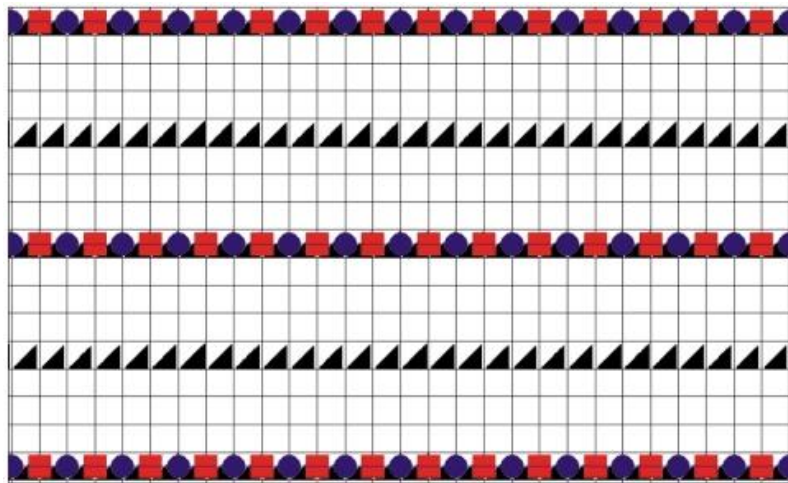


Figure 5. Swath survey bin offset; source points (red) and receiver stations (blue). Offset distribution within a select offset range of bins is excellent however there is inadequate sampling in the cross-line direction

The swath geometry has advantages in areas that are restricted in the sense of having room available to work. Because the swath geometry is simple it is easy to conduct however the poor azimuth and poor cross-line sampling must be considered.

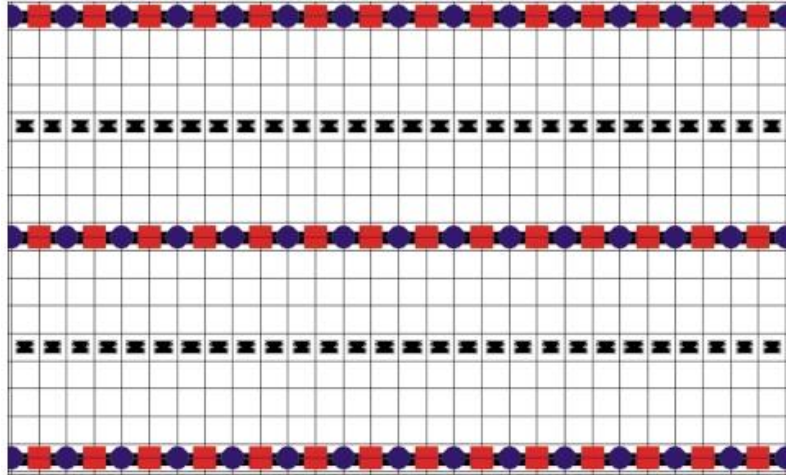


Figure 6. Swath survey bin azimuth; source points (red) and receiver stations (blue). The azimuth mix is narrow and depends on the number of live receiver lines and the line spacing

2.2.3 Orthogonal

The orthogonal field layout is perhaps the most intuitive of all designs and in this design the source and receivers are simply orthogonal to one another (Figure 7). Because of its simplicity the orthogonal design is easier for field crews to keep the source and receiver positioning and numbering in order, making it one of the most widely used designs.

The offset distribution (Figure 8) and azimuth distribution (Figure 9) are shown as a comparison to the full fold survey (Figure 2 and Figure 3). Close inspection (Figure 8) shows that not all offsets are sampled. Additionally, inspection of the azimuth distribution (Figure 9) reveals gaps. While it is evident that not all offsets and azimuths are sampled in the orthogonal design, the sampling in both cases is still very good. It becomes the survey

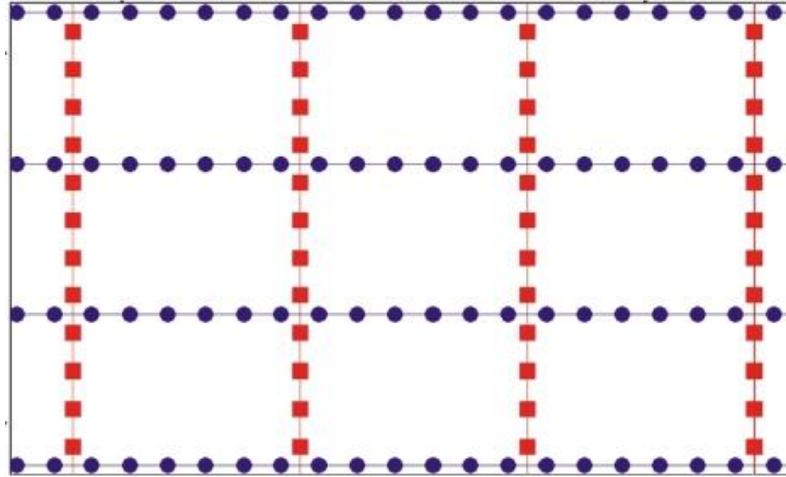


Figure 7. Orthogonal survey geometry; source points (red) and receiver positions (blue). The field layout is intuitive with the source and receivers simply orthogonal to one another

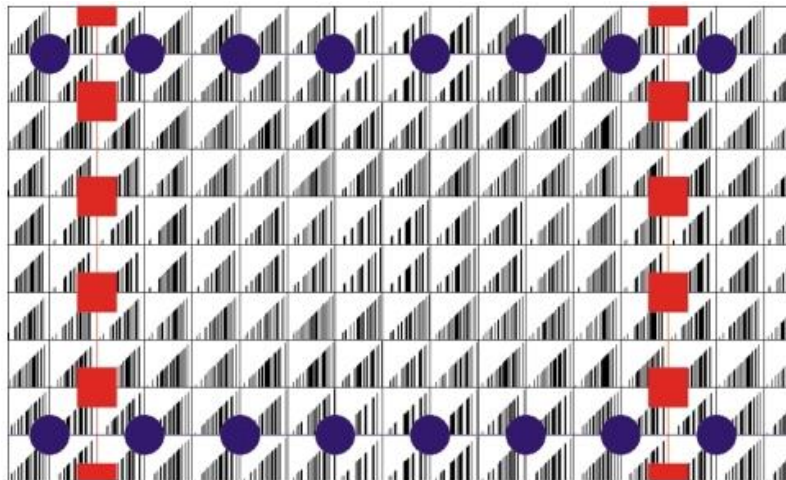


Figure 8. Orthogonal survey bin offset; source points (red) and receiver positions (blue). Inspection of the bin offset shows that not all offsets are sampled as illustrated by gaps within the blackened triangles within each bin

designer's responsibility to determine if the sampling is sufficient and if the benefits gained by reducing the number of source and/or receiver positions outweigh the loss of offset and azimuth distribution.

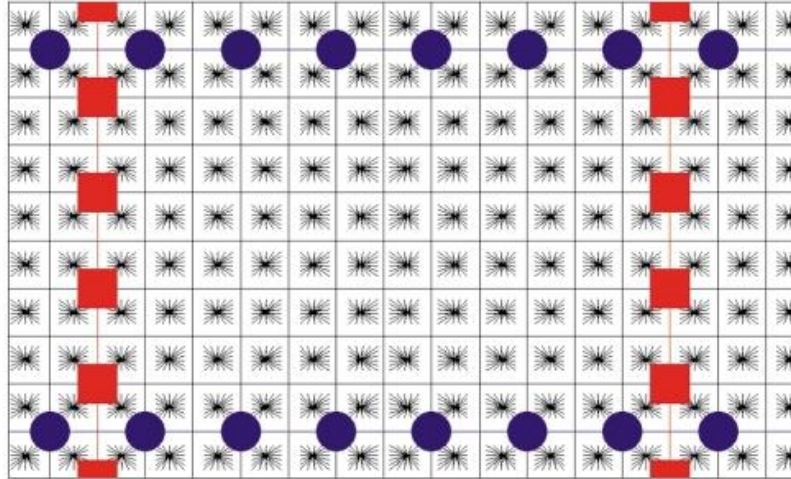


Figure 9. Orthogonal survey bin azimuth; source points (red) and receiver positions (blue). Inspection of the azimuth distribution within each bin reveals gaps

2.2.4 Brick

The brick pattern (Figure 10) was developed in an attempt to improve the offset distribution of the orthogonal method. To accomplish this source lines are split so they are no longer continuous but instead alternate in a brick like pattern. The brick design offers

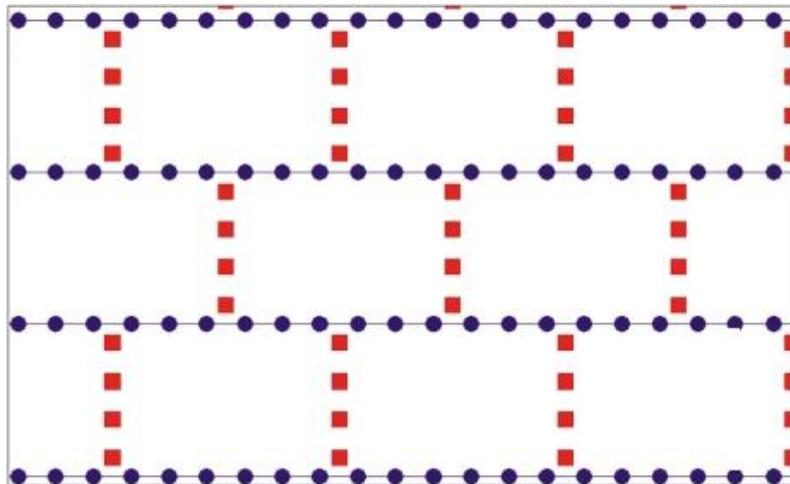


Figure 10. Brick survey geometry; source (red) and receiver (blue). Source lines are split and alternate in a brick like pattern

an improved offset distribution (Figure 11) and generally better azimuth distribution (Figure 12). While it may be difficult to quantify from the figures, comparison of offset and azimuth distributions to the orthogonal design (Figure 8 and Figure 9) shows a slight improvement in both.

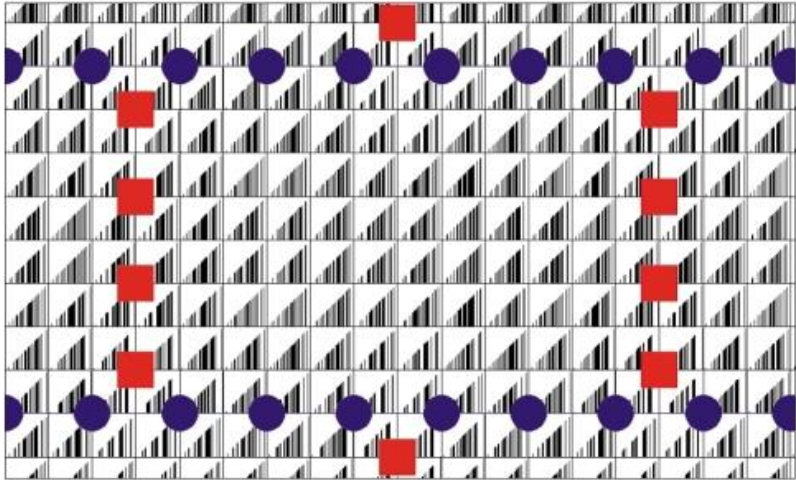


Figure 11. Brick survey bin offset; source points (red) and receiver stations (blue). The brick design offers an improved offset distribution over the orthogonal design

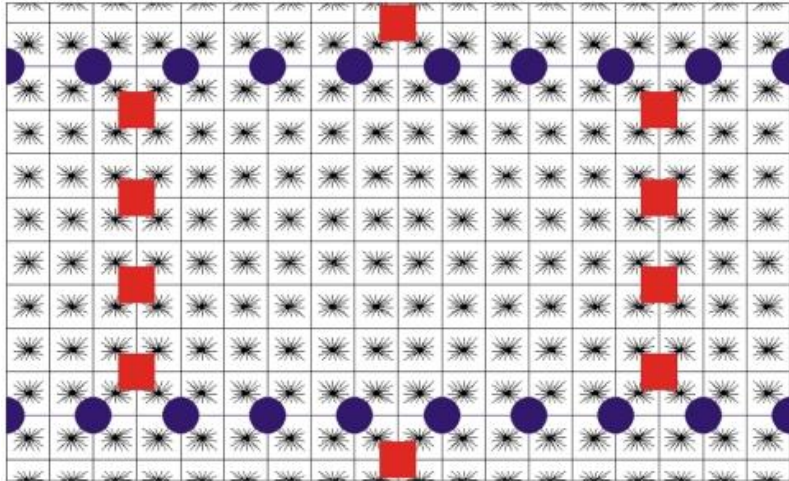


Figure 12. Brick survey bin azimuth; source points (red) and receiver stations (blue). The brick design offers a generally better azimuth distribution over the orthogonal design

2.2.5 Star

When acquiring data using the star (Figure 13) geometry the receiver lines are laid out in an arrangement that resembles the spokes on a bicycle wheel. The source points are then positioned along the receiver lines. Because of the simplicity of the star design, it is an

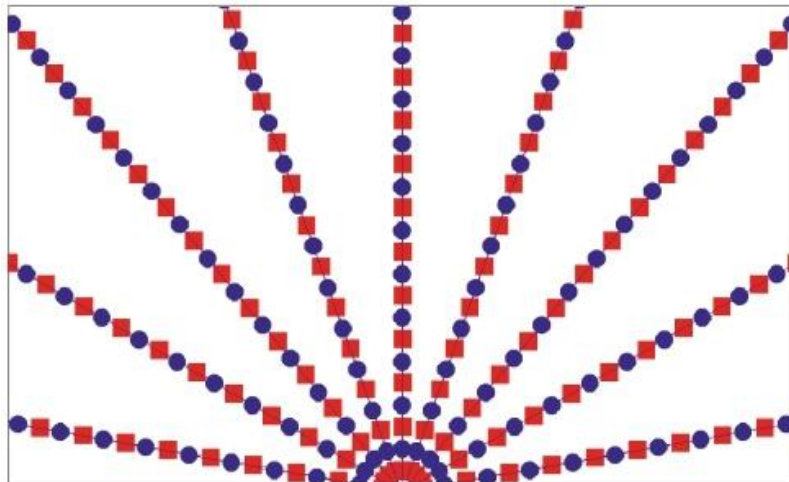


Figure 13. Star survey geometry; source points (red) and receiver positions (blue). Source points are positioned along the receiver lines and the simplicity of the design makes it easy to acquire

easy design to acquire. Inspection of the offset distribution (Figure 14) shows good distribution near each source and receiver line however gaps start to appear between each source and receiver line. Azimuth distribution (Figure 15) is also generally good however there is an azimuthal bias within most bins.

In the same category as the star geometry is the radial geometry. The radial design resembles the star geometry however source points are placed along concentric circles around the center of the survey. The radial design is mentioned because it is an improvement over the star design in that fold is superior and there is more areal coverage. It should also be noted that while the radial method provides some benefits the offset and azimuth distribution are generally very good but deteriorate quickly when moving away from the center.

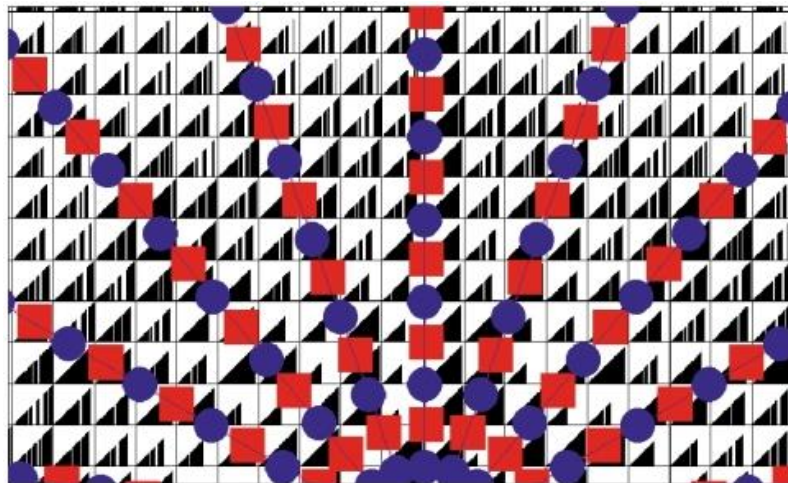


Figure 14. Star survey bin offset; source points (red) and receiver positions (blue). Offset distribution is good near each source and receiver line however gaps appear between each source and receiver line

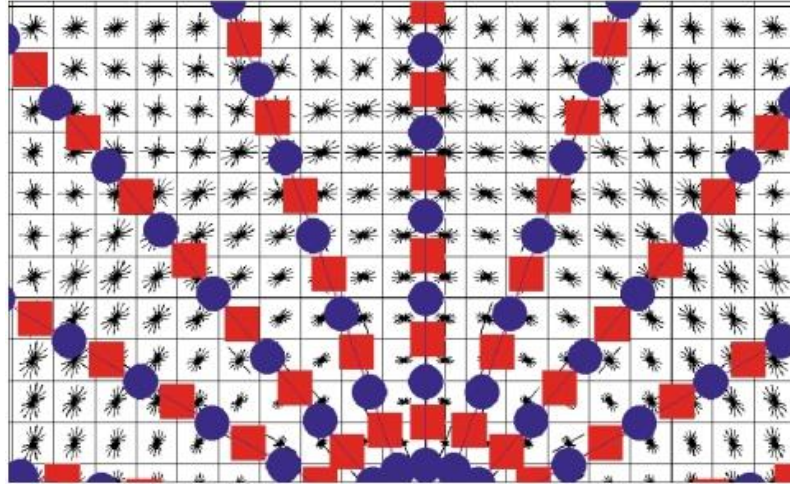


Figure 15. Star survey bin azimuth; source points (red) and receiver positions (blue). Azimuth distribution is generally good however there is an azimuthal bias within most bins

The designs above are simply a few of the many 3D survey geometries that have been described by the seismic community. While the orthogonal design remains perhaps the most commonly used each survey site will offer its own set of restrictions and requirements that will help guide a designer to the appropriate geometry. While there are many survey geometries to choose from the flexibility of professional 3D survey design software allows seismologists to model many different designs and produce the best strategy.

2.3 3D Survey Design

There are two general ways to approach 3D reflection survey design; the conventional method or the symmetrical sampling method. The conventional and more popular method designs a survey based upon regular offset and midpoint distributions as described in the previous section, whereas symmetrical sampling focuses on the equivalence of common shot gathers and common receiver gathers. Symmetrical sampling is discussed later within this chapter under the Symmetrical Sampling section. A detailed design based on the method is

also provided within the Symmetrical Sampling Method section of this chapter. Either method can be applied to any type of field geometry (i.e. orthogonal, brick, etc.). The conventional method of 3D survey design has been developed over the last 30 years and provides robust guidelines for developing a survey. The symmetrical sampling method was introduced approximately 12 years ago.

2.4 Design of a Near-surface 3D Reflection Survey

There are many ways to begin designing a survey and the specific sequences of steps that follow are only a general guide. As a start the following sequence may be used: 1) determine the depth of the target of interest which provides information in regards to the minimum and maximum offsets required; 2) based on the depth of the target and offsets determine the bin size; 3) twice the chosen bin size is the source and receiver station spacing; 4) determine the receiver line spacing; 5) decide the in-line and cross-line rolls; 6) ensure obstacles will not prohibit the needed offset and azimuth distributions; 6) estimate time, effort and costs. In addition to access and mobility within a field site any survey design must take into account: 1) the shallowest layer to be imaged; 2) the deepest layer to be imaged; 3) the maximum recorded frequency; 4) the minimum velocity; 5) maximum dips expected; 6) necessary fold and 7) size of target.

For 3D data the bin is the basic building block for the survey and it depends on the target size, required spatial resolution and economics. All of the traces that fall within a bin will be stacked (i.e. summed) creating a trace which represents that bin position by a point (i.e. a stacked trace). As a general rule we would like to have at least three traces per bin illuminating the target. The bin is a square or rectangular area whose dimensions are defined

as one half of the receiver interval in the in-line and cross-line directions. All traces falling within each bin will be added during the stacking process. As a general rule of thumb the bin size should be one third the size of the target of interest. The bin size in both the in-line and cross-line directions can be calculated as shown in equation 1 (Cordson et al., 2000)

(Eq. 1)

$$A_{x,y} = \frac{V_{\min}}{2 * F_m * \sin(\beta)}$$

Where: V_{\min} = minimum velocity
 F_m = maximum frequency
 β = dip of bed (where $\beta > 0$)

Calculating the bin size

This defines a natural bin size based upon the receiver geometry. The natural bin size is generally sufficient however it can be changed during processing. The bin size is usually not decreased but can be increased by combining adjacent bins in order to assist in velocity analysis.

2.4.1 Receiver and Source Interval

The receiver and source intervals are perhaps the easiest parameters to calculate. Both the receiver and source intervals are simply twice the bin size in both the in-line and cross-line direction.

2.4.2 Receiver and Source Line Interval

The receiver and source line interval are related to the shallowest (X_{min}) and deepest (X_{max}) layers to be imaged. X_{min} can be calculated as shown in equation 2 (Cordsen et al., 2000).

(Eq. 2)

$$X_{min} = \sqrt{RLI^2 + SLI^2}$$

Where: RLI = receiver line interval
SLI = source line interval

Calculating the shallowest layer (X_{min}) to be imaged

X_{min} should be less than the shallowest target of interest while X_{max} is approximately equal to the deepest layer of interest. X_{max} requires the receiver line interval and/or source line interval offsets to be large enough to image the deepest reflector. While the receiver line and source line intervals are not required to be the same it's generally best to keep them so to retain symmetry within the design.

2.4.3 Migration Apron

If data are to be migrated a migration apron must be considered. The migration apron is simply additional area that is added to the survey to increase the size of the area over which full fold is required. The migration apron can be calculated as shown in equation 3 (Cordsen et al., 2000).

(Eq. 3)

$$MA = Z * \tan(\theta)$$

Where: Z = depth
 θ = dip (where $\theta > 0$)

Calculating the migration apron

Near-surface seismic reflection data are generally not migrated; however if steep dips or diffractions are expected migration needs to be considered. Even though near-surface seismic data is generally not migrated, the move to 3D should give pause for more consideration. It could be argued that the 3D nature of the acquired data is reason enough for migration because it allows for proper positioning of reflected energy originating out of the 2D plane of incidence.

2.4.4 Fold

The general rule for 3D fold is that it should be one-half the 2D fold, assuming that the signal-to-noise ratio for the 2D data is acceptable (Cordsen et al., 2000). When discussing fold for 3D surveys the fold pattern for both the in-line and cross-line component can be calculated as shown in equation 4 (Cordsen et al., 2000).

(Eq. 4)

$$\text{In-line Fold} = (\text{Total Number of Receivers} * \text{Receiver Interval}) / (2 * \text{Source Line Interval})$$

$$\text{Cross-line Fold} = (\text{Source Line Length}) / (2 * \text{Receiver Line Interval})$$

$$\text{Total Nominal Fold} = \text{In-line Fold} * \text{Cross-line Fold}$$

Calculating fold

2.5 Symmetrical Sampling

The main criteria of symmetric sampling can be summarized as; 1) the source station interval should equal the receiver station interval; 2) the source line interval should equal the receiver line interval; 3) the maximum in-line offset should equal the maximum cross-line offset; 4) center-spread acquisition for shots and receivers; 5) source arrays are required as much as receiver arrays (Vermeer, 1998). These criteria form the basis of the concept which can then be applied to 3D survey geometries. Essentially, the symmetric sampling approach to 3D seismic survey design is a straightforward extension of the 2D symmetric sampling approach (Vermeer, 1990). 2D symmetric sampling was first described by Anstey (1986) in which he introduced the stack-array approach. The stack-array approach involves determining the appropriate source interval versus group interval for various shooting methods.

Three-dimensional symmetric sampling focuses on the equivalence of common-shot gathers and common-receiver gathers (Vermeer, 2002). The goal of symmetrical sampling is to have common-receiver gathers look like common-shot gathers. The benefit of having common-receiver gathers look like common-shot gathers, and vice-versa, produces data with

the same quality and character in both the in-line and cross-line direction (Vermeer, 1998). This is useful during processing because both gathers are equally suitable to various pre-stack processing steps such as f-k filtering and pre-stack noise suppression. Along with pre-stack processing there are other advanced processing techniques that can take advantage of the equal gathers in addition to improved AVO analysis and inversion.

While the concept of symmetrical sampling offers many benefits, to date, the very dense source and receiver requirements of the method make it uneconomical. However the relatively new advancement of very large channel-count systems may provide a means of acquiring data using 3D survey geometries based upon symmetrical sampling.

2.6 3D Survey Designs Applied to the Autojuggie

2.6.1 Conventional Methods

Three-dimensional near-surface seismic reflection at The University of Kansas has progressed around the design of the Autojuggie. Because this research makes use of the Autojuggie examples are provided to illustrate 3D survey design in regards to it. As an example, reflectors of interest, ranging from eight to 25 meters, have been chosen. The following design is based upon a design that was developed at an early stage in this research.

2.6.2 Survey Geometry

To image the target reflectors a receiver grid consisting of 10 lines of eight geophones for a total of 80 geophones per receiver patch will be used. A patch refers to all of the receivers that are live for any given source location. In this example all geophones are live for each shot so the patch consists of 80 geophones, the entire receiver array. To maximize

the geophone spacing within the Autojuggie a receiver interval of 1.0 meter and a receiver line interval of 0.5 meter. To build sufficient fold over the target area the patch (Figure 16) will be rolled half the receiver spread. A receiver spread refers to the length and width of the receiver grid. In this example there are eight geophones, spaced at 1.0 meter intervals, in the in-line direction and 10 geophones, spaced at 0.5 meter intervals in the cross-line direction. Rolling the patch a half-spread length in the in-line direction results in an in-line move of 4.0 meters. Rolling the patch a half-spread length in the cross-line direction results in a cross-line move of 2.5 meters. For this example the patch was rolled three times in the in-line direction and twice in the cross-line direction. The source and source line interval are four meters with 13 source lines of 9 source locations per line. Accounting for the 12 patch locations results in a total of 1,404 source positions.

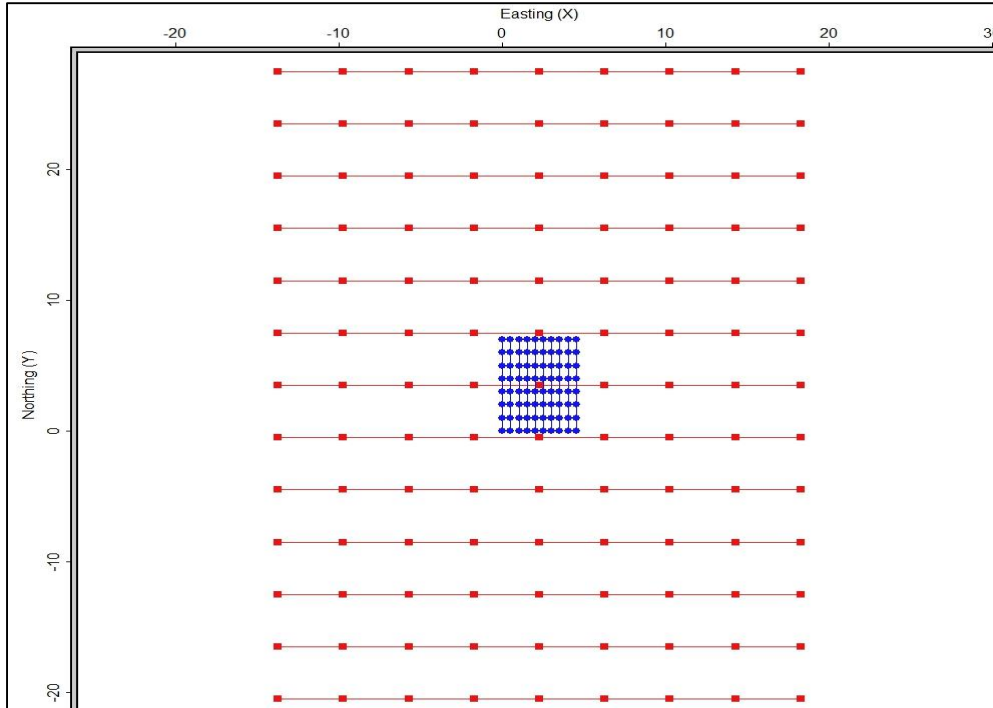


Figure 16. Autojuggie patch geometry, building sufficient fold over the target by rolling the receiver spread. The receiver spread is rolled half a spread length in both the in-line and cross-line directions

2.6.3 Fold

Although fold generally ramps up quickly in well-designed 3D reflection surveys, acquiring full fold over a target area must be quantified. Based upon this design an area of 990 square meters (44 meters in-line and 22.5 meters cross-line) is represented by an area of 0-30 fold. Additionally, an area of 592 square meters (18.5 meters in-line and 32 meters cross-line) is represented by an area of 24-30 fold (Figure 17). Lastly, a fold of 30 covering an area of 324 square meters (13.5 meters in-line and 24 meters cross-line), represents the area of the target of interest. Because the subsurface consists of relatively flat, cyclic Pennsylvanian age cyclothems characteristic of eastern Kansas (Knapp, 1988, Knapp and

Watney 1987), this design should be sufficient to image the subsurface geology within the vicinity of a small target area in Lawrence, Kansas.

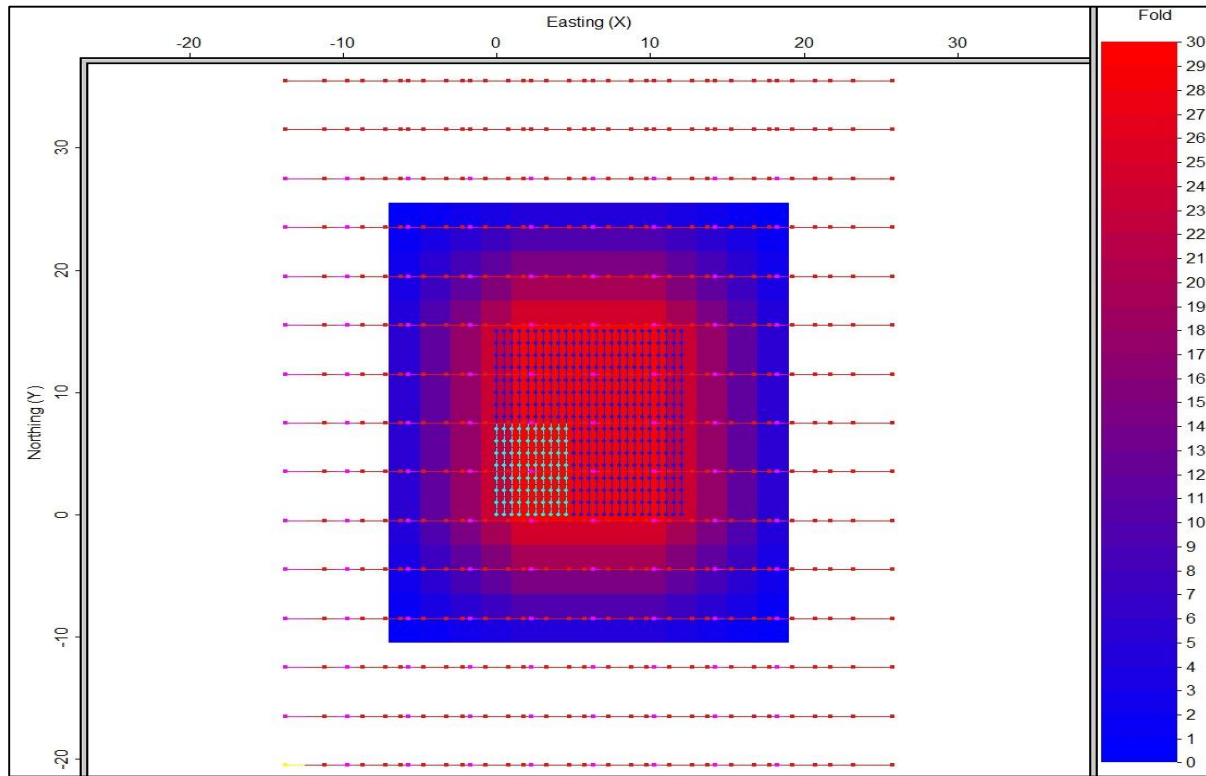


Figure 17. Autojuggie fold, building fold over the target of interest. Fold map of an area of 990 square meters with the highest fold reaching 30, covering an area of 324 square meters

2.6.4 Offset and Azimuth Distribution

For nearly all 3D seismic reflection surveys a broad range of offsets is important to properly sample the subsurface and for velocity analysis. Figure 18 shows the offset distribution over a portion of the area of full fold. The image illustrates good offset distribution over the area of interest and surrounding areas. Azimuth distribution must also be considered and a portion of the target area of the survey is shown (Figure 19). The survey design leads to a narrow azimuth as result of the rectangular receiver grid. Because the

underlying geology of the area is simple, narrow azimuth distribution is acceptable. If the geology were more complex the design would have to be reconsidered.

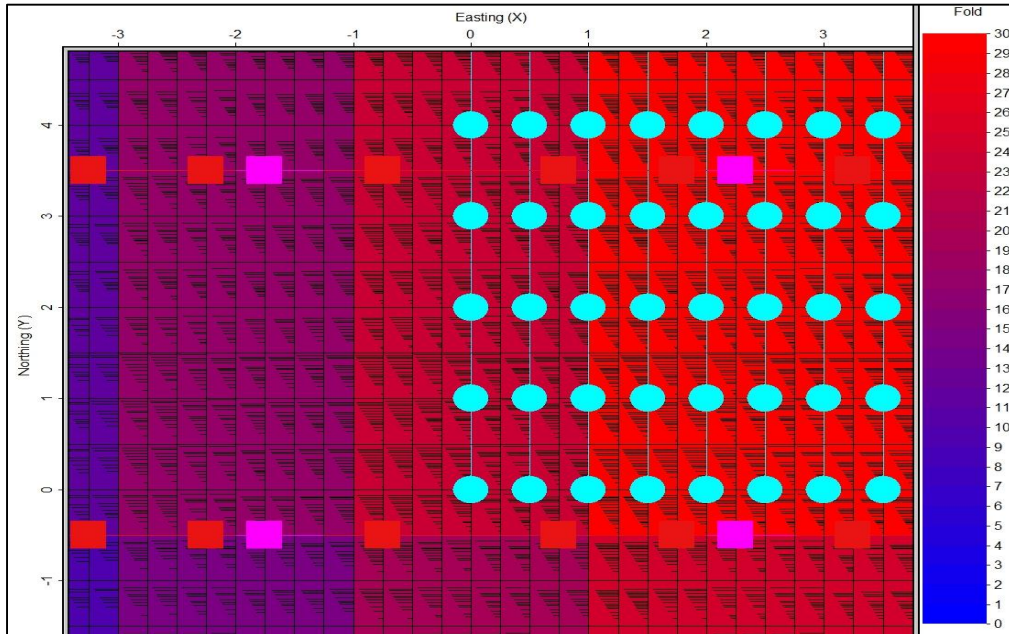


Figure 18. Autojuggie offset distribution over a portion of the area of full fold. Good offset distribution is illustrated within the area of interest and surrounding areas

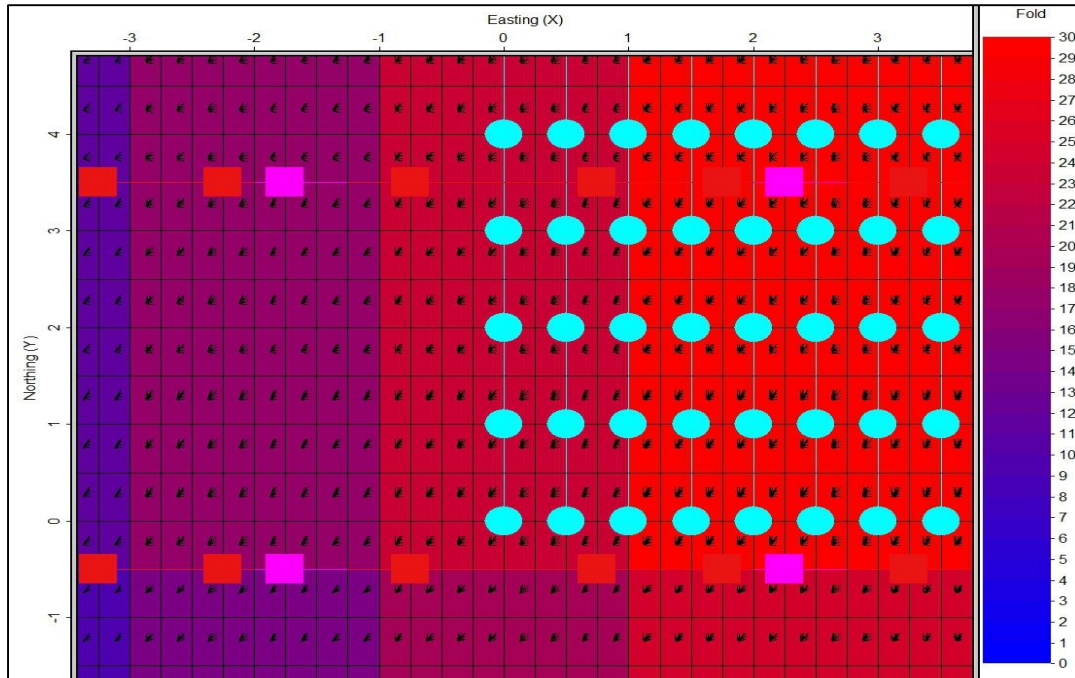


Figure 19. Autojuggie azimuth distribution. A portion of the target area is shown and the survey design leads to a narrow azimuth as result of the rectangular receiver grid

2.6.5 Trace Count

It is important to quantify that enough traces fall within the offsets and azimuths of interest. Several thousand traces illuminate the desired offset range of 8 to 25 meters (Figure 20). It can also be seen that these same traces represent a large number of traces illuminating a narrow range of azimuth (Figure 21).

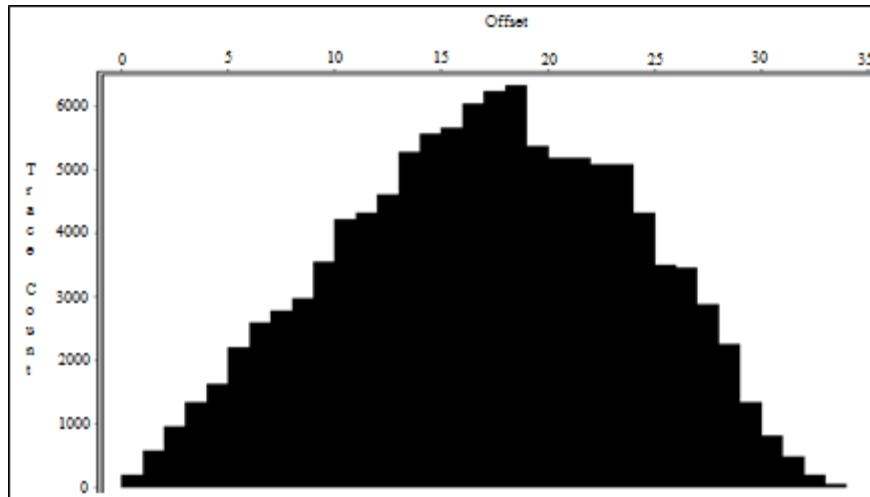


Figure 20. Autojuggie trace count vs. offset. Several thousand traces can be seen to illuminate the desired offset range of 8 to 25 meters

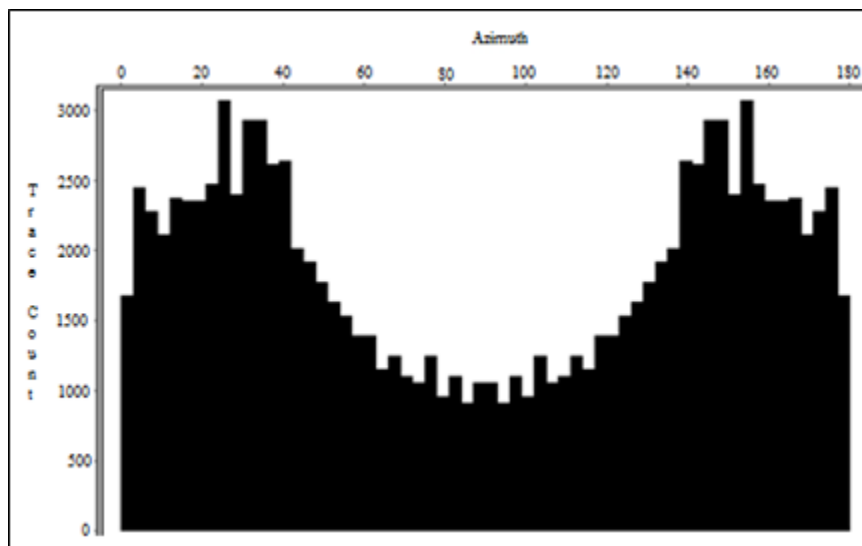


Figure 21. Autojuggie trace count vs. azimuth graph shows a large number of traces illuminating a narrow range of azimuth

2.6.6 Redundancy

The basic design of a 3D survey gives rise to many traces and mid-points and it's important to consider the redundancy of traces. Some redundancy helps increase the signal to

noise ratio however there is a point of diminishing returns. An excessive amount of redundancy leads to wasted effort and in the worst case scenario gives rise to a situation wherein velocity analysis cannot be properly performed because there are not enough unique offsets represented.

Redundancy plots are one method used to quantify the amount of redundancy in a survey design. When examining these types of plots a designer wants to see complete color coverage over the area of interest while at the same time not see an abundance of redundant traces. Some redundancy is inevitable and it is a survey designer's task to balance this redundancy. The offset redundancy plot (Figure 22) shows some redundancy; however it's at an acceptable level. The azimuth redundancy plot (Figure 23) shows that the majority of bins are being illuminated while redundancy is kept to a minimum.

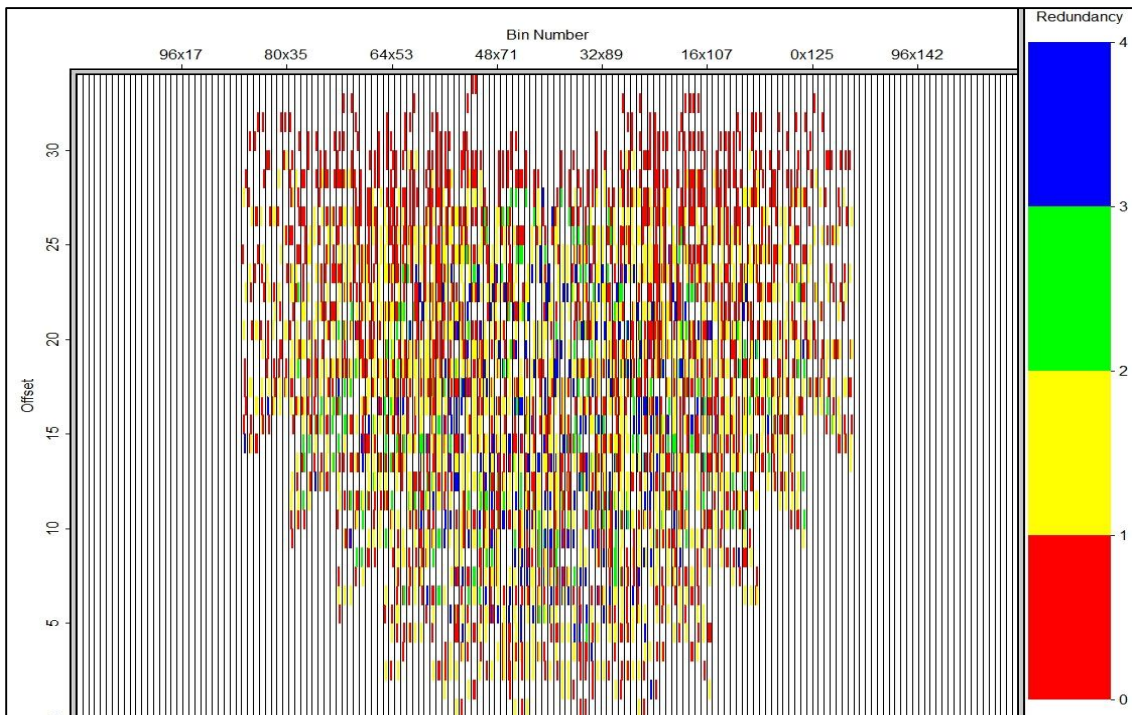


Figure 22. Autojuggie bin offset distribution. The design leads to some offset redundancy however, the redundancy is at an acceptable level

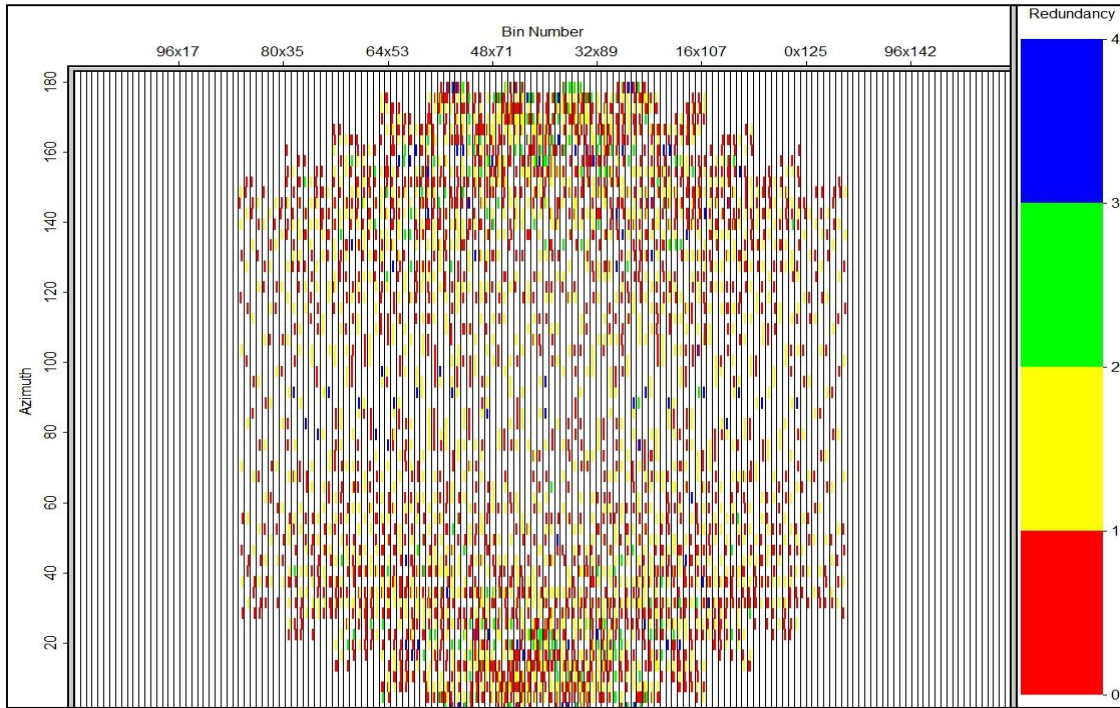


Figure 23. Autojuggie bin azimuth distribution. The majority of bins are being illuminated while redundancy is kept to a minimum

2.6.7 Symmetrical Sampling Method

As a comparison the symmetrical sampling design method was applied to design a 3D survey to image reflectors between 8 and 25 meters. The symmetrical sampling method recognizes that, based upon its methodology, large source and receiver counts are inevitable and offers guidelines to help reduce these numbers.

2.6.8 Survey Geometry

To determine the line interval, spread length and source and receiver spacing based upon the symmetrical sampling the following steps can be used:

- 1) Calculate the line interval:

Shallowest horizon to map, fold coverage (M) = 8
Shallowest time of that horizon (Tsh) = 28 ms
Maximum offset for that horizon (Xsh) = 8 m
Line interval (S) = $Xsh / \text{Sqrt}(2 * M) = 8m / \text{Sqrt}(2 * 8) = 2.0 \text{ m}$

2) Calculate the spread length

Deepest horizon to map (S) = 25 m
Deepest time of that horizon (Tdp) = 40 ms
Maximum offset for that horizon (Xdp) = 25 m
Spread length (rough estimate) = $2 * Xdp = 50 \text{ m}$

3) Calculate the sampling interval:

$$\Delta X = V_{\min} / (2 * F_{\max}) = 370 \text{ m/s} / (2 * 500 \text{ s}^{-1}) = 0.37 \text{ m} = 0.4 \text{ m}$$

According to the symmetrical sampling method; 1) the source and receiver line interval must be the same; 2) the spread length (offset) must be the same; 3) the source and receiver spacing must be the same. This would result in a final receiver and source grid consisting of 25 source and receiver lines with 125 source and receiver positions per line spaced at 0.4 meter intervals, totaling 3,125 source and receiver locations (Figure 24).

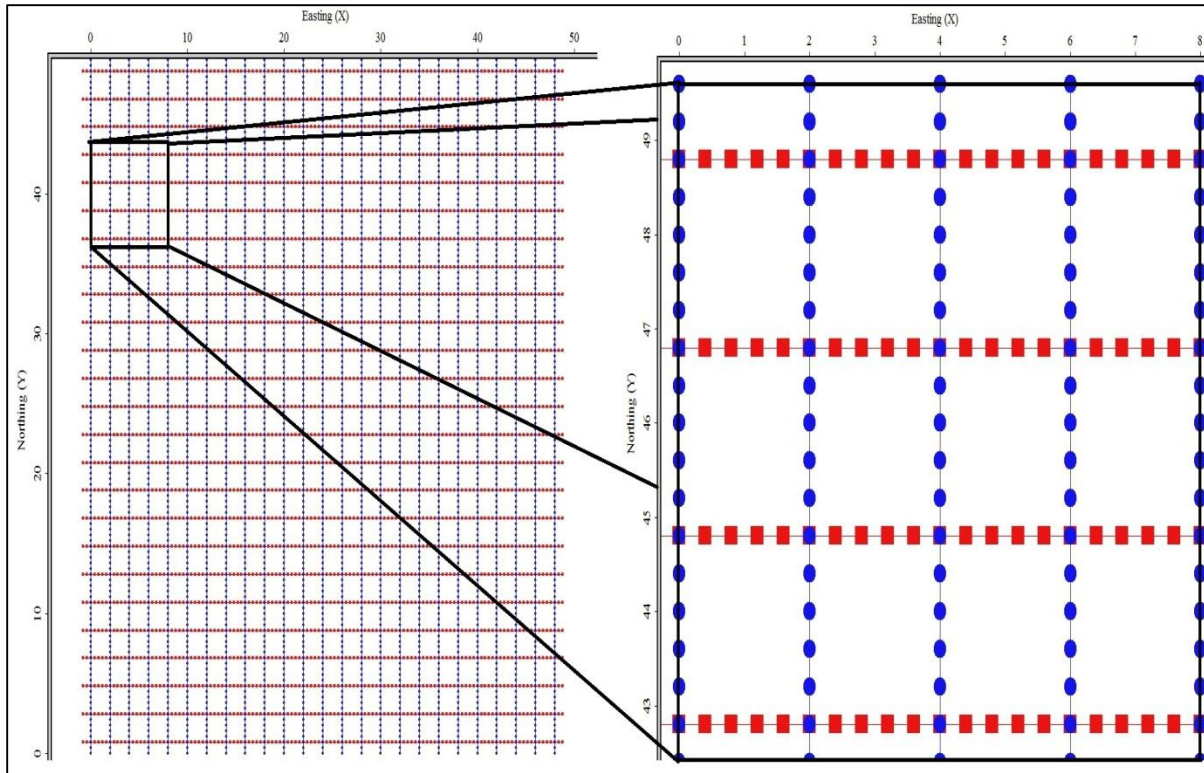


Figure 24. Symmetrical sampling field geometry, full survey grid (left), close-up view (right). This geometry would require 25 source and receiver lines with 125 source and receivers per line

2.6.9 Fold

In comparison to the previous survey it can be seen that fold (Figure 25) becomes very high in a symmetrical sampling design. While fold is important, achieving a fold of this magnitude is generally not required. The high fold is simply a result of the large number of source and receiver positions needed to sample the full subsurface wavefield.

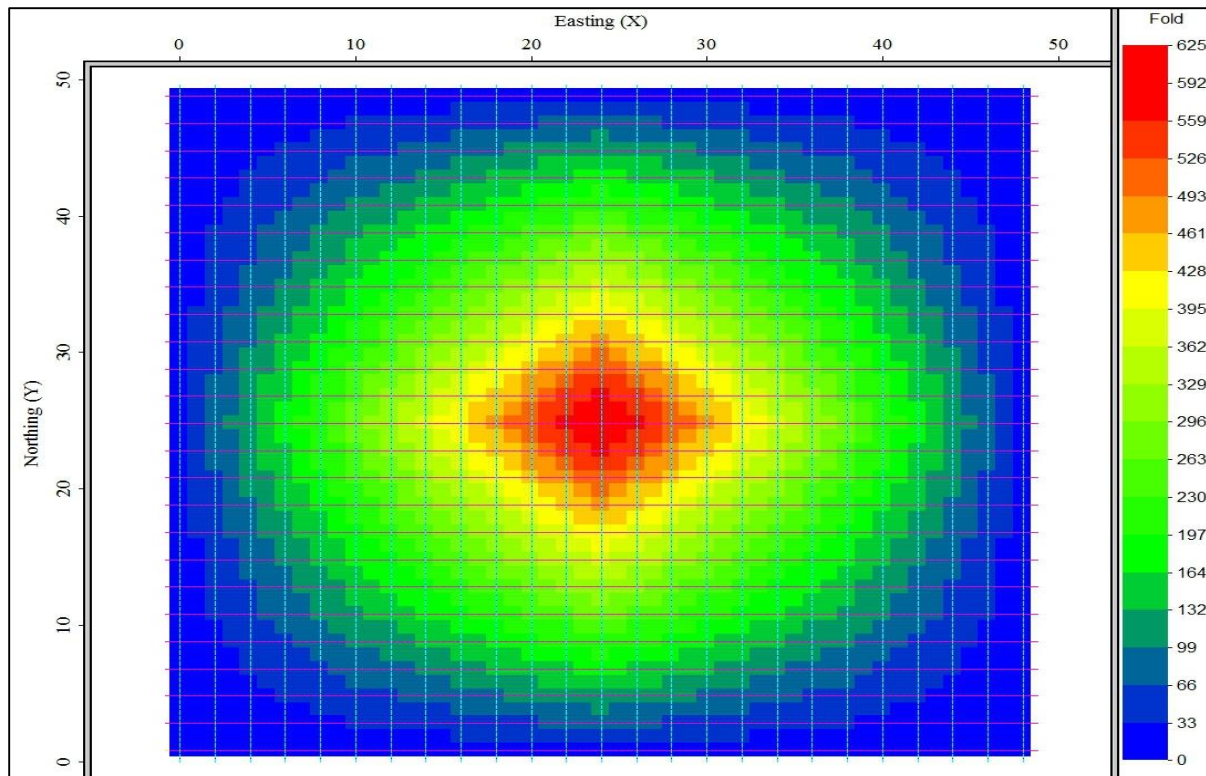


Figure 25. Symmetrical sampling fold. In comparison to the other survey designs fold becomes very high in a symmetrical sampling design

2.6.10 Offset and Azimuth Distribution, Trace Count and Redundancy

The offset distribution (Figure 26), azimuth distribution (Figure 27), trace count versus offset (Figure 28), trace count versus azimuth (Figure 29), bin offset redundancy (Figure 30) and bin azimuth redundancy (Figure 31) are shown. Because of the many source and geophone positions the figures show dense coverage for all of these parameters. This illustrates the reasoning for the high density of source and receiver points, the resulting subsurface coverage is excellent.

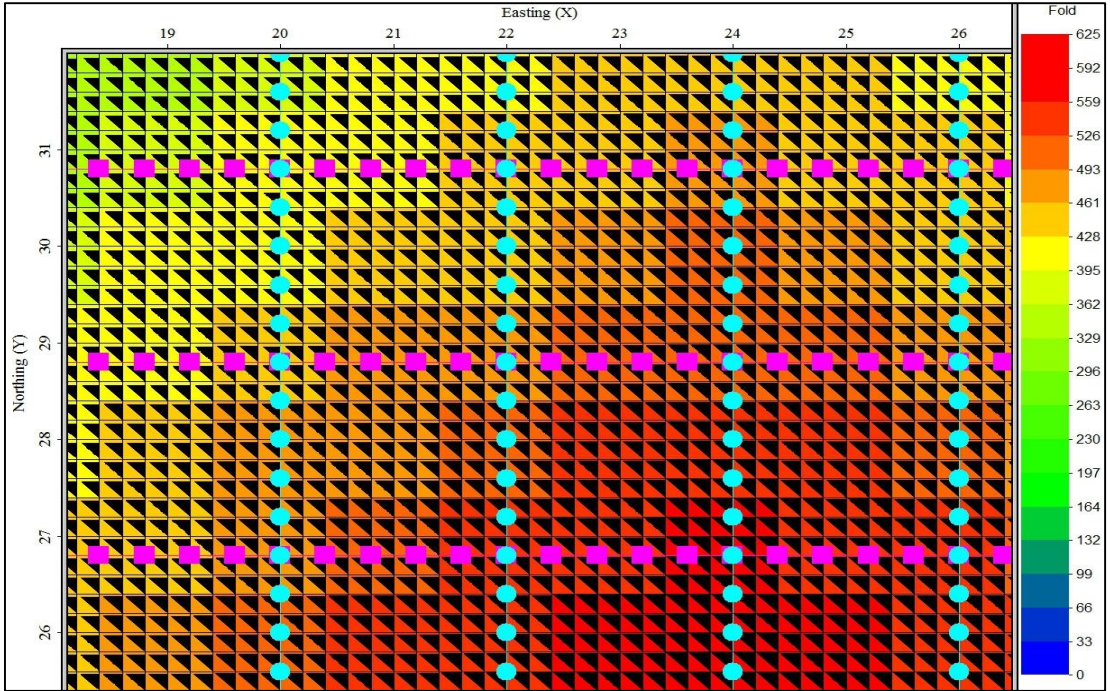


Figure 26. Symmetrical sampling offset distribution. There is a well sampled range of offset distribution within each bin as indicated by the blackened triangles within each bin

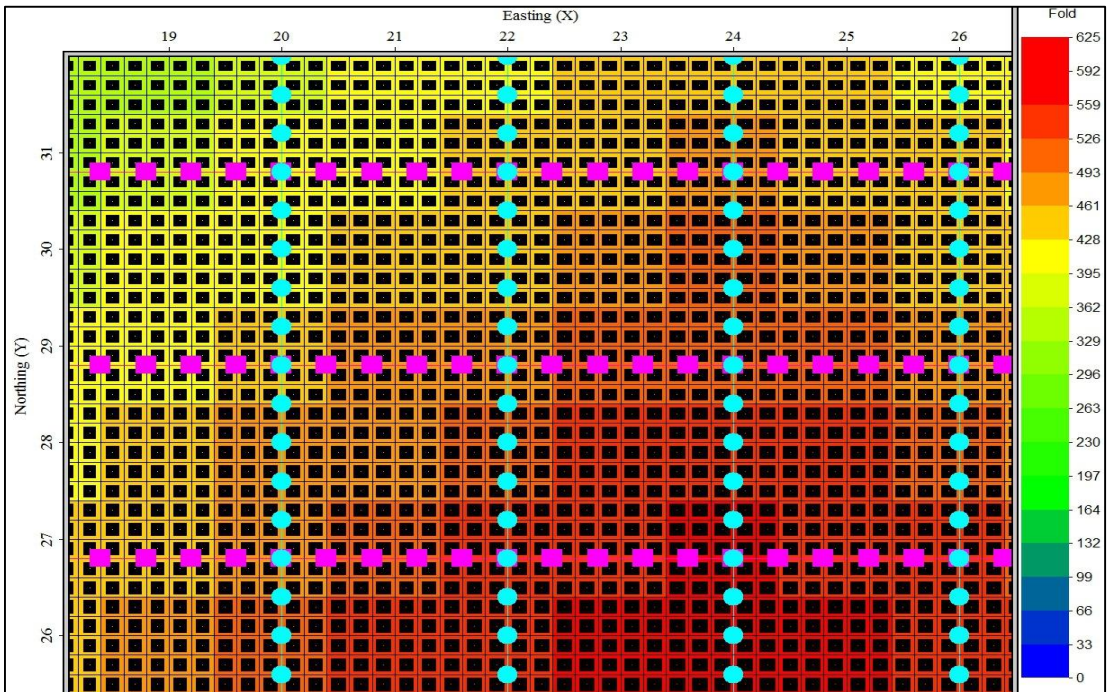


Figure 27. Symmetrical sampling azimuth distribution. Azimuth is well sampled within each bin as indicated by the blackened triangles within each bin

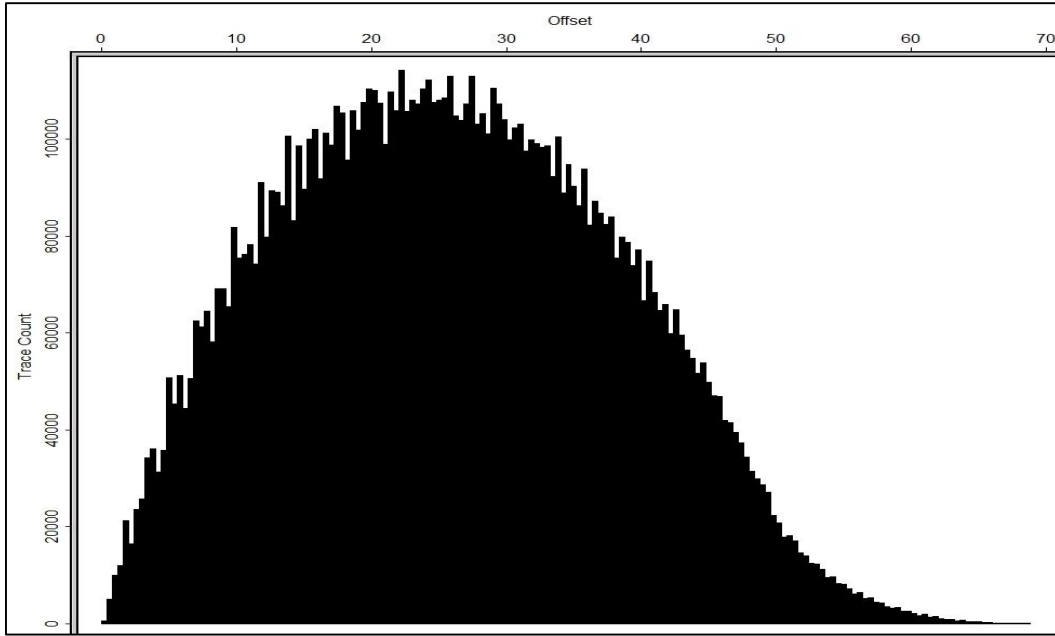


Figure 28. Symmetrical sampling trace count vs. offset. A large number of traces sample offsets ranging from approximately 5-45 meters

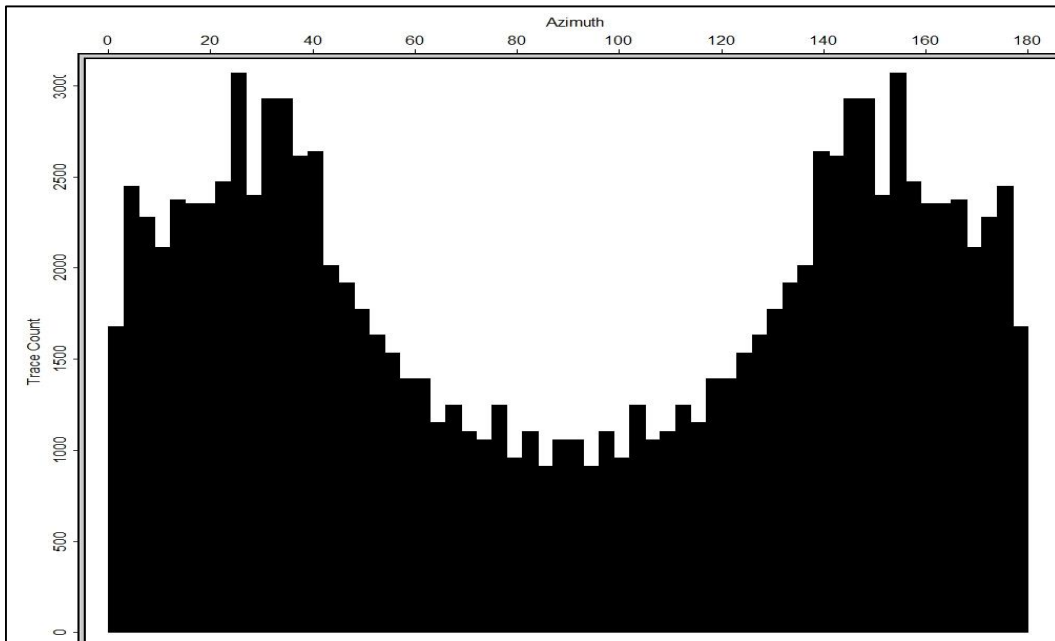


Figure 29. Symmetrical sampling trace count vs. azimuth. Traces are concentration within the 0-40 and 140-180 degree range

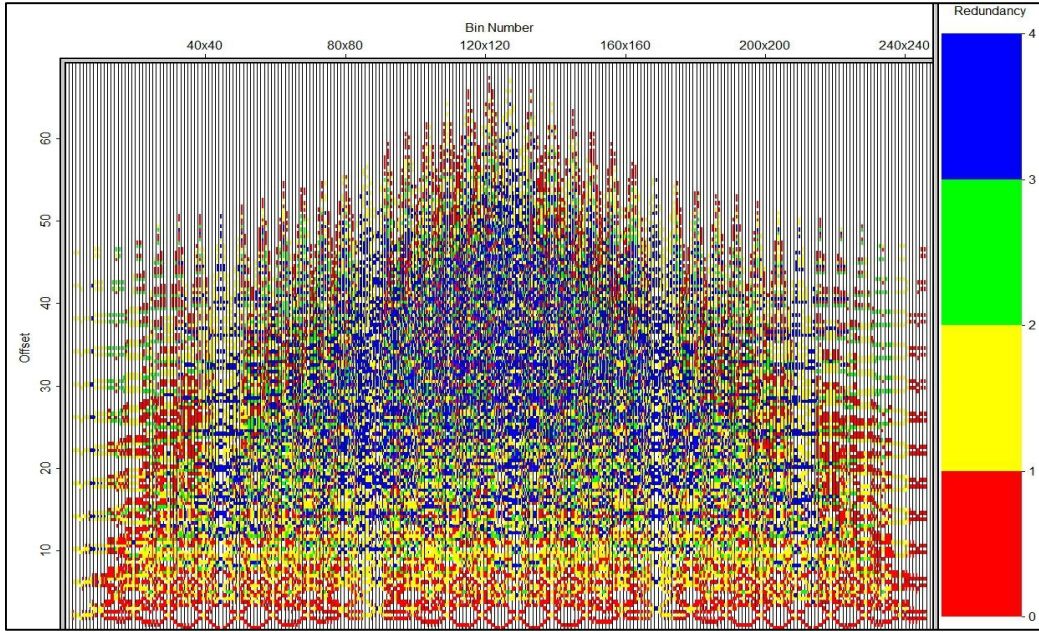


Figure 30. Symmetrical sampling bin offset redundancy plot. Bins are divided into colored blocks with the color indicating the number of times a particular offset was sampled

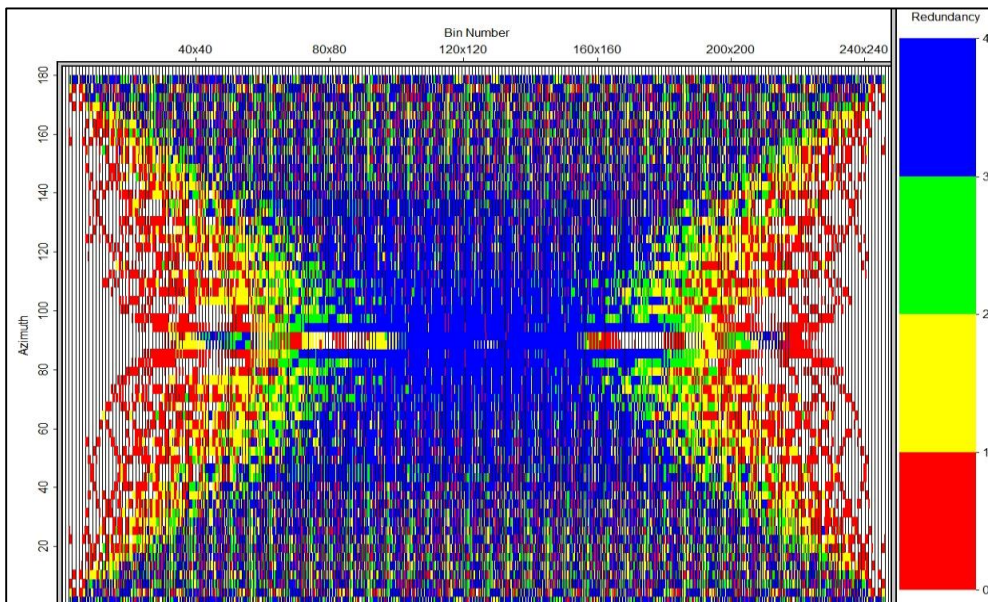


Figure 31. Symmetrical sampling bin azimuth distribution. The design leads to a number of redundant azimuths near the middle, however it is at an acceptable rate

2.7 Summary

The move from 2D seismic reflection to 3D has largely been driven by the search for hydrocarbons. However, technological advancements and decreased costs now allow near-surface seismic investigators to employ 3D methods. Conceptually the move to 3D simply includes the addition of coincident source and receiver lines and the introduction of azimuth. General guidelines can be used when developing 3D surveys however, because there are now more options available, and it is difficult to make changes to a 3D survey in the field, designers must be thorough and give additional consideration to the process.

Currently 3D survey design can be approached from one of two design methods. The conventional, and more popular, method designs a survey based upon regular offset and midpoint distributions whereas 3D symmetric sampling focuses on the equivalence of common shot gathers and common receiver gathers. Both methods can be applied to any type of field geometry (i.e. orthogonal, brick, swath, etc.) however the rigorous spatial requirements of the symmetrical sampling method make it uneconomical in most instances.

Chapter 3: The Autojuggie

3.1 Introduction

While 3D reflection has been established as the predominant seismic method for hydrocarbon exploration the same is not yet true for near-surface seismic investigations. While the benefits of 3D methods have been documented they are yet to be fully adopted by the near-surface community for engineering and environmental applications. There are a number of reasons for this; primary among them is the labor involved with planting large numbers of geophones. Further labor and time constraints come from the need to re-cable after each patch move. The amount of effort involved in these operations is likely part of the reason for the low number of published articles in regards to 3D investigations of the near-surface.

To help overcome these limitations The University of Kansas has developed a portable, automated seismic data acquisition system, known as the Autojuggie. The Autojuggie allows for efficient shallow seismic imaging and is capable of quickly performing non-invasive, high-resolution 2D or 3D seismic surveys by deploying a dense array of geophones.

3.2 Development of the Autojuggie

The Autojuggie has been in on-going development for more than a decade and has seen several significant design improvements. Initial tests (Figure 32) involved geophones mounted to a board (Steeple et al., 1999a). The results of these tests were surprising because they found little interference as a result of the rigid coupling of the geophones to the board. These initial tests were conducted with both .22 caliber and 30.06 caliber rifle sources. No interference was seen in the data acquired with the .22 caliber, however when filtering the 30.06 data with a high frequency pass band a wave mode of unknown origin appeared at

frequencies above 500 Hz. This unknown wave mode seemed to be related to the presence of the board. Even so, this mode did not interfere with the usefulness of the shallow reflection data.

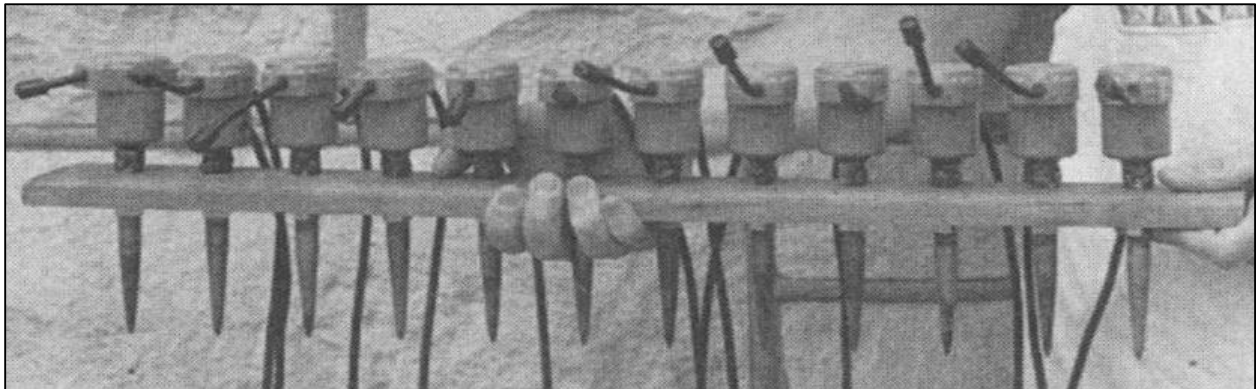


Figure 32. Early Autojuggie development. Initial tests started by mounting geophones on a board (from Steeples et al., 1999a)

Following the success of this initial test the design was modified and a farm tillage tool used to hydraulically plant 72 geophones mounted to lengths of channel iron (Figure 33). This new design allowed the authors (Steeple et al., 1999b) to plant 72 geophones in approximately two seconds. At further offsets the authors didn't find any deterioration of the signal as a result of the rigidly attached geophones however at close offsets slow moving waves were excited within the channel iron.

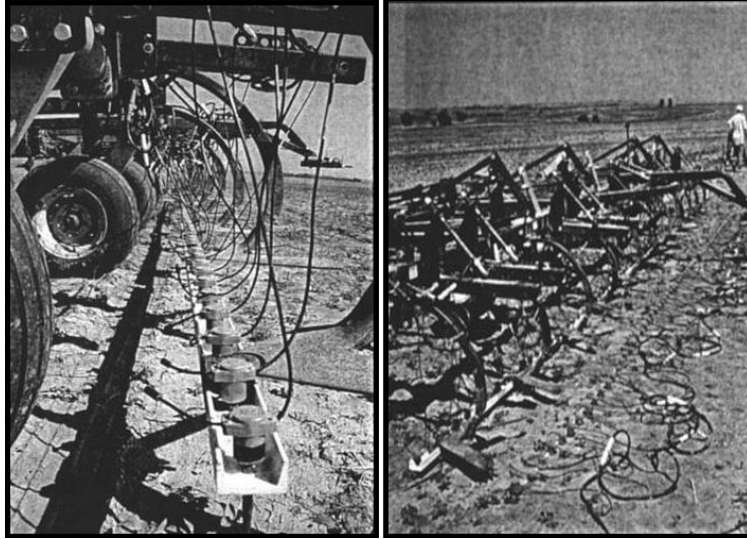


Figure 33. Early autojuggie development. Experiments continued by mounting geophones on lengths of channel iron (from Steeples et al., 1999b). As shown here the channel iron was adapted for deployment using farming equipment

Two important questions emerged from these initial experiments; whether rigidly mounted geophones could record seismic reflections and, whether the source of an anomalous mode found in the earlier study could be isolated (Schmeisner et al., 2001). The authors were able to answer these questions by comparing data acquired with the geophones mounted to channel iron versus data from hand-planted geophones and found that it was possible to acquire high quality reflection data. Additionally, they were able to isolate the anomalous noise seen in the earlier tests by detaching the channel iron geophone array from the farm tillage equipment. Once detached the noise was no longer present showing that it was not attributable to the channel iron but instead to the connection of the channel iron geophone array with the planting equipment.

The results of this study led to an important conclusion in the development of the Autojuggie. In the authors words, “depending on the method of automation, the planted

geophones may have to be detached from the planting mechanism during data acquisition and then reattached before they are moved to the next location” (Schmeisner et al., 2001).

While efficient acquisition has been the primary motivation for development of the Autojuggie, the ability to process data acquired with the Autojuggie was also investigated. Spikes et al. (2005) demonstrated that rigidly attached geophones (Figure 34) can accurately record common mid-point data. To show this the authors acquired data using the channel iron geophone array and data acquired using a control line. Both were processed to a common mid-point stacked section for comparison. Negligible differences between the two showed that conventional processing could be used to stack reflections from data acquired using rigidly connected geophones.

Several additional studies were undertaken to inspect the nature of the square channel iron. Blair et al. (2003) tested five shapes to determine if the shape of the tubing had any influence on the quality of the recorded data. Based upon amplitude coherency, airwave damping and noise content their findings show that the square tubing was the best of all the shapes. Clark et al. (2004) further refined the testing by including different configurations of geophones attached to steel and PVC tubing. Their results conclude that square steel tubing was also the best medium because of its rigidity and high signal-to-noise ratio over the largest range of offsets.



Figure 34 Early autojuggie development. Geophones mounted on channel iron to demonstrate that rigidly attached geophones can accurately record common mid-point data (from Spikes et al., 2005). As shown here, the channel iron is being deployed using a series of hydraulic cylinders

Experiments were also conducted to look at source air wave interference change with azimuth for geophones rigidly attached to square tubing. Because many source and receiver azimuths get defined during the course of a 3D reflection survey it's important to know if there's an azimuthally dependent interference arising from the channel iron. A zone of approximately 60 degrees was found where the airwave degraded off of both ends of the linear geophone array, as evidenced by a sharp reduction in the coherency and amplitude of the recorded airwave (Vincent et al., 2004).

Experiments using the Autojuggie have also been performed to acquire three component data and surface wave data. Properly planting and leveling three-component geophones takes considerable time and effort. In an attempt to increase the efficiency with which three component geophones can be deployed the concept of mounting Galperin type, three component geophones to channel iron was explored. Use of Galperin geophones allows

the vertical, radial and transverse components of motion to be derived. Ralston et al. (2001) found that the amplitude and phase characteristics of the vertical component of the wave field, as was found in previous studies, were undistorted and can be successfully recorded. However, the radial and transverse components of motion were distorted by interfering seismic modes propagating within the acquisition device (Ralston et al., 2001). Further research by Ralston et al., (2002) produced a linear inverse filter that can be applied to the radial and transverse components to remove interfering seismic modes. The filter is site specific so it would need to be calculated for every survey but the end result is data of equal quality as hand planted three-component geophones.

Development of the Autojuggie has focused on body waves, particularly the vertical component. However, some preliminary work has been done showing how the Autojuggie could be used to acquire surface wave data. Tian et al. (2003) concluded that the Autojuggie could be used with the Multichannel Analysis of Surface Wave (MASW) method with no variation from the geometry of a common mid-point survey. The importance of this research was to show that the Autojuggie can be used to record body and surface waves simultaneously.

The next stage of development was the move to a 2D array of geophones (Figure 35) that could be deployed simultaneously in a 3D survey mode (Tsoflias et al., 2006). The receiver grid measures 2.2 x 1.0 meters and is able to hold 72 geophones with a 0.2 x 0.2 in-line and cross-line spacing. A tractor was used to move and plant the receiver grid without any human contact with the geophones. One major developmental change was that all of the geophones could be automatically decoupled from the frame, leaving each geophone free standing, just as if they were hand planted. The reason for the decoupling was to totally eliminate any cross

feed through the rigid frame (Czarnecki, 2006). Decoupling also eliminates the azimuthally biased air wave discussed by Vincent et al., (2009).



Figure 35. Early autojuggie development. 2D geophone array that could be deployed simultaneously in a 3D survey mode (from Tsoflias et al., 2006). At this stage the geophones were entirely decoupled from the planting device

A brief summary of the Autojuggie would state that it is an acquisition device consisting of a rigid steel platform used for positioning, planting, and transporting geophones and a hydraulically controlled mechanism for decoupling the geophones from the platform during seismic data recording. In its current configuration (Figure 36) the Autojuggie is approximately 11.5 meters long, 5.0 meters wide and has a mass of approximately 6,350 kilograms. It was designed so that it can be legally towed on public roads to a research location with a heavy duty truck. The side wings can be hydraulically raised and lowered; during transportation the wings are secured in an upright position. When in an upright position they reach a height of approximately 3.5 meters.

The Autojuggie is built in three sections which include the main body and two hydraulically retractable side wings. In all there are eleven receiver lines; five lines make up



Figure 36. The Autojuggie in its current stage of development. The side wings are in an upright position allowing it to be towed on residential streets

the main body and two wings each having three lines. These lines which act as receiver lines are 5.1 cm steel square tubing running the length of the frame. To hold geophones, 20 holes slightly larger in diameter than a geophone were drilled at 0.5 meter intervals along each line. In addition to the 0.5 meter geophone spacing along each line each receiver line is also separated by 0.5 meters. When the wings are lowered the receiver grid measures 9.5 x 5.0 meters giving the Autojuggie the capability of deploying 220 geophones at 0.5 x 0.5 meter spacing in both the in-line and cross-line directions in under a minute. To move the spread and

deploy the next receiver patch the Autojuggie can pick up all 220 geophones simultaneously in the same amount of time.

Along with a gasoline engine mounted to the frame to power the hydraulics there is a control unit located at the front of the Autojuggie that allows a single operator to plant and retrieve all geophones within the receiver array. The general operating procedure for planting geophones is as follows (Figure 37). From an upright position hydraulic cylinders lower the wings into place. The entire trailer body is then lowered by hydraulically retracting the wheels. The geophones are housed in the steel square tubing of each receiver line and a steel frame runs along the top of the geophones to hold them in place as they are planted by the weight of the trailer. Once the geophones are planted hydraulic cylinders push the two steel frames apart so that each geophone is free standing. To pick up the geophones, the sequence is simply reversed.

For the work described in this dissertation I adapted the Autojuggie to deploy geophones mounted on base plates. Aside from the details to follow, the operating procedure is the same as described above. When deploying geophones mounted to base plates the geophones are not held in position by the two rungs of the frame and the weight of the Autojuggie is not used to plant the geophone base plates. Instead, the hydraulics lower the bottom rung of the trailer which in turn lowers the nylon strapping used to connect the base plates to the Autojuggie. When the base plates have been deployed tension from the nylon strapping is removed and the base plates are free standing.



Figure 37. Planting spiked geophones: Before planting begins (left), geophones being planted using the weight of the Autojuggie (middle), separation of the bars leaving geophones free-standing (right) (from Sloan et al., 2009)

As discussed previously, a significant development in the design of the autojuggie was a mechanism that allows the geophones to automatically decouple from the rigid platform, thus eliminating the interference of complex seismic modes generated by the planting instrumentation (Tsoflias et al., 2006). As will be discussed later, the Autojuggie has been adapted to deploy geophones mounted to base plates. Figure 38 shows deployment of geophones mounted to base plates providing the option of performing 3D reflection surveys on pavement. The hydraulic separation of the upper and lower bar allows either geophone base plates, or spiked geophones to be planted and entirely decoupled from the frame of the Autojuggie. Automatically planted geophones were shown to be capable of recording the same quality of 3D seismic data as hand planted geophones (Sloan, 2009), with only a small fraction of the time and effort required to acquire conventional shallow 3D data.



Figure 38. Geophones mounted on base plates. The geophones have been deployed and are ready for data acquisition. While deployed the geophones are not in contact with the Autojuggie and tension has been removed from the nylon strapping.

Part of the labor and time saving benefits provided by the Autojuggie comes from not having to disconnect equipment such as the geophone cabling, batteries and seismographs when rolling the patch. Because the cables are secured to the Autojuggie and the remainder of the equipment is contained on a platform at the back of the Autojuggie (Figure 39) nothing has to be disconnected to roll. All of the equipment simply moves with the Autojuggie as it is moved to the next position. Because the receivers are at fixed locations within the Autojuggie there's the added benefit of relieving the field crew of having to measure geophone locations. This reduces considerable time from a survey while at the same time improving the accuracy of in-line and cross-line receiver positioning.



Figure 39. The seismic equipment and cabling remain connected to the Autojuggie when moving the receiver grid to the next position. The seismographs, networking cables and batteries are housed at the rear of the Autojuggie

3.3 Prior Autojuggie Research

3.3.1 Early Autojuggie Application (Case Study 1)

Throughout its evolution the Autojuggie has been used for research within the Lawrence, Kansas area. One of the earlier applications was documented by Tsoflias et al. (2006) and Czarnecki et al. (2006). In that study the Autojuggie was used to investigate a shallow water table and a paleo-channel. At that point of development (Figure 35) the Autojuggie consisted of a 2D array of seventy two geophones spaced 20.0 cm apart in both the in-line and cross-line directions. As can be seen in Figure 35 hydraulic cylinders were used to lower the bottom portion of the frame to decouple the geophones from the Autojuggie and a tractor used to position the array.

The array was able to be moved and repositioned in under three minutes time and the top of the saturated zone (Figure 40) successfully imaged. These early accomplishments showed that the Autojuggie could significantly reduce the amount of time and effort required for performing 3D near-surface imaging.

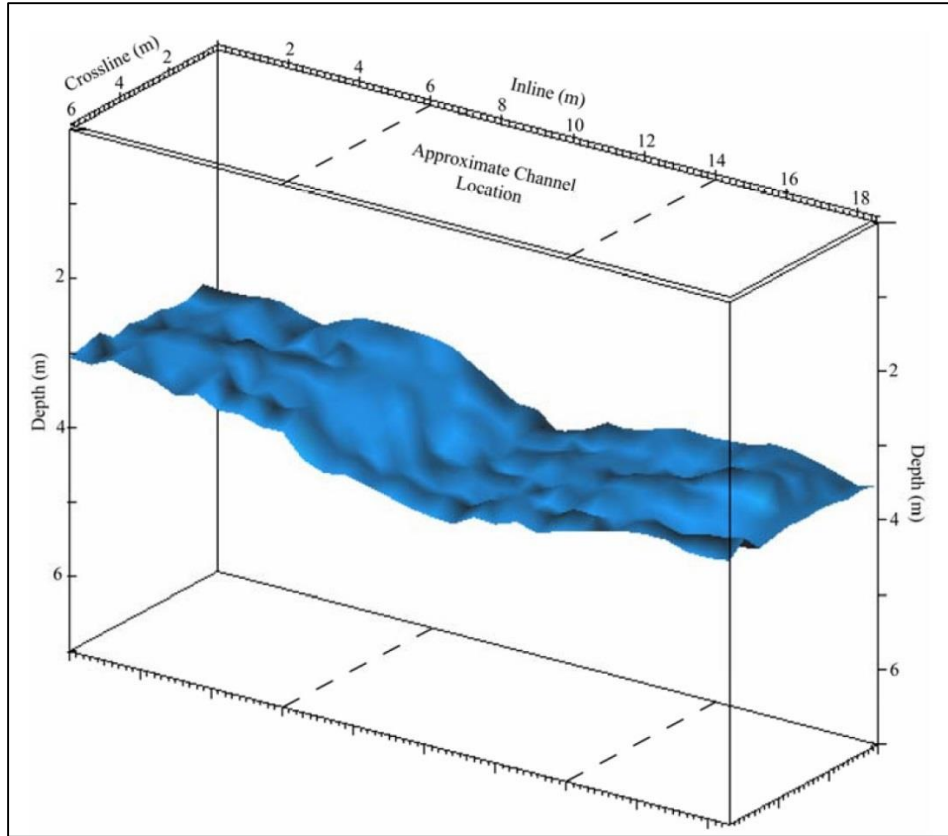


Figure 40. 3D image of the top of the water table from data acquired using a version of the Autojuggie during its developmental stage (from Czarnecki et al., 2006)

3.3.2 Recent Autojuggie Application (Case Study 2)

Sloan (2009) used the Autojuggie in its current state of development (Figure 36) to further investigate the earlier findings of Tsoflias et al. (2006) and Czarnecki et al. (2006). During the course of his research Sloan was able to image the top of the water table, consistent with earlier findings, two stratigraphic reflectors and bedrock (Figure 41).

This research marks an important step in near-surface 3D seismic reflection imaging. It showed that a robust, cost efficient acquisition device could be developed and used to quickly image the near-surface by acquiring high-resolution seismic reflection data. In comparison with a previously acquired 3D survey (Sloan et al., 2009) at the same test site, an

18% increase in square meters covered per hour, a 60–67% decrease in labor, and a 500% increase in fold was achieved (Sloan, 2009).

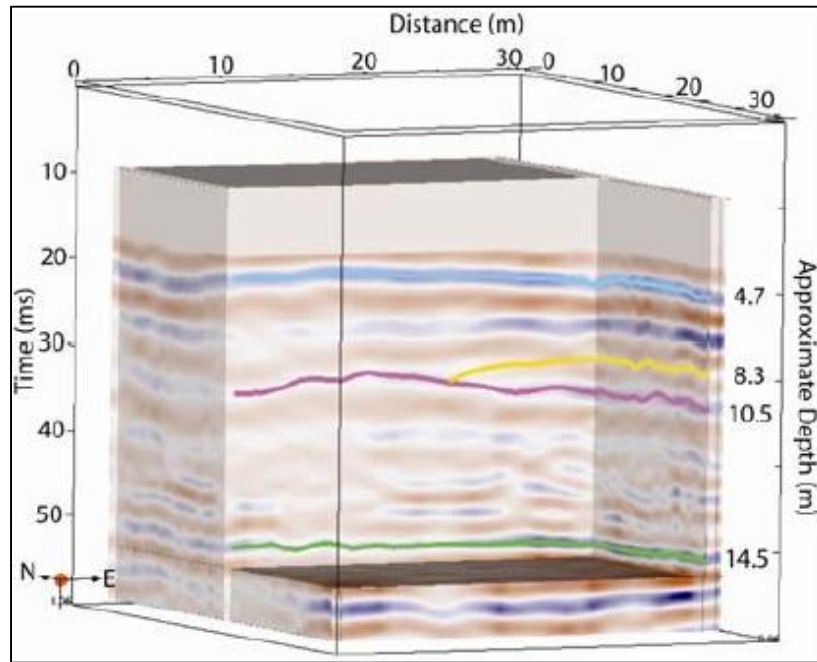


Figure 41. 3D diagram from data acquired using the Autojuggie in its current stage of development. Interpreted horizons: top of the saturated zone (blue), two stratigraphic boundaries (yellow and pink), and bedrock (green) (from Sloan et al., 2009)

3.3.3 Recent Autojuggie Application (Case Study 3)

Characterizations of near-surface material properties are of importance to transportation infrastructure projects and cost effective methods for bedrock and soil mapping are commonly the main objective (Sirles and Haramy, 2006). In an effort to address these considerations I fabricated geophone base plates that would allow the Autojuggie to deploy geophones on paved surfaces (Figure 42). Several plate sizes were tested and a plate size of 10.0 x 15.0 x 0.6 cm size proved to provide adequate signal while maintaining a reasonable size. In addition to developing a way to deploy geophones on blacktop three-

component tests were also conducted. To deploy the base plates the threaded rod supporting the Galperin geophone was placed through the hole on the lower frame of the Autojuggie. This allowed the plate to be raised using the lower frame of the Autojuggie, moved into position, and lowered into place.



Figure 42. Early base plate design (left) and seismic source (right). Early base plate designs used thin metal for the base with both vertical and Galperin geophones attached. A small sledge hammer is to strike the top of the metal rod

The seismic source was also a consideration (Figure 42). I tested several sources, all consisting of a sledge hammer and striking plate. Initial testing had the source operator standing upright swinging down on a plate set on the blacktop. When striking, the hammer was often at an angle with the plate driving it into the blacktop. Multiple strikes in this fashion started to damage the blacktop surface. One of the conditions of working at the site was that the blacktop could not be damaged. An alternative striking plate of heavy rubber was then tested. While this resulted in no damage to the blacktop it was difficult to inject sufficient seismic energy into the subsurface. It was also discovered during these tests that having the source operator bend over to pick up and move the plate each time was taxing.

While this would not be an issue for a survey with several hundred source positions when considering a survey with 1,000 or more source locations it was restrictive. To address these issues a free-fall sledge hammer source mounted to a Betsy Seisgun base (Figure 43) was constructed. While this source provided sufficient signal using a rubber striking plate it was difficult to move. A modified striking plate and small sledge hammer proved to be the most efficient source (Figure 42). The striking plate is constructed of a 20.0 x 15.0 x 2.0 cm iron base with a 90 cm length of 4.0 cm diameter iron rod welded to the plate. The modified striking plate provided excellent signal while decreasing the amount of time and energy required in moving the source to each station.



Figure 43. Free-fall seismic source. A heavy sledgehammer is connected at the end of a length of square iron which in turn is connected to the base of a Betsy Seisgun

Figure 44 shows a field record and Figure 45 a common mid-point stacked section from data I acquired using the geophone base plates. One item of note is that before surveying commenced modeling clay was adhered to the bottom of each base plate and the base plate then firmly seated to the blacktop. This was necessary as the base plates were

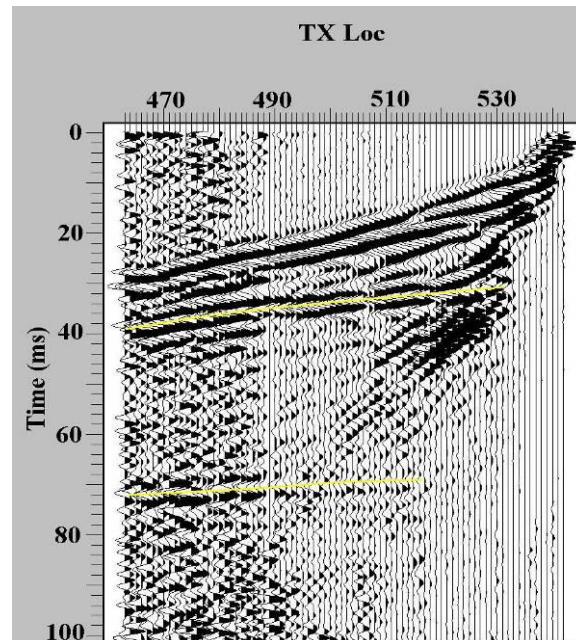


Figure 44. Field file from a 2D survey conducted using geophones mounted to base plates. A 125 ms AGC window, 350-450 Hz Butterworth filter and 2dB pre-rasterization gain have been applied

made of thin metal and had poor coupling. The survey site is located in the park-and-ride lot on the west campus of The University of Kansas. For recording a networked series of geodes were used with a record length of 250ms and a sampling interval of 0.125ms. Because of reduced signal at far offsets a vertical stack of three was employed at each source station. The receiver and source intervals were both 0.5 meters and acquisition was completed in one day. Processing consisted geometry assignment, muting, velocity analysis, normal moveout

and CMP stacking. Velocity analysis shows the velocity of the 32ms reflector is 1700m/s and 1900m/s for the 70ms reflector. Inspection of the stacked section reveals continuous, relatively flat reflectors at 35 ms and 70 ms. A well log record from the Kansas Geological Survey (Appendix E) was used to correlate the CMP stacked section with known subsurface lithology. Depth calculations from the seismic data were then compared to the well log record. The reflectors are in agreement with the well log data and record the cyclic nature of the Pennsylvanian age cyclothems characteristic of eastern Kansas (Knapp, 1988; Knapp and Watney, 1987).

The results of this study show the Autojuggie can be successfully adapted for performing high-resolution 2D seismic reflection surveys over paved surfaces in support of transportation related projects. It also proved to be a quick method for determining two of the top three most common geophysical applications in transportation projects; bedrock and soil mapping.

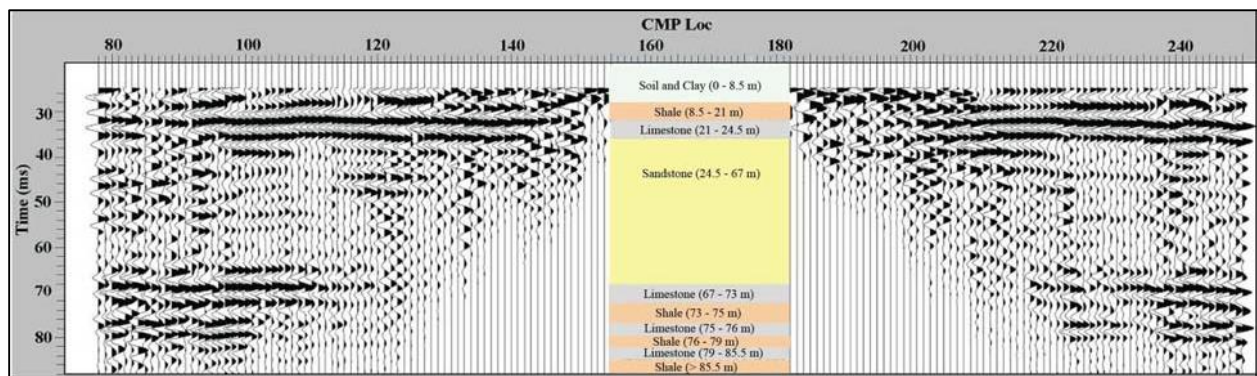


Figure 45. Interpreted stacked section correlated to well log records from a 2D survey conducted using geophones mounted to base plates. A 125 ms AGC window, 350-450 Hz Butterworth filter and 2dB pre-rasterization gain have been applied

3.4 Summary

The Autojuggie started from the idea of determining if good quality seismic data could be acquired from geophones rigidly mounted to a board. These initial tests proved successful and started the development of the Autojuggie which has been ongoing for more than 10 years. During this time several interesting research projects have looked at the effects of rigidly mounting geophones to material and the effect of the material on the seismic response. Results of these projects have been taken into consideration throughout development and have led to the Autojuggie in its current state. Over the last several years the Autojuggie has been successfully applied to research projects within the Lawrence, Kansas area. Results of these investigations show that the Autojuggie meets the objective for which it was originally designed; to significantly reduce the time and effort involved in acquiring high-resolution, near-surface seismic data.

Chapter 4: Development of Near-Surface Acquisition Designs

4.1 Introduction

The results of previous 3D near-surface seismic reflection surveys acquired using the Autojuggie (Sloan, 2009; Miller, 2009) have shown that it can acquire good quality data with significant savings in both time and effort. With the efficiency of acquisition having been demonstrated, efforts were made to look into ways to further increase efficiency. One option is a larger version of the current Autojuggie. The wings could be expanded so that each was wider and/or the Autojuggie could be made several meters longer. Both of these options are feasible and could potentially add several dozen more geophones for deployment. However, there are difficulties that arise with this approach. The Autojuggie is already a large piece of equipment and increasing its size would make towing it more difficult. The possibility exists of transporting it via a flatbed trailer however this would result in increased costs.

While these options are available acquisition designs appear to offer the most effective method to further increase efficiency. With this in mind designs were explored to try and find one that can decrease acquisition time, particularly by reducing the number of source positions. As presented in the Land 3D Survey Geometries section of Chapter 2 the standard 3D design is the orthogonal. The orthogonal layout is attractive because of its symmetry and ease of implementation. However, for near-surface surveys the dense number of source positions required for continuous coverage can exceed 1,000 source locations requiring several days of acquisition. To properly image a complex subsurface it may be necessary to have a large number of source positions. However, in areas of relatively simple geology the number of source points may be reduced drastically while still adequately imaging subsurface reflectors.

Prior 3D surveys acquired with the Autojuggie used an orthogonal acquisition design. While the Autojuggie proved to be a valuable tool for efficiently moving and deploying large numbers of geophones, the number of times the receiver patch moved was limited to a small number for an entire survey. After some analysis it was determined that a more efficient way to acquire 3D data would be to model the Autojuggie after a towed marine streamer. In looking at the Autojuggie it is not difficult to envision the seismic research truck as a marine vessel pulling a series of marine streamer hydrophones (Figure 46).



Figure 46. The Autojuggie deployed for marine streamer type acquisition

While part of the efficiency of the Autojuggie is being able to deploy large numbers of geophones simultaneously the other part is being able to move the receiver array quickly. The previous orthogonal designs were based upon a few receiver grid positions with a large number of source points. The marine streamer concept approaches design from the opposite direction by having the receiver patch roll many times, with a limited number of source

points. With these criteria in mind I developed a survey based upon this concept to take advantage of the speed and ease which the geophones can be moved.

There were several objectives for this study. First was to develop a method that would allow the Autojuggie to deploy geophones on pavement systems. The ability to deploy geophones on hard surfaces allows for the opportunity to conduct seismic surveys where they may not otherwise be performed such as residential roads, highways and runways. Secondly, the newly developed geophone base plates and the Autojuggie would be used to image reflectors underlying the west campus of The University of Kansas.

4.2 Base Plate Development

Geophone base plates for deploying geophones on paved surfaces are commercially available. However, because of their design it would have been difficult to develop a way to connect these base plates to the frame of the Autojuggie for deployment. As an alternative I decided to purchase materials and construct the base plates myself. Several different sizes and thicknesses were tested before deciding on a 4x6x $\frac{3}{4}$ inch metal plate as the base. To allow a geophone to be mounted on the plate a hexagonal nut was welded to the top of the plate and a geophone is then simply screwed into the nut. Initial testing showed that the unevenness of a parking lot surface, along with debris such as small rocks, resulted in the base plates not lying flat. Much of the surface area of the bottom of the plate was not in contact with the parking lot resulting in poor coupling. This is equivalent to a bad plant when using traditional geophone spikes. To correct for this three, $\frac{3}{4}$ " long bolts were welded to the bottom of each plate. The bolts act as legs for each base plate allowing even contact with the parking lot surface even when there are slight surface irregularities and debris.

To deploy the base plates a method had to be developed that would allow the plates to attach to the lower frame of the Autojuggie so they could be raised and lowered hydraulically. I tested several methods before deciding upon nylon strapping that runs the length of each receiver line. To connect the nylon strapping with the base plates and Autojuggie, brass grommets were secured in holes punched within the strapping. To connect a base plate to the strapping a bolt was placed through a grommet and then screwed into a nut that was welded to the top of each base plate. The strapping was then attached to the lower frame of the Autojuggie by placing a bolt through a receiver hole that would otherwise house a regular spiked geophone when the Autojuggie is used to perform surveys on soil (Figure 47). Note that in Figure 47 there are two geophones mounted on a single base plate. This image is from a previous test wherein two geophones (28Hz and 100Hz) were mounted on each plate. This idea was later abandoned and only single 28Hz geophones mounted to each plate were used for this study. When the base plates are fully deployed the tension within the nylon strapping is released and the base plates are free standing. This removes the possibility of unwanted noise travelling through the strapping from vibrations within the frame of the Autojuggie. The cost of the material for the base plates, nylon strapping and various nuts and bolts was approximately \$2,000.00. Fabrication and construction was completed at the University of Kansas geophysics workshop so aside from my own time there was no cost for labor.

One of the primary benefits of using nylon strapping is that all of the geophones were attached to the Autojuggie before going to the field site. The receiver takeouts were also secured to the Autojuggie and the geophones connected to the takeouts (Figure 48). Equipping all of the cabling before leaving the geophysics shop saved considerable time and

once at the field site the only items that had to be hooked up were the seismographs, network cables and batteries, which could be completed within an hour. Additionally the same held true at the end of the day. To breakdown only the seismographs, network cables and batteries



Figure 47. Geophone base plates and nylon strapping. The nylon strapping is secured to the Autojuggie using holes within the lower rung which house spiked geophones when performing surveys on soil

had to be disconnected. The Autojuggie, along with the geophones and receiver takeouts were then towed back to the geophysics shop. Because the survey presented here only required the Autojuggie to be towed several miles lower speeds could be maintained and spotters used to make sure none of the cabling came loose and that none of the geophones were dragging. Prior surveys wherein all of the setup was undertaken at a field site required approximately four hours with a crew of five. For longer distances alternatives are available for having the cabling and geophones in place during travel. One possibility is to use industrial plastic wrap and run it underneath the geophones and across the top of the lower

frame to which the nylon strapping is connected. Once at the survey site all that would need to be done is to cut the plastic away and connect the seismographs and batteries.



Figure 48. The Autojuggie as it was transported to the field site. Once at the field site only the seismographs, network cables and batteries need to be connected

4.3 Survey Design and Acquisition

The survey location is a blacktopped parking lot located on the west campus of The University of Kansas that is used for the university's park-and-ride operations (Figure 49). Near-surface material is characterized as a Wabash Series silty clay loam (Dickey et al., 1977) while bedrock consists of alternating layers of shale and limestone that individually range from one to several meters in thickness. These layers are characteristic of the cyclic nature of the Pennsylvanian age cyclothem of eastern Kansas (Knapp, 1988, Knapp and Watney 1987) and well log records from the Kansas Geological Survey indicate a thick sandstone from approximately 24 to 67 meters depth.

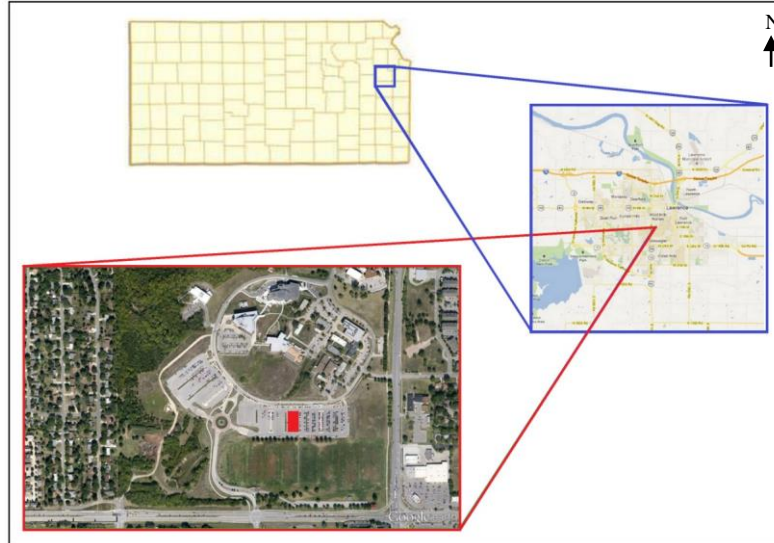


Figure 49. The University of Kansas west campus Park-and-Ride parking lot. The site is located on university property within Lawrence, KS and the survey location is marked in red

To have the widest patch possible all eleven receiver rows of the Autojuggie were used and the design results in an in-line area of full fold of 10.0 meters and a cross-line area of full fold of 6.5 meters (Figure 50), acquisition specifics are provided later in this section. This survey was a proof of concept to show how the Autojuggie could be used to quickly perform a 3D survey covering a substantial amount of area. In practice, future work using this design could simply continue to roll in-line to cover more area vertically. Additionally, rolling the receiver patch a full spread length in the cross-line direction has the effect of building up an area of continuous full fold laterally since the fold map will be a carbon copy when rolled cross-line.

One of the most important criteria in designing a survey of this type is that the shot points must occupy very specific locations (Figure 50, Figure 54). Source positioning is important because the edge locations of fold that are being built upon are dictated by the source location. To maintain a continuous area of full fold coverage the source locations

must be precise and consistent. Imprecise source locations will lead to fold stripping and/or fold gaps. While it is not difficult to accurately mark source locations extra time and consideration needs to be taken.

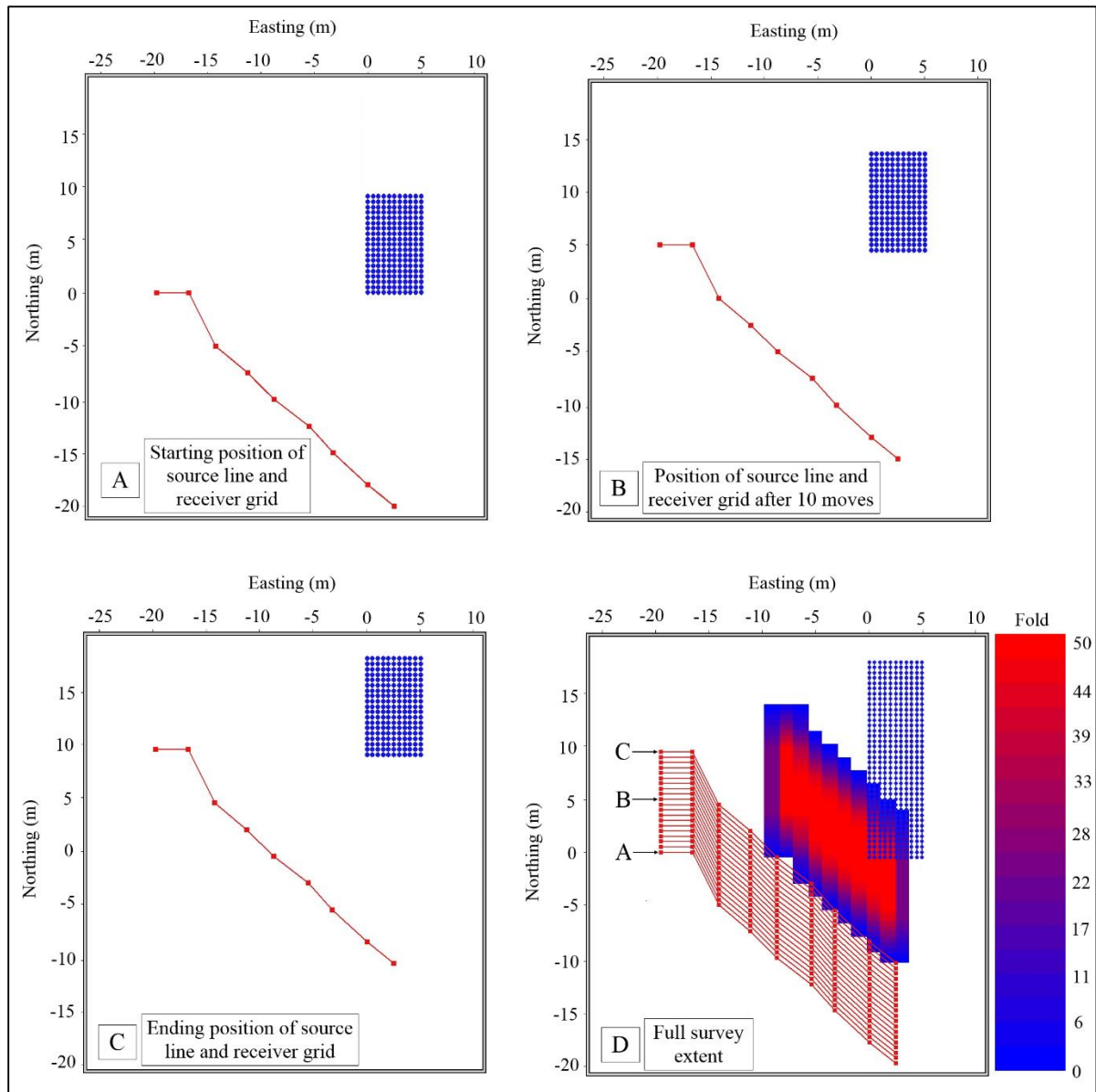


Figure 50. Roll parameters and fold map for the marine streamer acquisition survey design. The receiver grid and source lines occupied a total of twenty positions (D). Several of these positions (A-C) are shown to illustrate how the survey progressed. The source positions are represented in red and receiver positions in blue. Moving the receiver grid results in geophone positions being occupied multiple times

Another important item, as in all survey designs, is the depth of the reflector of interest. In the case of this survey a known reflector at approximately twenty-four meters depth was the target. Based upon the target depth the survey was designed with a range of offsets from approximately fifteen to twenty-five meters (Figure 51). Figure 51 illustrates the narrow range of offsets with the trace count for offsets outside of 15.0-25.0 meters falling off quickly.

As with offset, azimuth is a consideration for 3D surveys. While the local geology is not complicated, an azimuth distribution that may be suitable for a more complicated subsurface was implemented in the design of this survey. To capture a wide range of

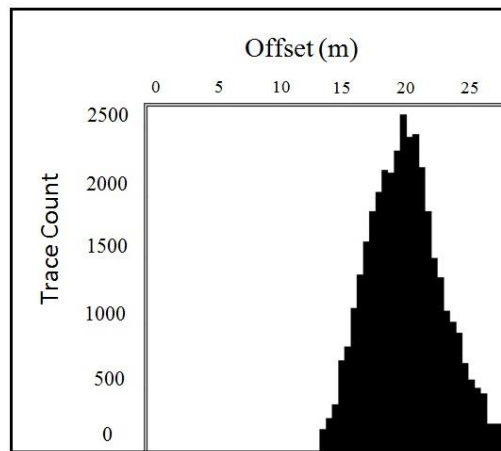


Figure 51. Trace count vs. offset range for the survey. There is a narrow range of offsets with trace counts for offsets outside of 15.0-25.0 meters falling off quickly

azimuth the shots were moved along a path of forty-five degrees from zero degrees in-line to ninety degrees cross-line, perpendicular to back of the receiver patch. The resulting coverage was ninety degrees of azimuth. There were nine source locations per patch and Figure 52 (A-I) illustrates how bin fold is distributed for each shot. The final image (Figure 52, J) shows

the complete bin fold for the entire survey. For small uncomplicated areas it may be safe to extrapolate the results from the collected angle of azimuth to 180, if not 360 degrees.

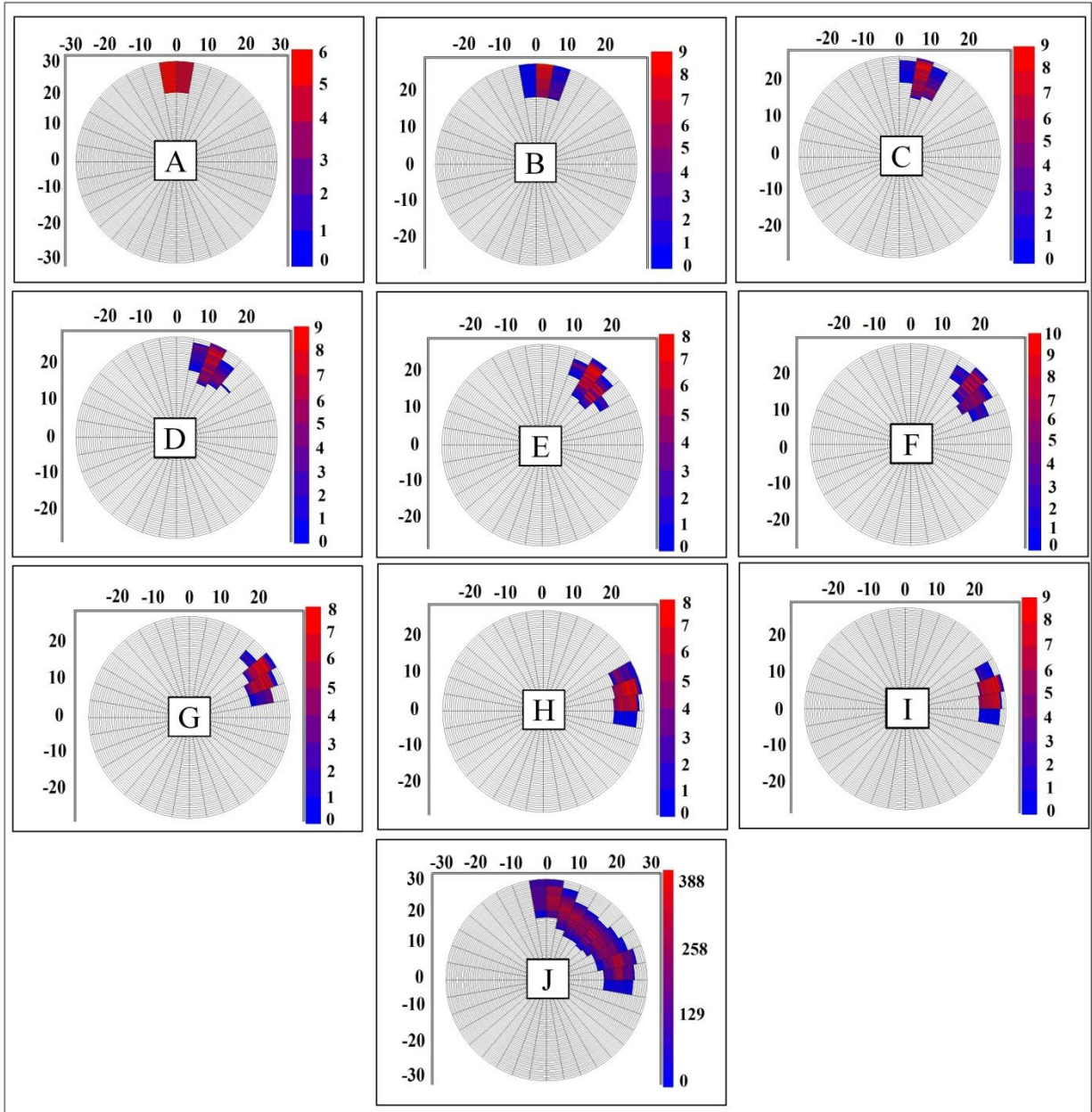


Figure 52. Azimuth coverage for each shot within a patch (A-I) and total survey azimuth coverage (J). To capture a range of azimuth shots were moved along a path of forty-five degrees with a resulting coverage of ninety degrees of azimuth

For recording eleven 24-channel Geometrics Geode seismographs with 24-bit A/D conversion and Mark Products 28 Hz vertical component geophones were used. Recording time was 1.0 second with a sampling interval of 0.125 ms. Lower frequency geophones and a long recording time were used because this survey, as will be discussed in a subsequent chapter, was designed to acquire data for both reflection and surface wave analysis. Prior work at this site showed that the 28 Hz geophones were adequate to image the target reflectors. Base plates were used to deploy geophones and a small sledge hammer and metal striking plate were used as the source. Because of the longer offsets a vertical stack of three at each source location was necessary.

Close inspection of Figure 46 and Figure 48 shows wood blocks that were placed at the corners and within the frame of the Autojuggie. These blocks were used to ensure that none of the geophones would be damaged by the lower rung of the Autojuggie when deployed. The wood blocks were taller than the combined geophone and base plate so that once the base plates were fully deployed any further downward movement of the hydraulic lower frame would be stopped by the wood blocks before crushing any geophones. Figure 53 shows the recording equipment housed within the framework of the Autojuggie. Containing the recording equipment within the interior of the Autojuggie allowed them to stay connected during each roll and saved a significant amount of time during surveying.



Figure 53. Deploying geophone base plates (left), note the seismographs, cables and batteries on the far left of the image. Close-up view of the recording equipment contained within the Autojuggie during survey (right)

The patch consisted of eleven source positions and eleven receiver lines each with nineteen geophones per line. The receiver interval and receiver line interval were both 0.5 meters and the patch was rolled nineteen times at a distance of 0.5 meters for each in-line roll. No cross-line rolls were performed. Although there were eleven source points per patch two of those eleven shot positions were used for surface wave work. They were removed during processing and are not included in the reflection data presented here. The source line interval was 0.5 meters however, because the way the source points are distributed there is no source interval as it is traditionally defined. Placing the source points in an Cartesian coordinate system, with the geophone located at the back left rail (driver's side of the seismic truck) of the receiver grid as position (0,0) the source points are given in Figure 54.

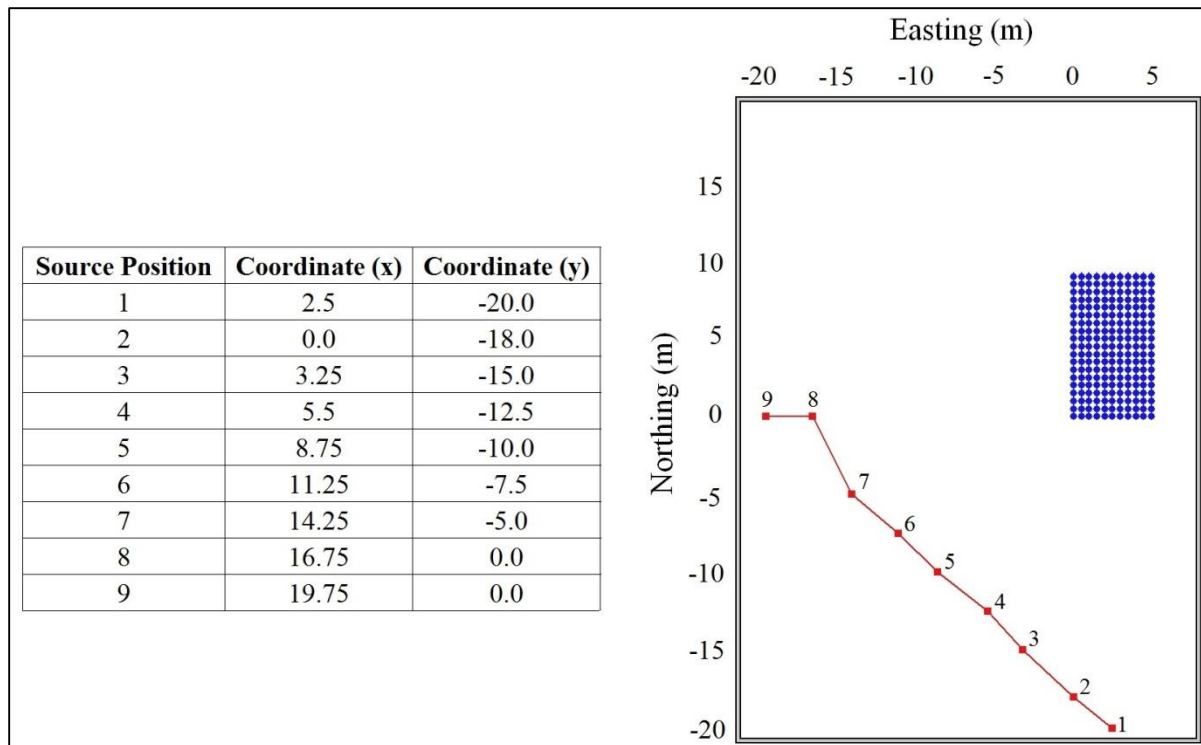


Figure 54. Source positions for each patch. To locate source positions each shot was placed within a Cartesian coordinate system for the source operator to follow

Throughout the survey the seismic research truck remained connected to the Autojuggie. This saved considerable time during receiver patch rolls. Previous experience, wherein the truck had to be moved because it interfered with source positions, has shown it can take upwards of twenty minutes to connect the geophysics truck, move the patch and then disconnect the truck and move it away from the survey area. The time to perform this task would likely diminish after it was done several times but because the truck doesn't interfere with any source locations it was decided that it was not necessary to disconnect it from the Autojuggie while surveying.

As discussed previously, the order and positioning of the shot points took some consideration beforehand and requires field hands to be alert when marking source locations.

Because each source point needs to be precisely located a method using a rope with position markers was used that allowed the source operators to progress along a diagonal. While it was a simple enough method for the operators to follow they had to receive special instruction on its use and had to stay alert to be sure they were progressing as designed.

The survey was conducted in the course of one day starting at approximately 7:00 a.m. and finishing around 6:00 p.m. Aside from three receiver lines, the geophones and receiver takeout lines had been attached to the Autojuggie prior to going to the field. Once we arrived at the field site all we needed to connect were the geophones for three receiver lines along with the seismographs, network cables and batteries. The three rows of geophones could have been connected beforehand, however because of timing issues it had to wait until we were at the field site. There was a field crew of four and not including the time for setup and tear down approximately six hours were spent surveying. Shooting each patch took less than twenty minutes and lifting the geophones, repositioning the Autojuggie and re-deploying the geophones could be completed in less than three minutes.

4.4 Data Processing and Interpretation

4.4.1 Initial Data Processing

Data were processed using the Parallel Geoscience Seismic Processing Workshop (SPW) software and processing consisted of: geometry assignment, binning (0.25 x 0.25 m) trace editing, early mute, ground roll mute, air wave mute, velocity analysis, CMP stacking, frequency filtering and 3D post-stack Kirchhoff migration. A 125–250 Hz Butterworth filter with 18 dB/octave rolloff slopes and a 60ms AGC window were applied to the stacked volume. Geometry definition consists of assigning the source and receiver locations into an

x, y coordinate system through the use of processing cards. This allows the processing software to sort and assign each trace to its respective common-midpoint (CMP) location. Bad channels were then removed from the data set. Next the data were binned using a rectangular bin size of 0.25 x 0.25 m. The bin size represents the area over which all traces that share a CMP location within that bin will be summed together and stacked.

Muting was applied to remove direct waves, refracted waves, air wave and ground roll. These seismic events are muted to avoid contaminating the final stacked volume with waveforms other than reflected signal. Normal moveout (NMO) velocity corrections of ~1700 m/s were determined using constant velocity stacks. To account for lateral velocity variations an iterative velocity analysis with velocity picks made in-line and cross-line and a velocity smoothing function applied before stacking. Lastly the data were migrated using a post-stack Kirchhoff time migration.

Because of the lack of very near offsets ground roll was not a concern and a combination of muting and frequency filtering were sufficient to reduce ground roll. Figure 55 illustrates a representative field record and a frequency-amplitude spectra is provided (Figure 56) for both an unfiltered and filtered shot record. A 2D line from the 3D volume is shown in Figure 57.

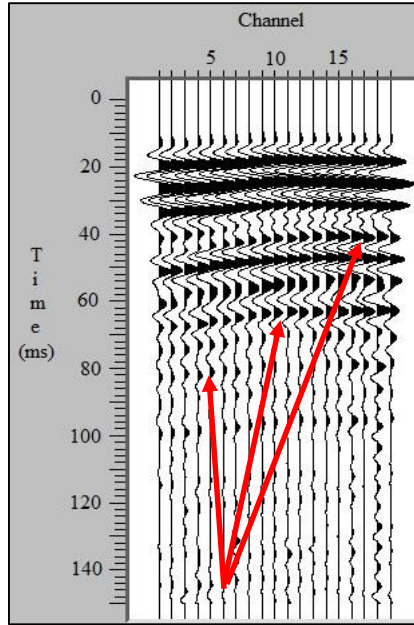


Figure 55. Field record filtered with a 125-350Hz Butterworth filter, 18db/octave rolloff slopes and a 125ms AGC window applied. The arrows indicate several reflectors

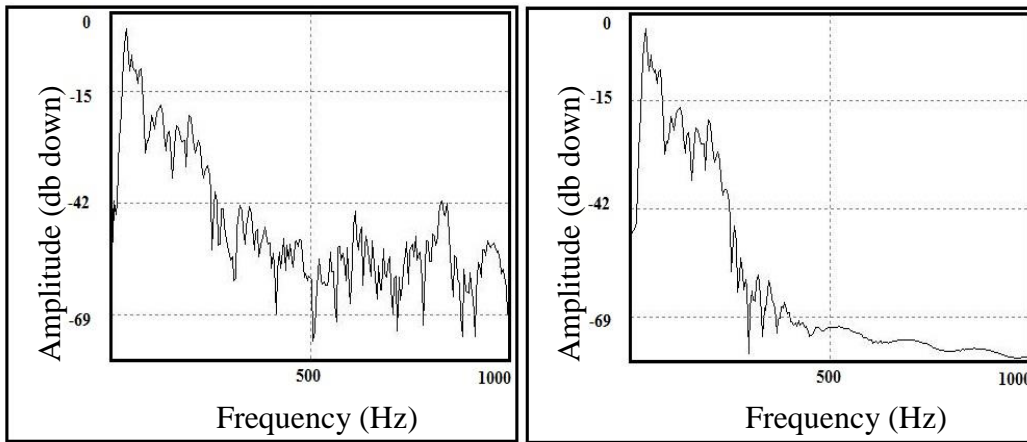


Figure 56. Frequency-amplitude spectra for a raw shot gather (left) and the same gather after applying a 60–350 Hz Butterworth filter (right)

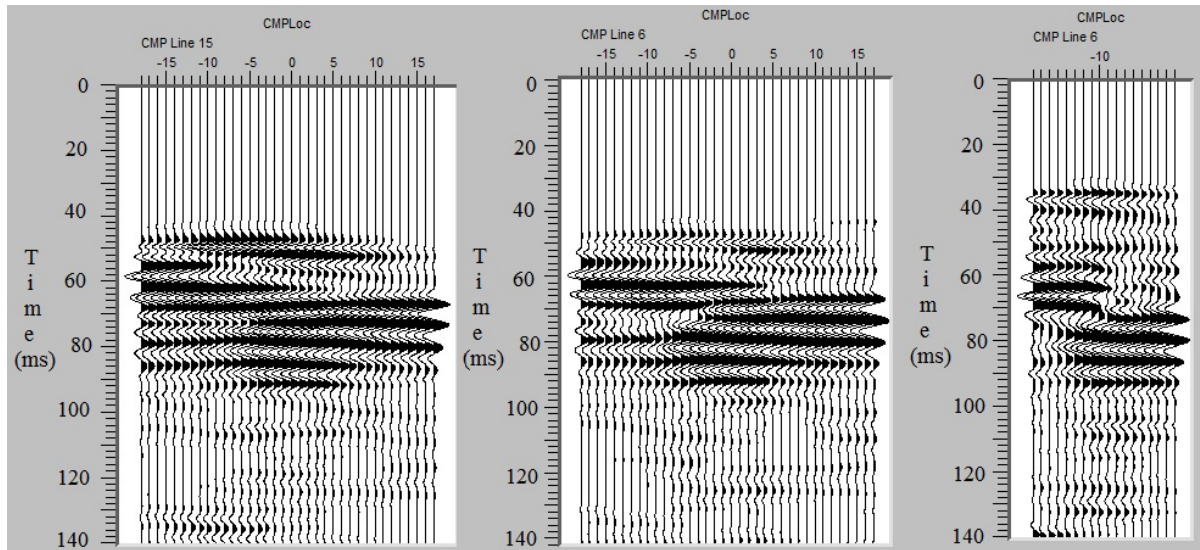


Figure 57. Stack comparison from 2D lines extracted from the 3D volume. Data from the streamer survey (left), single-offset (middle) and common-offset (right)

4.4.2 Secondary Data Processing

4.4.2.1 Single Offset

To explore the robustness of the modified marine streamer design two additional, secondary processing's of the data were undertaken. For the first test the only source point that was included was the one located directly behind the receiver array at an offset of 20.0 meters (Figure 58). The other processing steps and roll parameters remained as described previously. Because of the limited number of source positions and rolls fold is expectedly low. However, for 3D surveys the general guideline when high frequencies are expected is that fold should approximate the fold of a 2D survey. If the patch shown here continued to roll fold would grow and quickly reach that of 2D fold.

A 2D line from the 3D volume of the single offset processing is shown in Figure 57. The properties of the reflectors and geologic features that were seen in the previous two examples are also evident. The drawback to this design is that because of its single offset

azimuth is restricted to the ranges of 0-10 and 170-180 degrees. This being the case there are many applications for this design and it would be ideal for simple subsurface mapping.

4.4.2.2 Common-Offset

An additional processing test was to simulate a common offset seismic survey design in which only a single source position is used to image the subsurface. The intent is to roll the receiver grid an entire grid-length each time the patch is rolled. This results in single fold coverage, thus no common mid-points are recorded with multiple source locations. The benefit of this design is that it further reduces source positions and greatly increases the speed at which a survey can be performed. Because of the limited number of roll positions five source points, directly behind the Autojuggie at 20 meter offsets, were used for this simulation. The processing steps described previously were applied however because of the

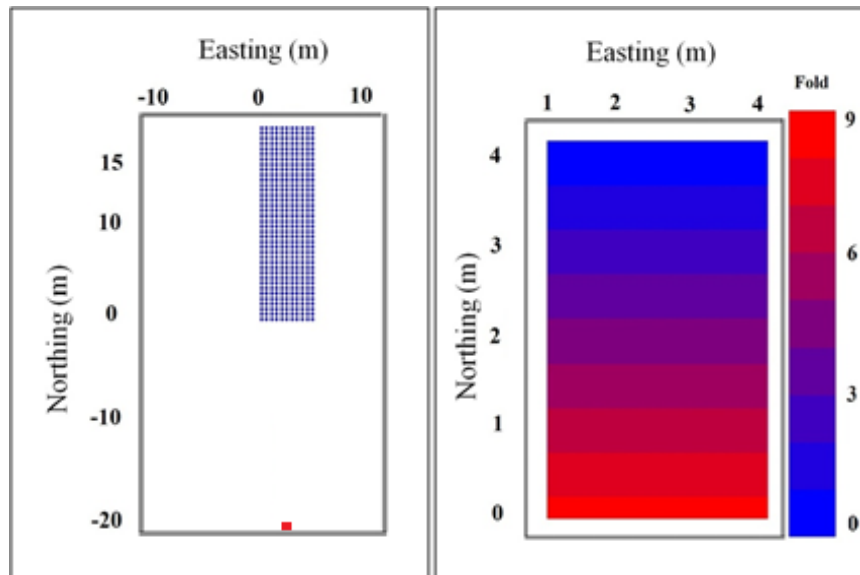


Figure 58. Geometry (left) and fold map (right) for the single offset marine streamer design. A source point located 20.0m behind the receiver array and a 0.5m roll interval were used

low number of shots processing was minimal and can be performed in a manner of a few minutes. Inspection of a 2D line from the 3D volume (Figure 57) shows several of the subsurface reflectors. There is agreement with the data shown previously illustrating that simple; near-surface layers can be mapped using this method. A 3D chair diagram of each of the surveys is shown in Figure 59.

The secondary data processing examples illustrate that for simple subsurface mapping the Autojuggie can be used to quickly and efficiently achieve this objective. This is a particularly effective method for applying the Autojuggie to transportation projects over roadways. The width and mobility of the Autojuggie is well suited for this type of work and a crew of three people consisting of a driver, source operator and recording operator could cover a substantial amount of ground in a single day. The receiver grid can be lifted and repositioned in under three minutes and the source shot only takes a few seconds to record.

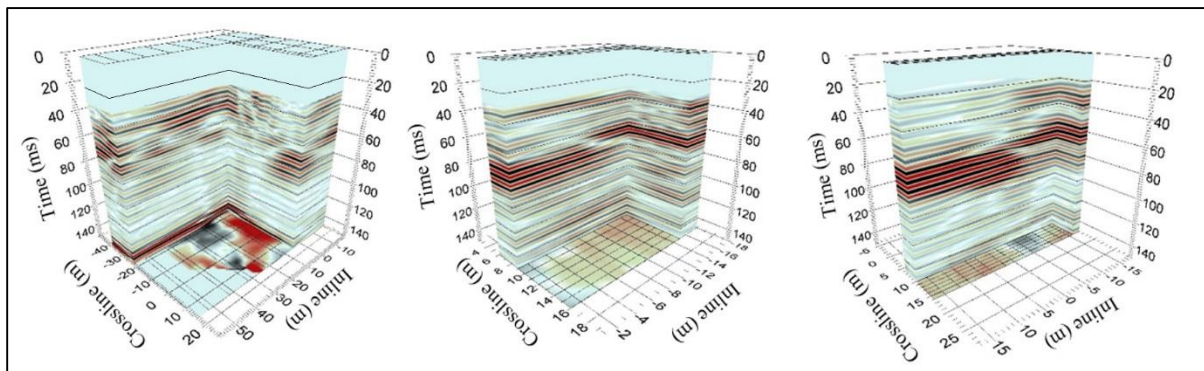


Figure 59. 3D Chair diagram stack comparison. Data from the streamer survey (left), single-offset (middle) and common-offset (right)

Using the 0.5m roll-parameters, 20 shots and 20 moves of the Autojuggie could be performed per hour covering approximately 15 meters of ground. Given an eight hour workday approximately 120 meters would have been traversed providing a three-dimensional image of the subsurface.

In comparison, using the common-offset technique wherein the receiver patch is rolled the full length of the Autojuggie, a substantial amount of area could be covered. The time to reposition the receiver grid wouldn't take any significant additional amount of time since the grid is simply being moved forward several additional meters. With this, 20 shots and 20 moves of the Autojuggie could be performed each hour. This allows for a traverse of 190 meters per hour or a total traverse of 1,520 meters per workday.

Near real-time data analysis could be implemented using simple processing routines. Processing could be performed after a pre-determined number of shots allowing initial data inspection to be performed in the field.

4.5 Base Plate Pitfalls

An orthogonal survey was designed and acquired using the Autojuggie equipped with base plates. Because many of the source positions were located near, or within the interior, of the Autojuggie much of the data is dominated by ground roll. This is a result of geophone coupling that is not as firm as traditionally planted geophones along with using a surface impact source of a hammer and striking plate. Although the orthogonal survey was not successful the details of the design and acquisition will be presented.

I designed a survey to target reflectors ranging from 21 to approximately 67 meters depth. To record the necessary offsets to image each of the reflectors the design consisted of a patch containing 10 receiver lines with 24 receivers each and 12 source lines with 12 source positions each (Figure 60). The largest minimum offset recorded (X_{min}) and the largest offset recorded (X_{max}) were 4.0 m and 32.0 m respectively. While a slightly larger X_{max} would have been preferable to record additional traces representing the reflector at 70 ms it would

have required two additional source lines to be added. Prior surveying at this location however has shown that a far offset of 32 meters is sufficient for the deepest reflector of interest so the additional source lines were not added to avoid increasing acquisition time. The receiver line and source line interval were 0.5 m and 4.0 m respectively with a receiver interval of 0.5 m and a source interval of 2.5 m. To build up fold and to cover a larger areal extent the patch was rolled three times in the in-line direction and once in the cross-line direction. Each roll was half a spread length, 12 receiver stations for each vertical move and five receiver lines for each cross-line move.

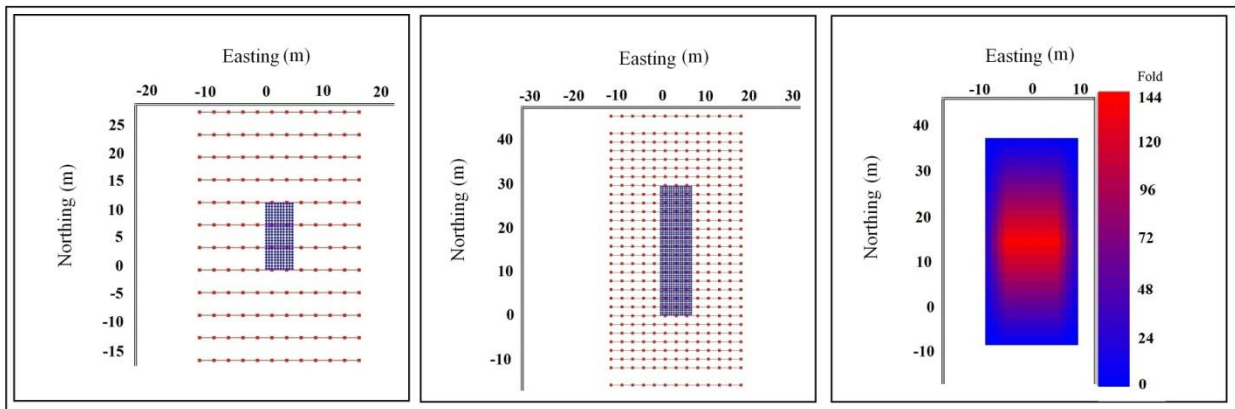


Figure 60. Patch (left), complete survey geometry (middle) and fold (right). The receiver grid (blue) contains 10 receiver lines with 24 receivers for each line. For each patch 12 source lines with 12 source positions (red) for each source line were used

When designing a 3D survey trace count vs. offset and trace count vs. azimuth must be considered (Figure 61). Trace count is an important criterion in determining if the subsurface and required offsets are being sufficiently sampled. The aspect ratio of the survey must also be taken into account. Three-dimensional seismic surveys are defined as either narrow or wide azimuth with the distinction being made based upon the aspect ratio of the

patches. The aspect ratio of a patch is determined by the ratio of the width of the patch to its length. Patches with an aspect ratio of less than 0.5 are considered narrow azimuth while patches with ratios of 0.5 and greater are considered wide azimuth. Based upon the design, this survey is wide azimuth with an aspect ratio of 0.625. While both narrow and wide azimuth designs have their benefits, wide azimuths have a more uniform distribution of offsets and azimuths which may be more appropriate for near-surface 3D surveys.

Inspection of the offset plot (Figure 61) shows that the majority of the traces fall between an offset range of 5.0-25.0 m with approximately 1,500 traces recording offset from 2.5-5.0 m and 25.0-27.0 m. The azimuth plot (Figure 61) shows a concentration of traces in

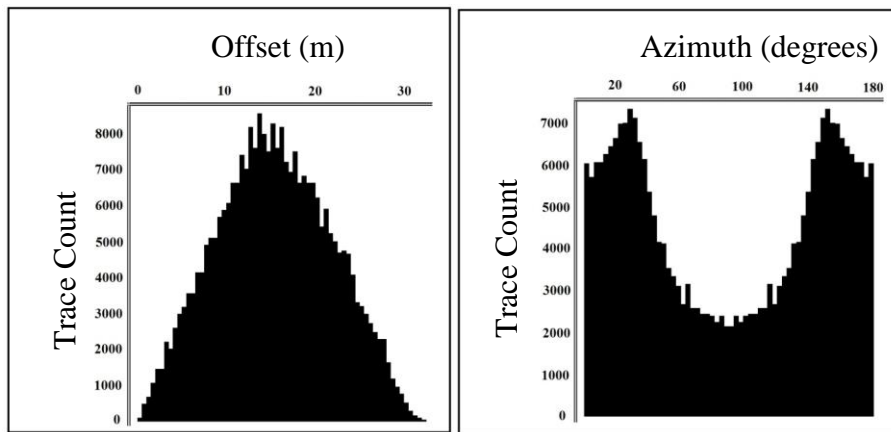


Figure 61. Trace count vs. offset (left) and trace count vs. azimuth (right). The majority of the traces fall between an offset range of 5.0-25.0 m with a concentration of traces within the 0-40 and 140-180 degree range

the 0-40 and 140-180 degree range. This is an effect of the elongated rectangular shape of the receiver grid with a higher percentage of source positions on the north and south sides of the receiver patch. Figure 62 is an offset-redundancy plot that displays the range of offsets sampled within each bin. Bins are represented by a vertical line divided into colored blocks,

where each block represents 0.25 m of offset. The color of the block indicates the number of times a particular offset was sampled.

For recording, ten 24-channel Geometrics Geode seismographs with 24-bit A/D conversion and Mark Products 100-Hz vertical component geophones were used. Recording time was 0.5 seconds with a sampling interval of 0.125 ms. Using 10 geodes was convenient because it allowed one geode to be assigned to each receiver line. This simplifies both cabling and processing by eliminating the need to cross takeouts between receiver lines. Originally ten rows of eighteen geophones per receiver line were to be used. This would have left six open channels at the end of each receiver line. There was enough nylon strapping and base plate material remaining from the construction of the main receiver lines to extend them beyond the back of the Autojuggie and use all 24 channels of each geode. Taking the

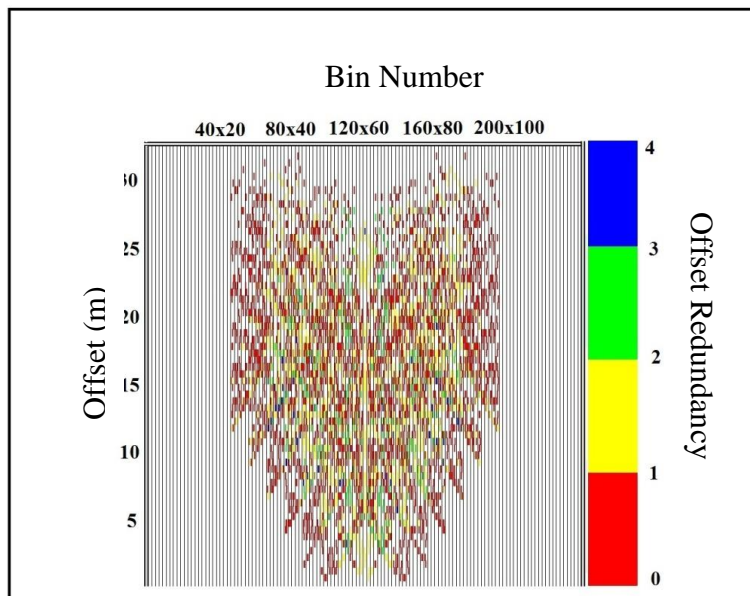


Figure 62. Bin offset redundancy plot. Bins are divided into colored blocks with the color indicating the number of times a particular offset was sampled

additional time to make the extenders was preferable than simply leaving the channels open. These extensions didn't add any significant additional setup time and when the patch rolled they were simply draped over the back of the frame of the Autojuggie to avoid dragging and potentially damaging the cables.

Because the survey took place on a blacktop surface the seismic source was a consideration. A modified striking plate and small sledge hammer proved to be the most efficient source. The striking plate consists of a 20.0 x 15.0 x 2.0 cm iron base with a 90 cm length of 4.0 cm diameter iron rod welded to the plate. The modified striking plate provided excellent signal while decreasing the amount of time required in moving the source to each station. The modified source also allowed for more consistent strikes from station-to-station. Using such a source on blacktop has the added benefit that there is no source position degradation when occupying the same source locations for different patch rolls. Re-occupying source locations is an outcome of the orthogonal design in which a given source position may be used several times throughout a survey. Reduced source signal at far offsets required a vertical stack of three to be employed at each source station. Vertical stack tests had shown that a single blow would be sufficient for near source-to-receiver offsets, however to image the deeper reflections longer source-to-receiver offsets were required.

Acquisition took place over four days from August 16-19, 2011 with significant delays during the first two days due to rain. The survey encompassed eight patches with 144 shots per patch with the total shots numbering 1,152. As discussed previously, all of the geophones and cabling were rigged to the Autojuggie at the geophysics shop before moving to the survey location. Once at the field site the Autojuggie was moved into position, the seismographs, network cables and batteries connected, base plates deployed and several test

shots taken. Generally several geophones within the patch would need to be adjusted because a base plate was tilted or a geophone was bad. The field crew met at the geophysics workshop at 8:00 am each day and accounting for transit, setup time, test shots and geophone adjustment we were ready to start surveying by approximately 9:30 each morning.

The field crew consisted of three people, one observer and two source operators with the goal to acquire two patches per day. Even with weather delays this was possible. Prior to shooting a line, chalk would be used to mark the source locations. Once the field crew was in a rhythm we were able to shoot through a line, consisting of 12 source positions, in approximately 6.5 minutes. The source positions within the interior of the Autojuggie slowed progress and on average it took approximately an hour and 40 minutes to shoot a patch. Rolling the patch required the Autojuggie to be hooked up to the seismic truck so it could be moved to the next location. Once the Autojuggie was positioned the truck was unhooked and moved away from the survey area. This process took approximately 20 to 25 minutes. Deployment time for the receiver patch was negligible as the geophones could be lowered into position in less than a minute.

Because we didn't want to leave the Autojuggie and equipment at the field site overnight it reduced the number of shots we could complete each day. If the Autojuggie had been left at the field site setup teardown wouldn't have been necessary and there would have been time to shoot three to possibly three and a half patches within a working day.

4.6 Summary

To illustrate the efficiency of using the Autojuggie along with a modified marine streamer acquisition design (Section 4.4.1) it's best to take a look at the details in regards to

the amount of time it took to complete the survey. The modified marine streamer survey was conducted in the course of one day starting at approximately 7:00 a.m. and finishing around 6:00 p.m. Not including the time for setup, tear down and field crew breaks, a total of approximately six hours were spent surveying. Nineteen in-line rolls at 0.5 meter intervals were performed producing an area of full fold of ten meters in-line and six meters cross-line. Each patch had a total of eleven shot points per receiver grid. Two of these shot points were used for surface wave analysis and were not included in the reflection processing. The two additional source points are noted because they would be removed from future reflection surveys and further reduce the time required to shoot each patch. Although it doesn't reduce the amount of time considerably per patch, over the course of a days' work it can add additional time savings. Shooting each patch took less than twenty minutes and lifting the geophones, repositioning the receiver grid and re-deployment could be completed in less than three minutes.

The work presented here has shown that the Autojuggie, along with a modified design incorporating only far-offsets, can successfully deploy geophones mounted on base plates for the purpose of performing 3D seismic reflection surveys on pavement systems. Outfitting the Autojuggie with base plates allows 3D reflection surveys to be performed in areas that restrict the use of spiked geophones such as roads, highways and runaways. With the addition of the modified marine streamer design, use of the Autojuggie for transportation projects is even more feasible. Because the source locations are restricted to a narrow range, or even a single offset (Section 4.4.2), it makes an ideal design for surveying roadways. Further reduction of source locations, as shown by the common-offset test (Section 4.4.2), illustrate that simple subsurface mapping can be achieved very efficiently and quickly. Because

processing is minimal with the common-offset method data could be acquired and processed in nearly real time.

A drawback to using base plate mounted geophones is that source positions near the base plates will be contaminated by ground roll and unusable for processing and interpretation. This is a result of coupling that is not as rigid as traditionally planted geophones along with the use of a hammer and striking plate source. Further work is needed to determine the appropriate source-offset distances for use with an impact source and geophones mounted on base plates deployed on pavement.

Chapter 5: Developing 3D Surface Wave Methods

5.1 Introduction

During a seismic reflection survey several wave modes are created by the source and subsequently recorded as part of the seismic record. Among these various wave forms are reflected waves and surface waves. Although the Autojuggie was designed for acquisition of shallow reflection data a surface wave analysis may also be performed based upon the recorded seismic wave modes. While surface waves and reflected waves provide different information about the subsurface both can be used for near-surface investigations. Surface waves, or ground roll, make up as much as two-thirds of a seismic field record (Heisey et al., 1982). In reflection seismology ground roll has been treated as noise that masks reflected waves and most of the efforts in regards to seismic reflection processing have been to attenuate ground roll through acquisition and processing techniques (Lombardi, 1955; Anstey, 1986; Knapp, 1986). During reflection processing much of the recorded wave information, including surface waves are muted in an effort to isolate reflections. This eliminates a great deal of information that might otherwise be useful for subsurface investigations.

Surface wave methods can complement reflection surveys by providing information in regards to shallow layers that may not otherwise be available. Reflection methods may be unable to image reflectors when the near-surface target is beyond resolution limit and in these cases near-surface layers may be detected by the characteristic dispersion property of ground roll. Methods, as will be discussed, have been developed allowing a way to construct 1D vertical shear wave velocity (V_s) profiles through inversion of surface waves. Multiple 1D V_s profiles along a single traverse can then be used to generate a continuous 2D V_s profile. Analysis of these profiles can make it possible to detect near-surface features that can

be difficult to detect using high resolution seismic reflection methods. This section presents the application of the multichannel analysis of surface waves (MASW) method with geophone base plates mounted to the Autojuggie. Typically MASW surveys are performed using a single receiver line. However, the multiple receiver rows of the Autojuggie allows for simultaneous acquisition of surface waves among each of the receiver lines. Surface waves recorded in this manner offer a new way to visualize near-surface shear wave velocities, the output from MASW, in three-dimensions.

5.2 Historical background, near-surface surface wave methods

In general, there are two types of surface waves most widely observed in seismic investigations and earthquake seismology; Rayleigh and Love waves (Dobrin and Savit, 1988). If a vertical seismic source is used the type of resulting surface waves are Rayleigh waves, if a shear source is used then Love waves will be generated. Rayleigh wave particle motion has a vertical direction, whereas Love wave particle motion is horizontal. Because of the horizontal particle motion of Love waves they are not usually recorded during seismic surveys employing a vertical source and vertical receivers. Ground roll is a Rayleigh type surface wave that is in most cases always generated in near-surface seismic reflection surveys and makes up a large percentage of each shot record.

In a layered medium in which seismic velocity changes with depth, both types of the surface waves have a dispersive property that is indicative of elastic moduli of near-surface earth materials. Short wavelengths penetrate shallower depths and longer wavelengths deeper depths. The propagation velocity for each wavelength, called phase velocity (Bath, 1973), depends primarily on the shear wave velocity of the medium over the penetration depth and

is influenced only slightly by the p-wave velocity, density and Poisson's ratio. Therefore surface wave velocity is a good indicator of V_s . It's generally assumed that the phase velocity of ground roll is approximately 92% of V_s (Stokoe et al., 1994), and the ratio changes between 0.88 and 0.95 for the entire range of Poisson's ratio (0.0 - 0.5) (Ewing et al., 1957). Therefore, by analyzing the dispersion feature of ground roll represented in seismic data, near-surface V_s profiles can be constructed and the corresponding shear moduli calculated.

Surface waves have long been used to study the subsurface and development of surface wave methods date back to the 1950s when the steady state method was first used (Van der Pol, 1951; Jones, 1955). Initial studies were based entirely on the Rayleigh wave fundamental mode assumption and all other types of waves including higher modes and body waves were ignored. These early methods eventually became known as the Continuous Surface Wave (CSW) method (Matthews et al., 1996).

Spectral Analysis of Surface Waves (SASW), introduced by Nazarian and Stokoe (1983) was an advancement of the CSW method. The SASW method makes use of the Rayleigh wave dispersion property for the purpose of creating a near-surface V_s profile. A surface impact source is used to generate waveforms and two receivers record the ground roll. Because near-surface investigations are generally interested in different depths, and because only two geophones are used, the test needs to be repeated with many different source and receiver spacing. The goal is to have the receiver separation replicate the wavelength for a given depth of investigation. To account for the effect of potential internal phase shifts due to receivers and instrumentation the test is also performed in two directions to (Nazarian et al., 1983). The SASW method assumes the fundamental mode of the

Rayleigh wave is the only mode contained with the data and higher mode frequencies are not considered.

There are several considerations when using the SASW method. Among them is the time and labor required due to the repeated source and receiver spacing. Also, because only two receivers are used there are effects from the inclusion of other wave modes, such as body waves, air wave, higher modes and non-planar surface waves (Sheu et al., 1988; Hiltunen and Woods, 1990; Foti, 2000).

A progression from the SASW method was the development of the multi-channel analysis of surface waves (Park et al., 1999; Xia et al., 1999; Ivanon et al., 2005; Miller et al., 2008). One of the main benefits of MASW is that it uses multi-channel acquisition. The focus of surface wave analysis has been the creation of a shear wave velocity profile. That same concept continues through the analysis of surface waves using the MASW method. Surface waves are unique in that they are dispersive. The dispersive nature of surface waves, which body waves lack, allow different wavelengths to penetrate different depths and propagate with different velocities. The corresponding phase velocities then represent the elastic properties within the penetrating depths.

Performing an MASW investigation usually consists of four steps: 1) acquiring surface waves on multi-channel seismic records, 2) generation of a dispersion curve, which is a plot of frequency versus phase velocity, 3) picking the fundamental-mode from each dispersion curve record and 4) inverting the dispersion curves to obtain 1D Vs profiles. By acquiring data in a roll-along fashion multiple 1D Vs profiles can be created showing a continuous subsurface Vs profile by creating a 2D Vs map. Spatial interpolation is used

between subsequent 1D Vs profiles and each 1D Vs profile, located in the middle of the receiver spread, is used to acquire the corresponding record (Park, 2005).

While planning and performing a MASW survey is generally straight forward there are several items to consider before acquisition. These include the depth of investigation, source and receiver offsets and both near and far field effects. Even though ground roll generally dominates a seismic record optimal recording of ground roll requires field configurations and acquisition parameters that are conducive to recording planar, fundamental mode Rayleigh waves (Park et al., 1999). Rayleigh waves require a certain amount of time to be developed into planar waves which usually does not occur until the near-offset is greater than half the maximum desired wavelength (Stokoe et al., 1994). Therefore the near-offset should be approximately the same distance as the minimum depth of investigation. The maximum penetration depth is approximately one wavelength and the general rule is that the maximum penetration depth is approximately half the longest wavelength (Rix and Leipski, 1991). Therefore the far-offset distance is usually selected to be twice the maximum investigation depth.

The first documented use of the multi-channel approach for surface wave analysis dates back to the early 1980s when investigators in the Netherlands used a 24-channel acquisition system to deduce the shear wave velocity structure of tidal flats. Park et al. (1999) later highlighted the effectiveness of the multi-channel approach by detailing advantages of multi-channel acquisition and processing for geotechnical investigations.

MASW is an attractive geophysical method because of its efficiency of investigating elastic properties of near-surface materials. In addition, it provides a way of getting subsurface information that may not be available from other methods. In regards to surface

waves, the inclusion of waves considered as noise, such as body waves, direct waves, refracted waves, and air waves (Sanchez-Salinerio et al., 1987), reflected waves (Sheu et al., 1988) and higher-modes (Gucunski and Woods, 1991); ground roll can be identified by its different coherency in arrival times on a multi-channel record.

5.3 Autojuggie MASW

Very early in the design of the Autojuggie it was shown that hydraulically deployed geophones have the ability to collect data suitable for MASW (Tian et al., 2003a,b). Because surface waves are recorded during a standard reflection survey acquisition designs were explored that would exploit this allowing the acquired data to be used for both 3D reflection and surface wave analysis. Through the analysis of both wave forms a method for performing a thorough investigation of the subsurface for geotechnical analysis exists. Reflection data can be used to investigate deeper geologic layers while the surface wave data can be used to investigate the upper portions of the subsurface that reflection methods may not be able to resolve.

Dual acquisition of reflection and surface waves requires additional source locations to be added to the survey design. The research presented here will illustrate MASW acquisition as an extension of the modified marine streamer discussed previously. It should be noted that because we are simply adding source locations dual acquisition can be accomplished with any 3D survey. During 3D reflection processing the surface wave locations are removed and vice-versa when processing the surface wave data.

As a brief recap of the survey design, there were eleven receiver rows each with nineteen geophones and the receiver patch was rolled nineteen times in-line at 0.5 meter

intervals (Figure 50). For recording eleven 24-channel Geometrics Geode seismographs with 24-bit A/D conversion and Mark Products 28 Hz vertical component geophones mounted to base plates were used. Recording time was 0.5 second with a sampling interval of 0.125 ms. A small sledge hammer and metal striking plate were used to generate the source signal and the source point was located directly behind the middle receiver line of the Autojuggie.

The general rule is that Rayleigh waves develop into planar waves when the near-offset is greater than half the maximum desired wavelength. A velocity of 500 m/s and a frequency of 60Hz results in a wavelength of ~8.0 meters and based upon this we should have used 4.0 meter near-offsets. Because the near-offset rule is only a generalization, the true velocity and frequency used to calculate the wavelength could be higher and because there is flexibility within the MASW method, a near-offset of 1.0 meters was sufficient. An additional source position at 0.5 meter near-offset was also collected and both the 0.5 meter and 1.0 meter offset data were processed and compared. There was no significant difference between the two and the data shown here is from the 1.0 meter offset.

Once the near-offset is chosen the far-offset is dictated by the fixed length of the Autojuggie which in this case provides a far source-receiver offset of 10.5 meters. The general rule for the maximum penetration depth is that the maximum penetration depth is approximately half the longest wavelength. A velocity of 500 m/s and a frequency of 60 Hz results in a wavelength of ~8.0 meters so the depth of penetration would be ~4.0 meters. As with the near-offset, the far-offset rule is a generalization, the true velocity and frequency used to calculate the wavelength could be lower, this being the case a far-offset of 10.5 meters was sufficient. The selection of offsets was based upon previous 2D seismic reflection work that showed that the shallowest reflector that could be imaged using seismic reflection

is at a depth of approximately 8.5 meters. Therefore the offsets chosen for MASW analysis would image approximately 1.0-4.0 meters depth and provide information that is not readily available with reflection methods.

Each receiver line was processed individually (Figure 63) using the SurfSeis software developed by the Kansas Geological Survey. Processing consisted of creating individual data sets for each of the receiver lines, reformatting the field data into the SurfSeis format, geometry assignment, generating dispersion curves, picking the fundamental mode for each dispersion curve and finally inverting for the Vs profile. An example of a picked dispersion curve is shown in Figure 64. Dispersion curves are picked for each positioning of the receiver grid. Since there were twenty total receiver grid positions covering the length of the survey there were twenty dispersion curves picked for each receiver line and several examples of picked dispersion curves can be found in Appendix A. Dispersion curves are graphical

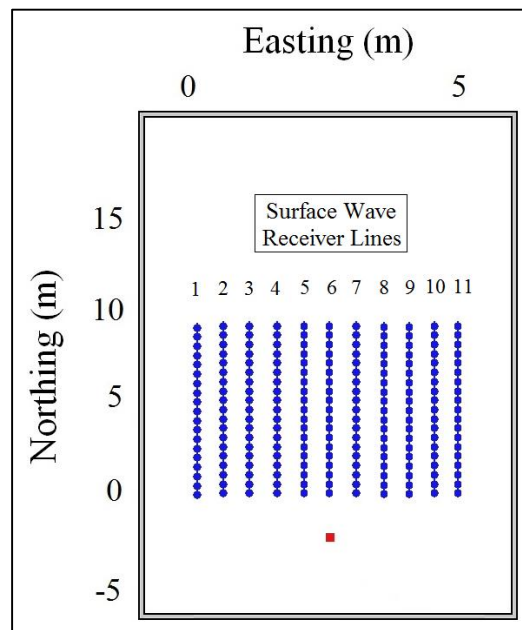


Figure 63. Surface wave receiver lines. Surface waves were acquired and processed individually for each receiver line

ways to represent phase velocity versus frequency. The picks are intended to follow the fundamental mode frequency and because the picks are used to invert for the 1D Vs profile they need to be made as accurately as possible. The individual 1D Vs profiles are then combined to create a 2D Vs profile. As can be seen, the phase velocities range between ~270-600 m/s with a frequency range of approximately 30-100 Hz.

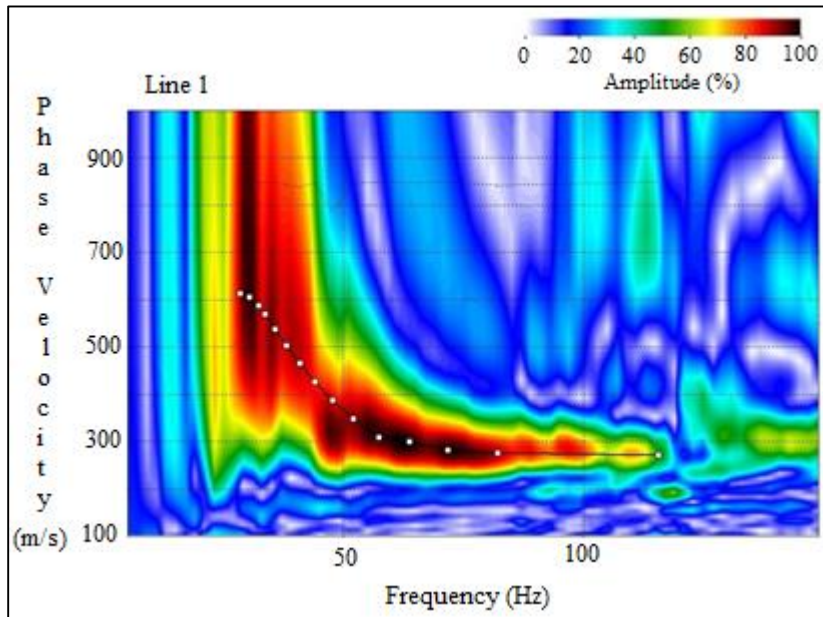


Figure 64. Dispersion curve for the first station of the first receiver line. Dispersion curves were picked for every shot position for each of the receiver lines

The final result of inverting the dispersion curves is a 2D Vs profile along the length of each receiver line (Figure 65). Images for each receiver row can be found in Appendix B. All of the Vs profiles for the receiver rows show the same general details. The subsurface to a depth of approximately 7.0 meters displays a layered subsurface with the shear wave velocity within the range of approximately 200-600 m/s and increasing with depth. One area of interest is around 1.8 meters depth. Close inspection of the Vs profile shows a velocity

inversion wherein there is a velocity decrease at this depth. Construction of the parking lot calls for a compacted subsurface, the velocity decrease at this depth is likely related to the effects of the transition zone from the compacted material into the natural underlying soils and clays. The continued increase in velocity through the remainder of the section shows the increase in material stiffness as a result of burial. Bedrock lies at approximately 9.0m, the highest velocities at 7.0m correlate to the transition from soils and clays to competent bedrock.

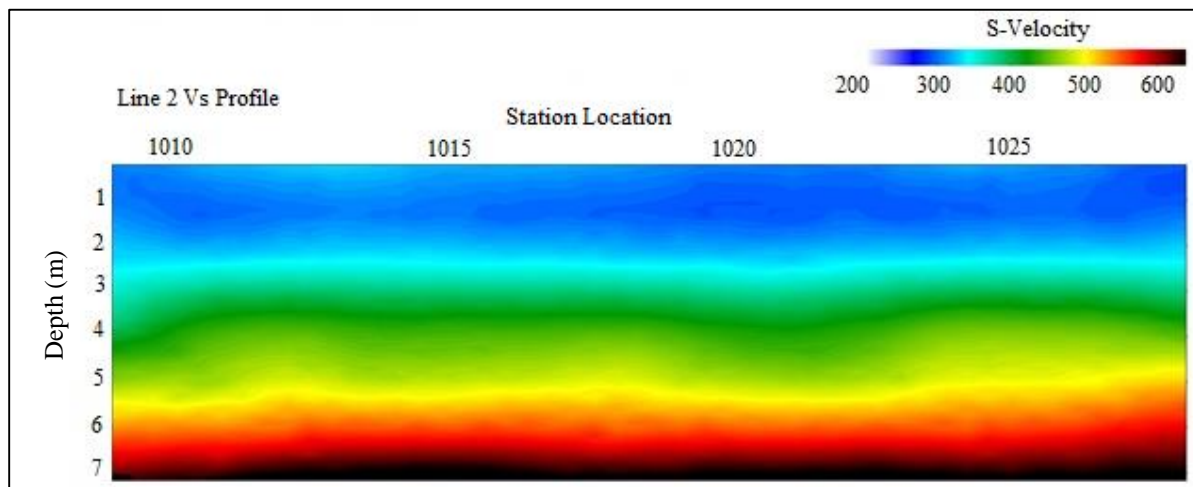


Figure 65. 2D Vs profile for line 2 of the survey. Depth of imaging is approximately 7.0 meters with shear wave velocities within the range of 200-600 m/s

5.4 Psuedo-3D Surface Wave Profiles

The MASW method is designed to create 2D Vs profiles from surface wave data. While these 2D profiles individually offer a great deal of information extending the visualization to 3D can have benefits such as being able to track subsurface features between 2D Vs profiles. In an effort to produce these types of plots several programs were developed using the MATLAB scientific programming language. One of the output files from SurfSeis

is a data file containing the V_s velocities at depth. Because multiple, coincident 2D profiles (i.e. surface wave data along each receiver line) were acquired pseudo-3D profiles can be created using the velocity data. Several profiles, which will be discussed subsequently, were constructed to show the versatility of viewing V_s data as pseudo-3D profiles.

5.4.1 Cross-line (vertical) Profiles

The V_s profiles produced by SurfSeis are in-line profiles which show the V_s velocity structure at depth along each receiver row. To help visualize how the velocity structure varies at depth in the cross-line direction a series of cross-line V_s profiles were created. By programmatically selecting the velocity values at depth for each position along corresponding receiver lines cross-line V_s profiles can be created. Because the velocity output for each receiver row from SurfSeis is at discrete intervals along each receiver line an interpolation was performed to obtain data values between these locations. By interpolating between points, cross-line V_s profiles can be created at 0.1 meter increments through the entire in-line range of the surveyed area. Figure 66 shows one example. Distances of 0.6, 1.6 and 2.6 meters are shown in the example and profile slices at 1.0 meter increments throughout the remainder of the surveyed area are provided in Appendix C.

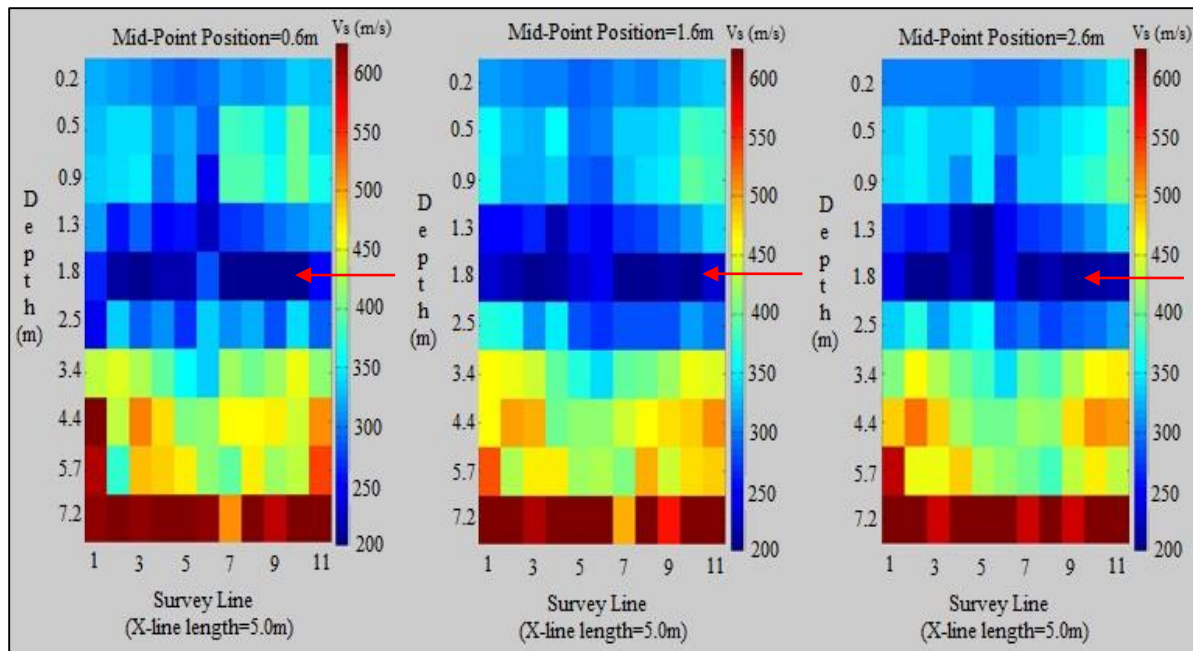


Figure 66. 2D Vs cross-line profiles. Distances of 0.6, 1.6 and 2.6 meters are shown and a velocity inversion around 1.8m is evident (red arrows)

The profiles (Figure 66) show the same velocity profile at depth as was seen in the 2D Vs profiles (Figure 65) created with SurfSeis. One item of note is the velocity inversion around 1.8 meters depth. While this velocity inversion can be seen in Figure 65 it is more evident in the cross-line Vs profile (Figure 66).

As an extension of the viewing capabilities of pseudo-3D surface wave data the vertical profiles can be graphed in 3D space (Figure 67). Figure 67 shows the same vertical profiles as Figure 66 however in this viewing style they can be seen as multiple in-line slices that span the entire cross-line length of 5.0 meters. This style of graph may make it easier to see Vs variations within the subsurface. While the profiles show an increase in Vs velocity with depth the velocity inversion illustrated previously is also seen clearly. As with the previous profiles, any positions throughout the surveyed area could have been selected at 0.1

meter increments. The remainder of the pseudo-3D cross-line profiles can be found within Appendix C.

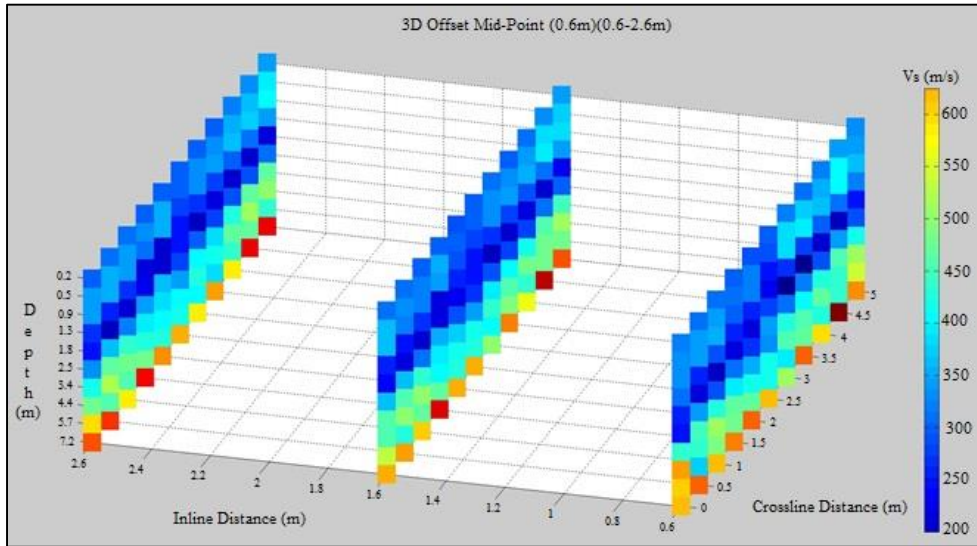


Figure 67. Pseudo 3D V_s cross-line profiles. Distances of 0.6, 1.6 and 2.6 meters are shown, however, profiles at 0.1 meter increments through the range of the survey area can be displayed

5.4.2 In-line (vertical) Profiles

To help visualize the velocity structure between each receiver row, in-line V_s profiles were programmatically created. Interpolation was performed between each receiver line so that V_s profiles could be extracted at 0.1 meter increments between each receiver row across the entire surveyed area. Figure 68 shows one example. Distances of 0.3, 1.3 and 2.3 meters are shown in the example and profile slices at 1.0 meter increments throughout the remainder of the surveyed area are provided in Appendix C.

As can be expected, the profiles (Figure 68) show the same velocity profile at depth as was seen in the 2D V_s profiles (Figure 65) and cross-line profiles (Figure 66). The

velocity inversion around 1.8 meters depth is still evident and the same structure can be seen in the additional in-line profiles provided in Appendix C.

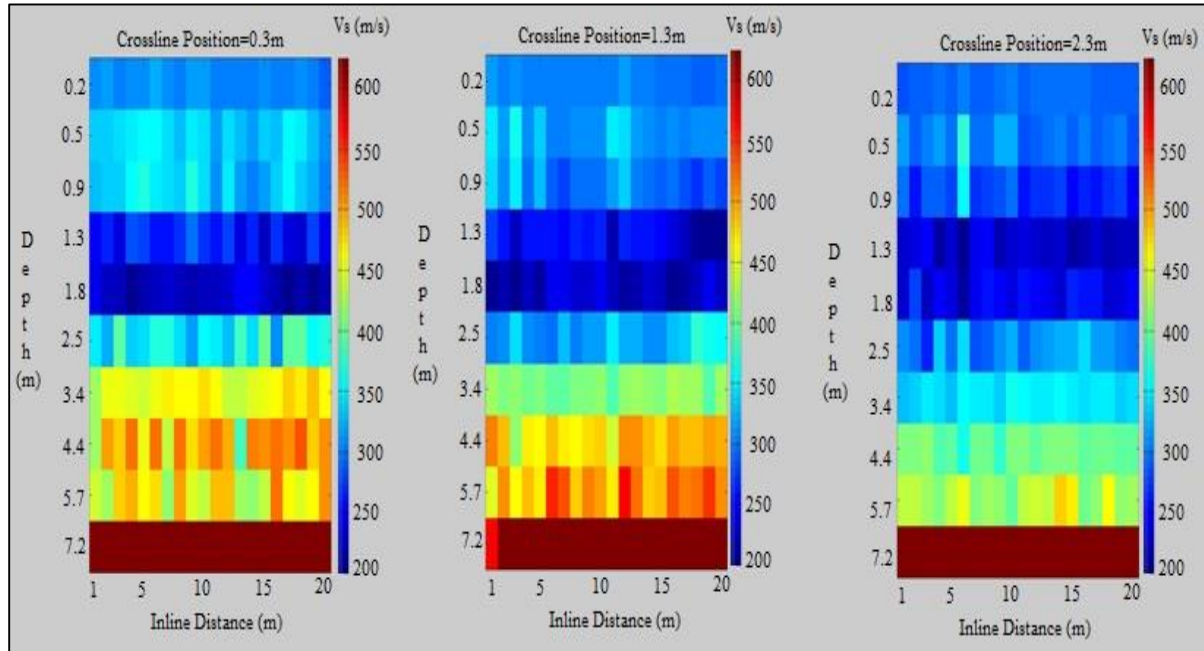


Figure 68. 2D Vs in-line profiles. The profiles shown span the entire length of the survey line at distances of 0.3, 1.3 and 2.3 meters in the crossline direction

Figure 69 is similar to the pseudo 3D cross-line profiles except in this case the figure shows Vs profiles with depth along the in-line direction, spanning the length of the surveyed area. The positions selected for display match the positions in Figure 68. The same Vs velocity increase with depth and velocity inversion seen previously is evident. Pseudo-3D profiles throughout the remainder of the survey area, at increments of 1.0 meters can be found in Appendix C.

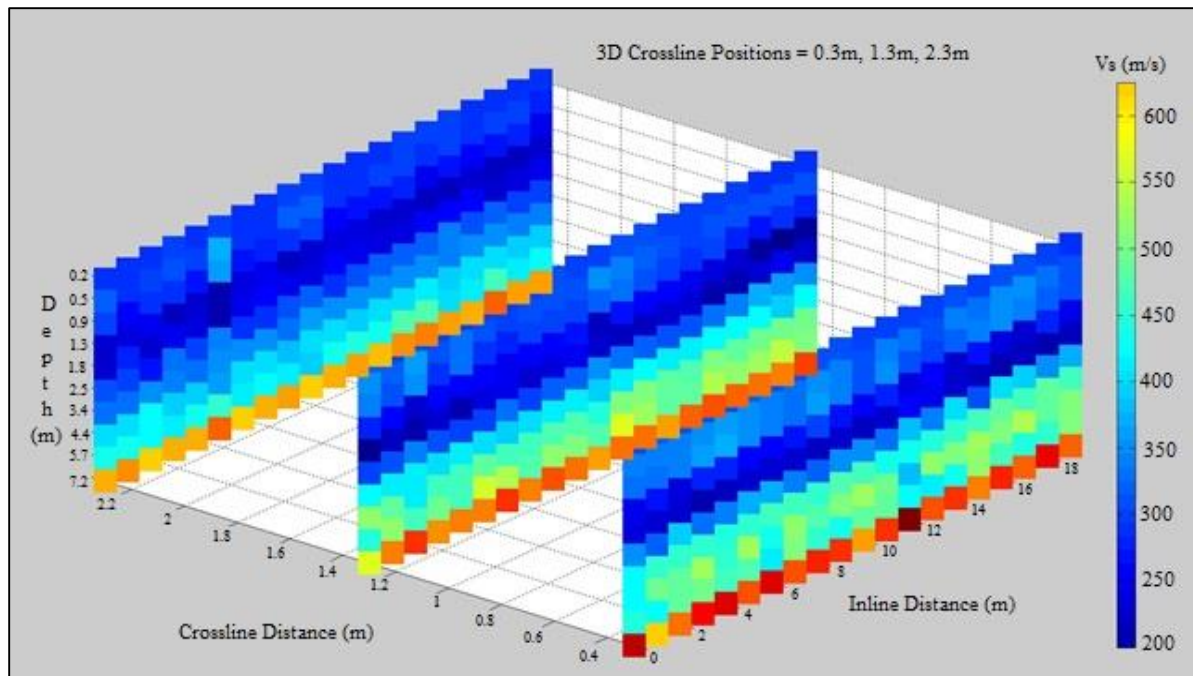


Figure 69. Pseudo 3D Vs in-line profiles. Distances of 0.3, 1.3 and 2.3 meters are shown however, profiles at 0.1 meter increments through the range of the survey area can be displayed

5.4.3 Depth (horizontal) Profiles

Arguably one of the most useful uses of the pseudo-3D displays is the ability to view shear wave velocities across the surveyed area at a given depth. Figure 70 shows a series of shear wave velocities at approximately 1.0, 4.0 and 7.0 meters depth. The remaining horizontal velocity profiles are provided in Appendix C. Because interpolation was not undertaken as a function of depth the velocities used are discrete shear wave velocities at depth as calculated by SurfSeis. If it was deemed that a finer horizontal velocity profile was necessary for a geotechnical investigation it is possible to interpolate with depth to produce this information.

The horizontal slices (Figure 70) are from shallow, mid and deepest depths and the velocity increase with depth is evident. Inspection of the remainder of the horizontal profiles (Appendix C) shows the increase of velocity with depth, the velocity inversion at ~1.85 meters is also evident.

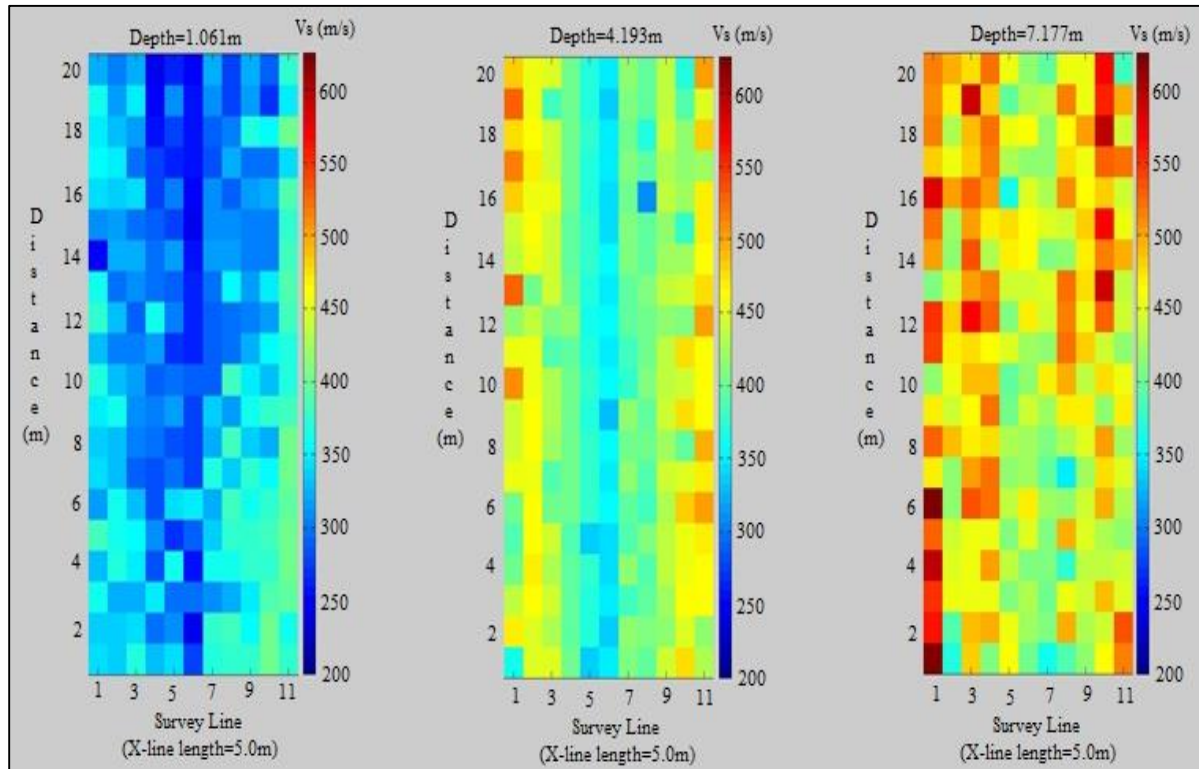


Figure 70.2D Vs horizontal (depth) profiles. Shown are depth plots from 1.061, 4.193 and 7.177 meters. The data shown within each plot spans the entire area of the survey

Contouring data sometimes reveals additional information that may not be evident otherwise. As an example of the type of analysis that may be performed using pseudo-3D data the horizontal Vs depth slices were contoured (Figure 71). The contoured data show the general increase in shear wave velocity to the bottom right of the survey area. It also reveals several areas of velocity highs, as indicated by the closely spaced contours. One item of note

is that there appears to be linearity (north-south) within the data. This may be a result of the survey design wherein the receiver grid is elongated in the in-line direction versus the cross-line direction. The contoured profiles shown correspond to the depths shown in Figure 70, the contour plot for additional depths can be found in Appendix C.

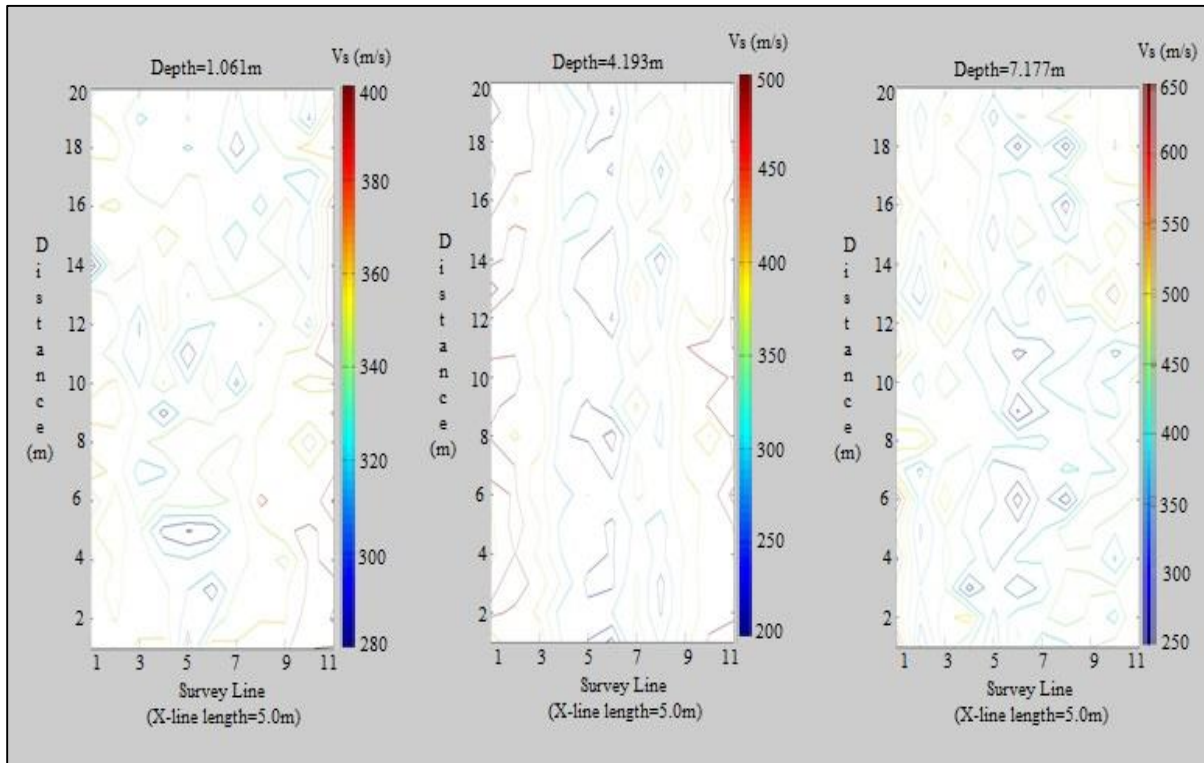


Figure 71. 2D Vs horizontal (depth) contoured profiles. The contoured profiles span the entire area of the survey and depths of 1.061, 4.193 and 7.177 meters are shown

5.5 Ground Penetrating Radar and Vs Comparisons

In an effort to determine the level of confidence that may be placed on the very shallow inverted surface wave velocities a ground penetrating radar (GPR) survey was conducted. A Pulse-EKKO system was used to acquire 50 MHz, 100 MHz and 200 MHz data along each of the eleven receiver lines. The data acquired with the lower frequency 50

50 MHz and 100 MHz antennae did not reveal any reflection events. A driller log (Appendix E) obtained from the Kansas Geological Survey water resources indicates the upper layer of the subsurface consists of soil and clay. The log is from a water well that was drilled on property owned by The University of Kansas. The well is located on Ohio Street in Lawrence, KS and is approximately 1.5 miles from the study area. The results of the 50 MHz and 100 MHz data seem to confirm the drill log in that the upper soil has high clay content. Data acquired with the 200 MHz antennae were able to image several reflectors (Figure 72). Construction records obtained from The University of Kansas Design and Construction Management that were developed for the Park-And-Ride lot show that construction designs called for an upper surface of 5.08 cm asphalt surface, 15.24 cm asphalt base and 22.86 cm chemically stabilized sub grade underlain by a compacted subsurface. Unfortunately the depth of the compacted

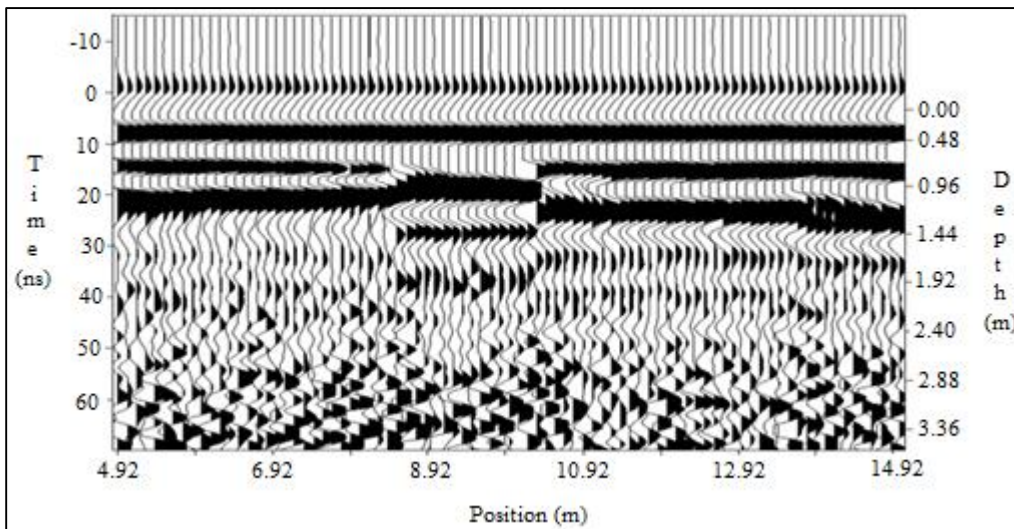


Figure 72. GPR profile corresponding to the second receiver row. Data were acquired using 200 MHz antenna along each geophone receiver line

surface wasn't specified within the design documents. While the GPR data was not able to resolve reflectors above 0.5 meters. Reflectors are evident between 1.9 and 2.4 meters. The GPR profiles for the other receiver lines show the same general layering however there are variations between the lines. The GPR profiles for the other receiver lines can be found in Appendix D.

Overlay images were created along each receiver line to compare the Vs profiles with the GPR data. To make the comparison the area from the 2D Vs profiles that correlated to the same distance and depth from the GPR profiles was programmatically extracted using MATLAB. It should be noted that a new Vs velocity color scale was generated based on the values within the smaller data subset. The two data sets were then superimposed to see if any correlation exists (Figure 73). Overlays for each of the receiver lines can be found in Appendix D.

Inspection of the overlay shows that the coloring of the Vs velocity field changes with the direct wave, air wave and reflection events. We can also see a color change around 2.4 meters depth where coherency within the traces is lost. Correlations of the events near the top of the section are of interest. The events from 0.0-0.56 meters are the direct and air wave arrivals. While in this instance these events by themselves don't offer any particular information of use, that the Vs velocities change along with these events indicate that the Vs velocities at these very shallow depths can be accepted with some accuracy. Although we don't have the resolution required to resolve the very shallow events that would define the construction of the parking lot surface it provides some basis for potential future research.

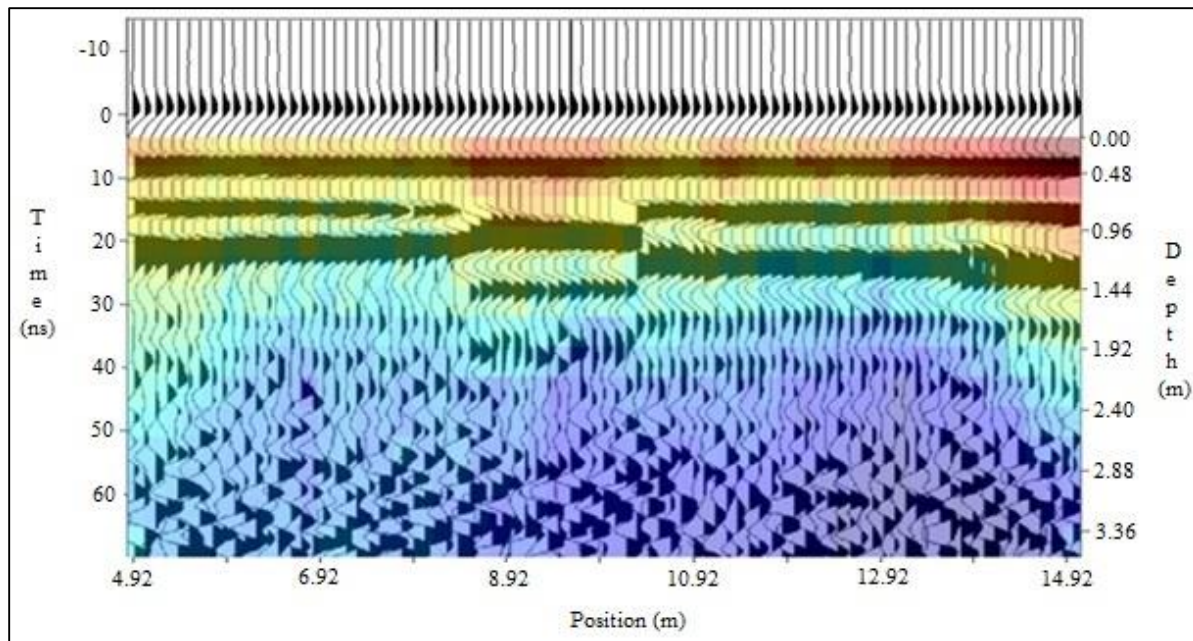


Figure 73. Superimposed Vs velocity field and GPR profile corresponding to the second geophone receiver row. Variation within the Vs velocity field can be seen to correlate with events imaged within the radar data

5.6 Summary

The Autojuggie is a versatile acquisition device that can be used for seismic reflection surveying, acquisition of surface waves for analysis using MASW or, most preferably, used to acquire both wave modes for a thorough analysis of the subsurface for geotechnical characterization. Through the use of modified survey designs and processing techniques both wave forms can be acquired during a single survey. The combined acquisition allows subsurface reflectors to be mapped in 3D and the very near-surface shear wave velocity structure determined. As has been shown here, surface wave data acquired along closely spaced, coincident receiver lines, can be programmatically formatted to create various profile views of the shear wave velocity structure. This style of combined seismic wave mode acquisition has many uses for geotechnical characterization such as determining depth to

bedrock, subsurface reflector geometries and potential faulting. Complimenting this, surface wave information can be used to determine the shear wave velocity of the upper several meters of the subsurface to detect potential voids, buried pipes and other near-surface features geotechnical surveys target.

References

- Allen, S. J., 1980, Seismic method., *Geophysics*, 45, 1619–1633.
- Anstey, N., 1986, Whatever happened to ground roll?: *The Leading Edge*, 5, 40–45.
- Bachrach, R. and T. Mukerji, 2001a, Fast 3-D ultra shallow seismic reflection imaging using portable geophone mount: *Geophysical Research Letters*, 28, 45–48.
- Bachrach, R. and T. Mukerji, 2004a, Portable dense geophone array for shallow and very shallow 3-D seismic reflection surveying—Part 1: Data acquisition, quality control, and processing: *Geophysics*, 69, 1443–1455.
- Bachrach, R., and T. Mukerji, 2001b, AVO analysis of shallow seismic data: feasibility and analysis of 2D and 3D ultra shallow reflections: *SAGEEP, Expanded Abstracts, Env. Eng. Geophys. Soc., Proceedings*.
- Bachrach, R., and T. Mukerji, 2004b, Portable dense geophone array for shallow and very shallow 3D seismic reflection surveying—Part 2: 3D imaging tests: *Geophysics* 69, 1456–1469.
- Barnes, K. M., and R. F. Mereu, 1996, An application of the 3-D seismic technique or mapping near-surface stratigraphy near London, Ontario: *J. Environ. Engin. Geophys.*, 1, 171–177.
- Bath, M., 1973, *Introduction to seismology*, Stuttgart, Birkhauser, Verlag, 395 p.
- Blair, J. D., Steeples, D. W., Vincent, P. D., Butel, N., and J. Powers, 2003, Analysis of the seismic response of rigidly interconnected geophones attached to steel media of various shapes: 73rd Annual International Meeting, SEG, Expanded Abstracts, 1263-1266.
- Büker, F., Green, A. G., and H. Horstmeyer, 1998, Shallow 3-D seismic reflection surveying: Data acquisition and preliminary processing strategies: *Geophysics*, 63, 1434-1450.
- Büker, F., Green, A. G., and H. Horstmeyer, 2000, 3-D high-resolution reflection seismic imaging of unconsolidated glacial and glaciolacustrine sediments: processing and interpretation, *Geophysics*, 65, 18–34.
- Cartwright, J., and Huuse, M., 2005, 3D seismic technology: The geological ‘Hubble’: *Basin Research*.
- Clark, J. M., Blair, J. D., and D. W. Steeples, 2004, Seismic response of geophones attached to tubing: 74th Annual International Meeting, SEG, Expanded Abstracts, 1452-1455.
- Convert, J. P., DeVault, J. L., and Pieuchot, M., 1976, Telemetry offers simplicity, accuracy: *Oil and Gas J.*, v. 74, October 25, p. 127-130.

- Cordsen, A., Galbraith, M., and J. Peirce, 2000, Planning Land 3-D Seismic Surveys: Geophys. Developments, 9, Soc. Expl. Geophys.
- Corsmit, J., Versteeg, W. H., Brouwer, J. H., and K. Helbig, 1988, High-resolution 3-D reflection seismics on a tidal flat: acquisition, processing and interpretation: First Break, 6, 9–23.
- Czarnecki, G. P., 2006, Automated three-dimensional ultra-shallow seismic reflection data acquisition using a two-dimensional geophone array: MS Thesis, The University of Kansas, Lawrence.
- Czarnecki, G. P., Tsoflias, G. P., Steeples, D. W., Sloan, S. D., and Eslick, R. C., 2006, An example of automated 3D ultra-shallow seismic acquisition: 76th Annual Mtg., Expanded Abstracts, Soc. Expl. Geophys., 1461-1465.
- Dickey, H. P., Zimmerman, J. L., Plinsky, R. O., and R. D. Davis, 1977, Soil survey of Douglas County, Kansas, United States Department of Agriculture Experiment Station publication, 73.
- Dobrin, M., B. and Savit, C., H., 1988, Introduction to Geophysical Prospecting, McGraw-Hill, 896 p.
- Dragoset, Bill, 2005, A historical reflection on reflections, The Leading Edge, Jan 2005, Vol. 24, No. s1.
- Ewing, W. M., and Jardetzky, W. S., 1957, Elastic waves in layered media: McGraw-Hill, Inc., 380 p.
- Foti, S., PhD Diss., 2000, Politecnico di Torino, Multistation methods for geotechnical characterization using surface waves.
- Green, A. G., Pugin, A., Beres, M., Lanz, E., Büker, F., Huggenberger, P., Horstmeyer, H., Grasmück, M., De Iaco, R., Holliger, K., and H. R. Maurer, 1995, 3-D high-resolution seismic and georadar reflection mapping of glacial, glaciolacustrine and glaciofluvial sediments in Switzerland: Ann. Symp. Environ. Engin. Geophys. Soc. (SAGEEP), Expanded Abstracts, 419–434.
- Gucunski, N., and Woods, R. D., 1991, Use of Rayleigh modes in interpretation of SASW test, Proc., 2d Int'l. Conf. on Recent Advances in Geotechnical Earthquake Eng. and Soil Dynamics, St. Louis, Missouri, 1399-1408.
- Hart, B. S., 1999, Definition of subsurface stratigraphy, structure and rock properties from 3-D seismic data: Earth-Science Reviews, 47.

- Heisey, J.S., Stokoe II, K.H., and Meyer, A.H., 1982, Moduli of pavement systems from Spectral Analysis of Surface Waves, *Transp. Res. Rec.*, v. 852, Washington D.C, p. 22-31.
- Hiltunen, D.R., and Woods, R.D., 1990, Variables affecting the testing of pavements by the surface wave method, *Transp. Res. Rec.*, v. 1260, p. 42-52.
- House, J. R., Boyd, T. M., and F. P. Haeni, 1996, Haddam Meadows, Connecticut: A case study for the acquisition, processing, and relevance of 3-D seismic data as applied to the remediation of DNAPL contamination, in Weimer, P., and Davis, T. L., Eds., *Applications of 3-D seismic data to exploration and production: Geophysical Developments Series 5: Soc. Expl. Geophy.*, 257–265.
- Ivanov, J., Park, C., Miller, R., and Xia, J., 2005, Analyzing and Filtering Surface-Wave Energy By Muting Shot Gathers, *Journal of Environmental and Engineering Geophysics*, Pg. 307–322.
- Jones, R., 1955, A vibration method for measuring the thickness of concrete road slabs in situ, *Magazine of Concrete Research*, v. 7, n. 20, p. 97-102.
- Kaiser, A. E., Horstmeyer, H., Green, A. G., Campbell, F. M., Langridge, R. M., McClymon, A.F., Detailed images of the shallow Alpine Fault Zone, New Zealand, determined from narrow-azimuth 3D seismic reflection data, 2011, *Geophysics*, Vol. 76, No. 1.
- Knapp, R. W., 1988, High resolution seismic data of Pennsylvanian cyclothems in Kansas *Geophysics: The Leading Edge Of Exploration*.
- Knapp, R. W., and D. W. Steeples, 1986a, High-resolution common-depth-point seismic reflection profiling: Instrumentation: *Geophysics*, 51, 276–282.
- Knapp, R. W., and D. W. Steeples, 1986b, High-resolution common-depth-point seismic reflection profiling: Field acquisition parameter design: *Geophysics*, 51, 283–294.
- Knapp, R. W., Watney, W., L., 1987, Seismic identification of Pennsylvanian cyclothems beneath Lawrence, Kansas *SEG Expanded Abstracts* 6, 338, DOI:10.1190/1.1892102.
- Lanz, E., Pugin, A., Green, A., and Horstmeyer, H., 1996, Results of 2- and 3-D highresolution seismic reflection surveying of surficial sediments: *Geophysical Research Letters*, 23, 491–494.
- Lombardi, L. V., 1955, Notes on the use of multiple geophones: *Geophysics*, 20, 215-226.
- Loper, G. B., and Pittman, R. R., 1954, Seismic recording on magnetic tape: *Geophysics*, 19, 104–115.

- Matthews, M.C., Hope, V.S. and Clayton, C.R.I., 1996, The use of surface waves in the determination of ground stiffness profiles. Proc. Instn. Civ. Engrs. Geotech. Engng., 119, April, 84-95.
- Mayne, W. H., 1962, Common reflection point horizontal data stacking techniques: Geophysics, 27, 927-938.
- Miller, B. E., Tsoflias, G., P. and Steeples, D. W., 2009, Automated geophone deployment on pavement for high resolution seismic reflection investigations in support of transportation infrastructure projects, 79th Annual Mtg., Expanded Abstracts, Soc. Expl. Geophys.
- Miller, Richard D., and Xia, Jianghai, 1999, Using MASW to Map Bedrock in Olathe, Kansas Open-file Report No. 99-9.
- Miller, RD, Xia, Jianghai, Park, C.B., Ivanov, J., 2000, Shear-wave velocity field from surface waves to detect anomalies in the subsurface, Geophysics.
- Miller, R. D., Raef, A. E. E., Byrnes, A. P., Lambrecht, J. L., and Harrison, W. E., 2004, 4-D high-resolution seismic reflection monitoring of miscible CO₂ injected into a carbonate reservoir in the Hall-Gurney Field, Russell County, Kansas: 74th Annual Meeting, SEG, Expanded Abstracts, 2259-2262.
- Miller, Rick, Xia, Jianghai, Park, Choon B, Ivanov, Julian M., 2008, The history of MASW, The Leading Edge, Vol. 27, No. 4, P. 568-568.
- Nazarian, S., K.H. Stokoe II, and W.R. Hudson, 1983, Use of spectral analysis of surface waves method for determination of moduli and thicknesses of pavement systems: Transportation Research Record No. 930, p. 38-45.
- Park, Choon, B., 2005, MASW-Horizontal resolution of 2D shear-velocity (Vs) mapping, KGS Open-file Report 2005-4.
- Park, C. B., Miller, R. D., and Xia, J., 1999, Multichannel analysis of surface waves (MASW), Geophysics, 64, 800-808.
- Ralston, M. D., Steeples, D. W., Spikes, K., and J. Blair, 2001, Near-surface three component seismic data acquisition using rigidly interconnected geophones: 71st Annual Meeting, SEG, Expanded Abstracts, 1411-1414.
- Ralston, M. D., Steeples, D. W., Spikes, K., Blair, J., and T. Gang, 2002, Analysis of an automated three-component shallow seismic acquisition system: 72nd Annual Meeting, SEG, Expanded Abstracts, 1551-1554.

- Rix, G. J., and Leipski, A. E., 1991, Accuracy and resolution of surface wave inversion: Recent Advances in Instrumentation, Data Acquisition and Testing in Soil Dynamics, Geotechnical Special Publication No. 29, ASCE, 17-23.
- Ryden, N., 1999, SASW as a tool for non destructive testing of pavements, MSc thesis, Univ. of Lund, Sweden.
- Ryden, N., and C.B. Park, 2006, Inversion of surface waves using phase velocity spectra: Geophysics, v. 71, n. 4, p. 49-58.
- Ryden, N., and Lowe M. J. S., 2004, Guided wave propagation in three-layer pavement Structures: Journal of the Acoustical Society of America, v. 116, p. 2902-2913.
- Ryden, N., C.B. Park, P. Ulriksen, and R.D. Miller, 2003, Lamb wave analysis for non-destructive test-ing of concrete plate structures: Symposium on the Application of Geophysics to Engineering and Environmental Problems (SAGEEP 2003), San Antonio, Texas, April 6-10, INF03.
- Ryden, N., C.B. Park, P. Ulriksen, and R.D. Miller, 2004, Multimodal approach to seismic pavement testing: Journal of Geotechnical and Geoenvironmental Engineering, v. 130, p. 636-645.
- Sanchez-Salinerro, I., Roesset, J. M., Shao, K. Y., Stokoe II, K. H., and Rix, G. J., 1987, Analytical evaluation of variables affecting surface wave testing of pavements: Transportation research record No. 1136, 86-95.
- Schmeisnner, C. M., Spikes, K. T., and D. W. Steeples, 2001, Recording seismic reflections using rigidly interconnected geophones: Geophysics, 66, 1838–1842.
- Schmelzbach, C., and Juhlin, C., 2007, High-resolution 3-D seismic imaging of the upper crystalline crust at a nuclear-waste disposal study site on Avro Island, southeastern Sweden, 76th Annual Meeting, SEG, Expanded Abstracts, 1396–1400.
- Sheu, J. C., Stokoe II, K. H., and Roesset, J. M., 1988, Effect of reflected waves in SASW testing of pavements: Transportation research record No. 1196, 51-61.
- Sirles, P., and Haramy, K., 2006, How Transportation Agencies Use Geophysics: Highway Geophysics – NDE Conference, 1428.
- Sloan, S., D., PhD Diss., 2008, The University of Kansas, Ultra-Shallow Imaging Using 2D & 3D Seismic Reflection Methods.
- Sloan S. D., Steeples D. W. and G. P. Tsoflias, 2009, Ultra-Shallow Imaging Using 3D Seismic Reflection Methods, Near Surface Geophysics, Special Issue on Hydrogeophysics Methods and Processes, Vol. 7, No. 5, p. 307-314.

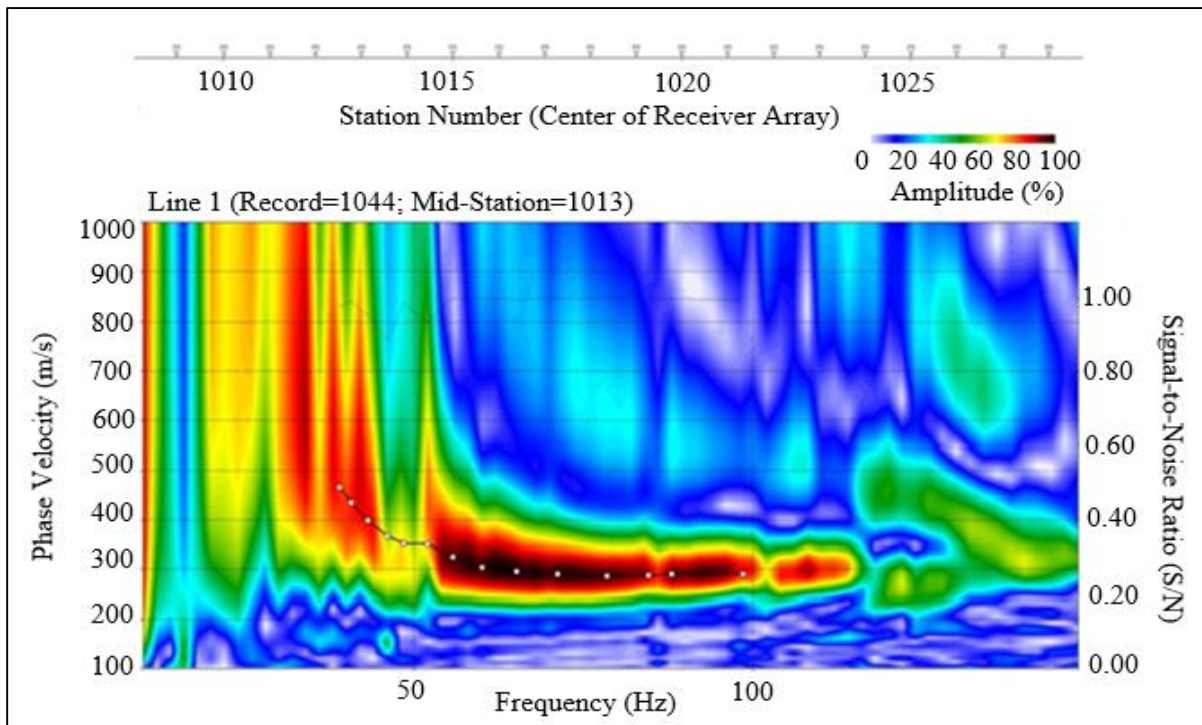
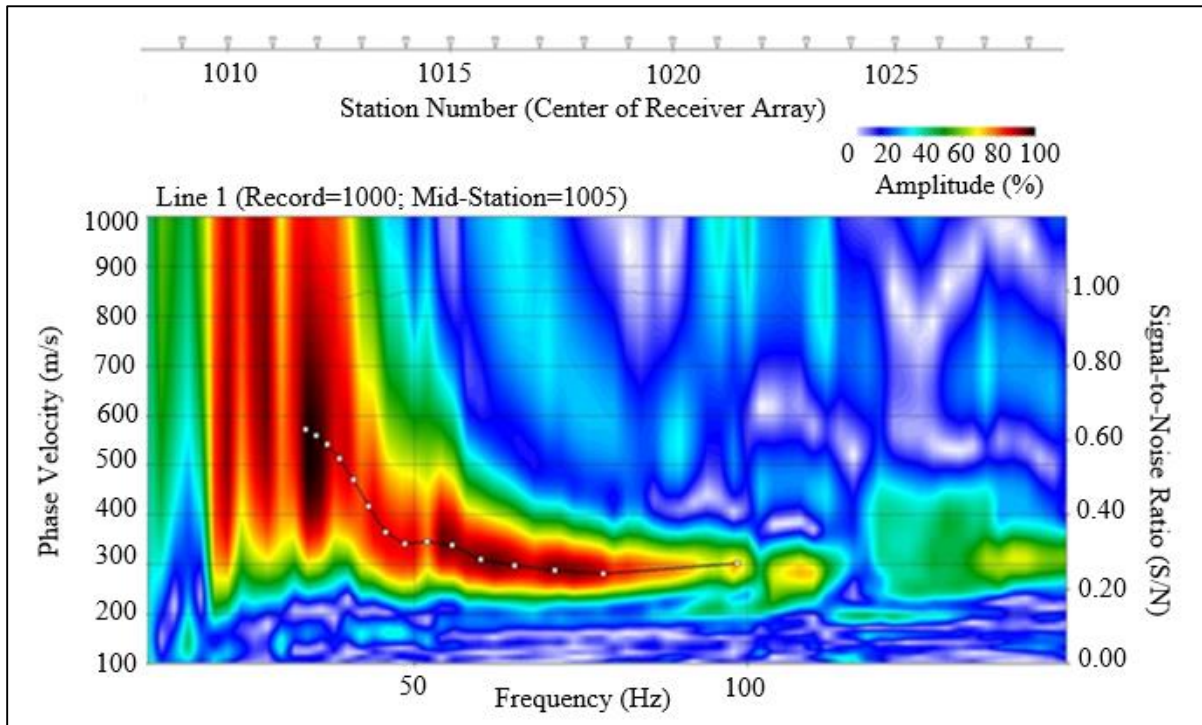
- Spikes, K. T., Vincent, P. D., and D. W. Steeples, 2005, Near-surface commonmidpoint seismic data recorded automatically planted geophones: *Geophysical Research Letters*, 32, L19302.
- Spitzer, R., Green, A. G., and F. O. Nitsche, 2001, Minimizing field operations in shallow 3-D seismic reflection surveying: *Geophysics*, 66, 1761–1773.
- Spitzer, R., Nitsche, F. O., Green, A. G., and H. Horstmeyer, 2003, Efficient acquisition, processing, and interpretation strategy for shallow 3D seismic surveying: A Case Study: *Geophysics*, 68, 1792–1806.
- Steeple, D. W., Baker, G. S., and C. Schmeissner, 1999a, Toward the autojuggie: Planting 72 geophones in 2 sec: *Geophysical Research Letters*, 26, 1085–1088.
- Steeple, D. W., Baker, G. S., Schmeissner, C., and B. K. Macy, 1999b, Geophones on a board: *Geophysics*, 64, 809–814.
- Stokoe, K. H., II, Wright, S. G., Bay, J. A., and Roësset, J. M., 1994, Characterization of geotechnical sites by SASW method, *Geophysical Characterization of Sites*, ed. R. D. Woods, Oxford & IBH Pub. Co., New Delhi, India, 15-25.
- Tian, G.; Steeples, D. W.; Xia, J.; Miller, R. D.; Spikes, K. T.; Ralston, M. D., 2003, Multichannel analysis of surface wave method with the autojuggie, *Soil Dynamics and Earthquake Engineering*, 23: 243 - 247.
- Tian, G.; Steeples, D. W.; Xia, J.; Spikes, K. T., 2003, Useful resorting in surface-wave method with the autojuggie, *Geophysics*, 68: 1906 - 1908.
- Tsoflias, G. P., Steeples, D. W., Czarnecki, G., and Sloan, S. D., 2006, 3-D Autojuggie: automating deployment of two-dimensional geophone arrays for efficient ultra-shallow seismic-reflection surveys, *Geophysical Research Letters*, 33, doi: 10.1029/2006GL025902.
- Van der Pol, C., 1951, Dynamic testing of road constructions, *J. Appl. Chem.*, 1 July, 281–290.
- van der Veen, M., Spitzer, R., Green, A. G., and P. Wild, 2001, Design and application of a towed land-streamer system for cost-effective 2-D and pseudo-3-D shallow seismic data acquisition: *Geophysics*, 66, 482–500.
- Vermeer, G., 1990, *Seismic Wavefield Sampling*, Geophysical Reference 4. Society of Exploration Geophysicists.
- Vermeer, G. J. O., 2002, *3-D Seismic Survey Design*: Geophysical Reference Series, 12, Society of Exploration Geophysicists.

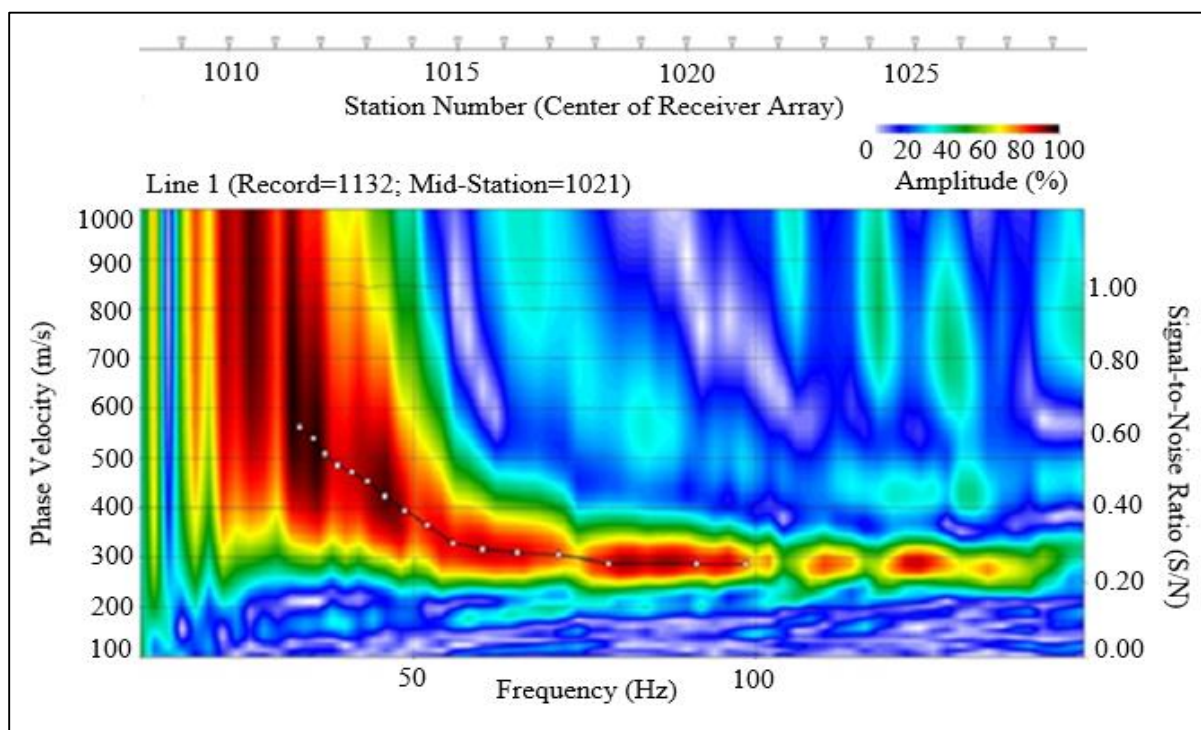
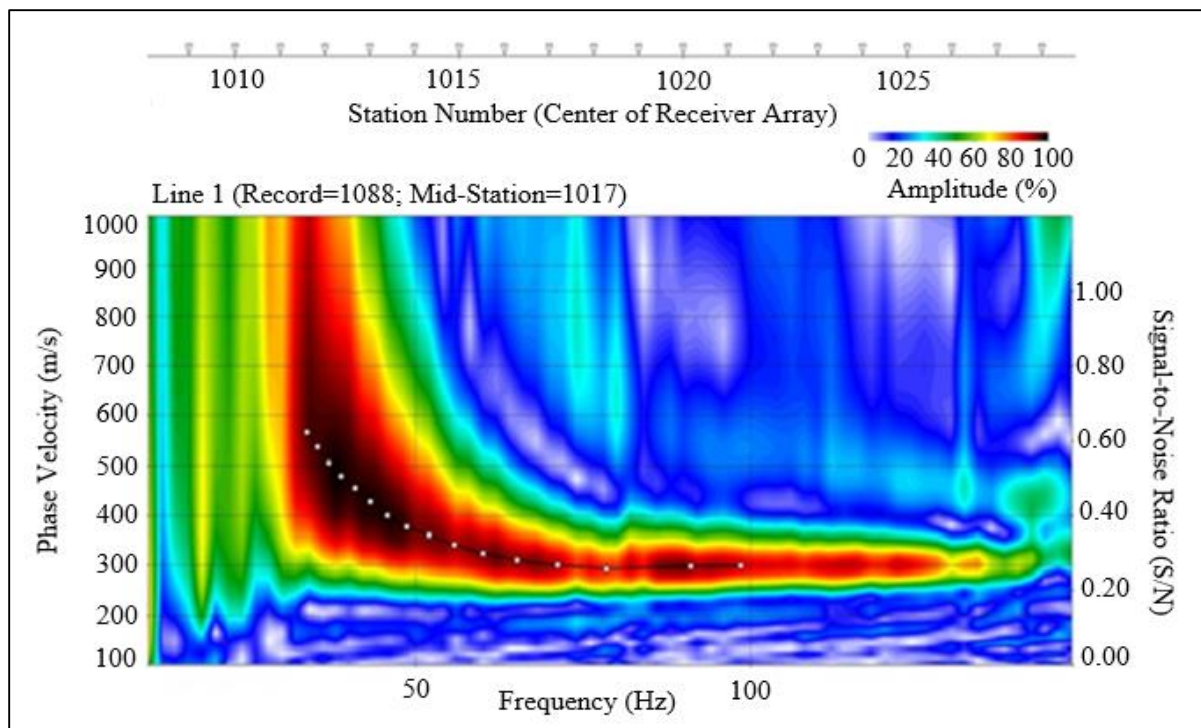
- Vermeer, G.J.O., 1998, 3-D symmetric sampling, *Geophysics* 63, 1629-1647.
- Villella, A. C., Xia, J., and Miller, R. D., 1997, Delineation of salt dissolution sinkholes using minimal deployment shallow 3-D seismic reflection surveying: 67th Annual Meeting, SEG, Expanded Abstracts, 780–783.
- Vincent, P. D., Blair, J. D., Steeples, D. W., and G. P. Tsoflias, 2004, Effect of orientation of hollow-bar-mounted geophones on airwave coherency: 74th Annual International Meeting, SEG, Expanded Abstracts, 1345–1348.
- Vincent, P. D., 2005, Frequency-domain least-squares filtering of data from square tubing mounted geophones: M.S. Thesis, The University of Kansas, Lawrence.
- Vincent P. D., Tsoflias G. P., Steeples D. W. and R. A. Black, 2009, Evaluating the Effect of the Joining Platform to Seismic Data Acquired by Geophones Mounted to Rigid Media, *Journal of Applied Geophysics*, Vol. 68, No. 2, p. 146-150.
- Walton, G., G., 1971, Esso's 3-D seismic proves versatile, *Oil and Gas J.*, 69, No. 13, 139-141.
- Walton, G., G., 1972, Three-dimensional seismic method, *Geophysics*, 37, 417-430.
- Weatherby, B. B., 1948, The history and development of seismic prospecting: in *Geophysical Case Histories*, 1, 7–20, Society of Exploration Geophysicists.
- Weidehold, Helga, 2005, “Poor Man’s 3D” – A simple approach to 3D seismic surveying: A case history, *Near-surface geophysics, Investigations in geophysics*, No. 13, Society of Exploration Geophysicists.
- Xia, Jianghai, Miller, Richard D., and Park, Choon B., 1999, Estimation of near-surface shear-wave velocity by inversion of Rayleigh waves, *Geophysics*, Vol. 64, No. 3, Pg. 691–700.

Appendix A

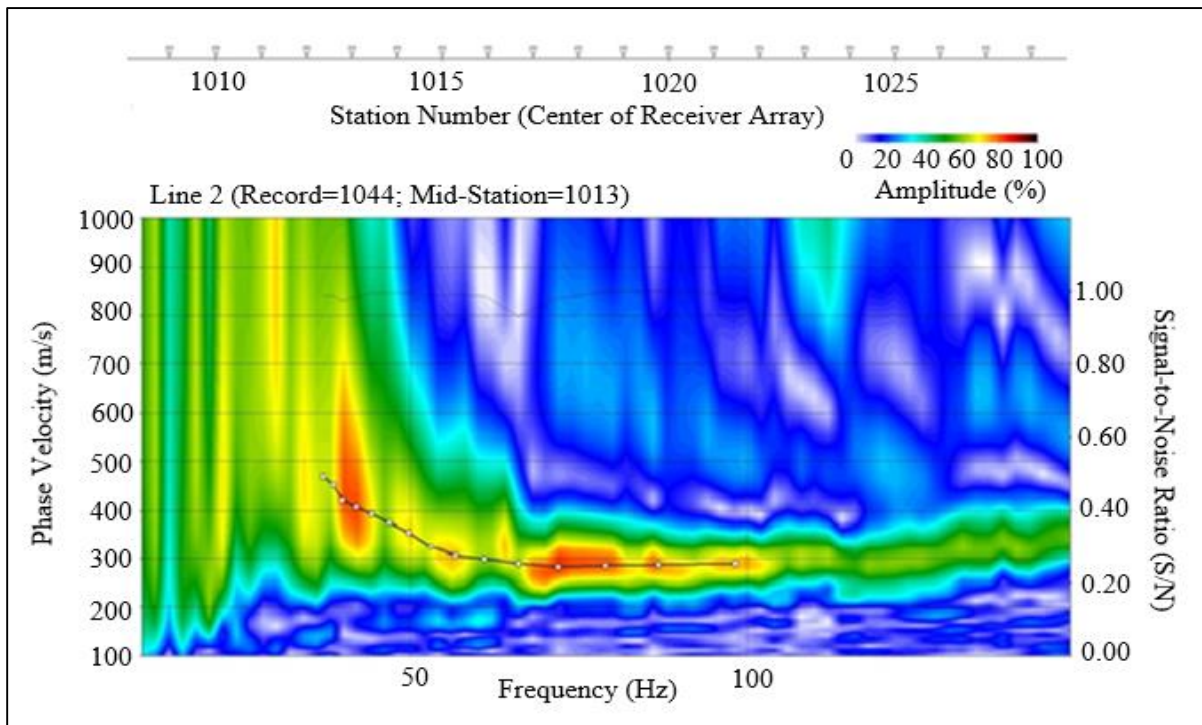
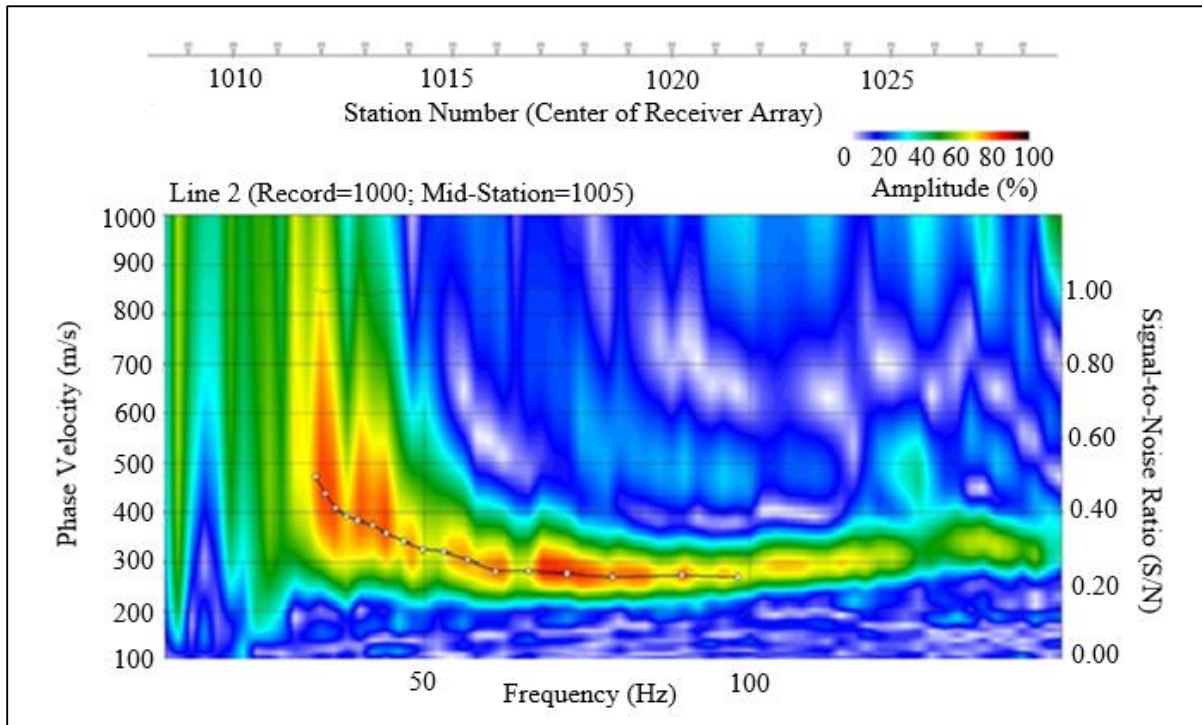
Example MASW Surface Wave Dispersion Curves

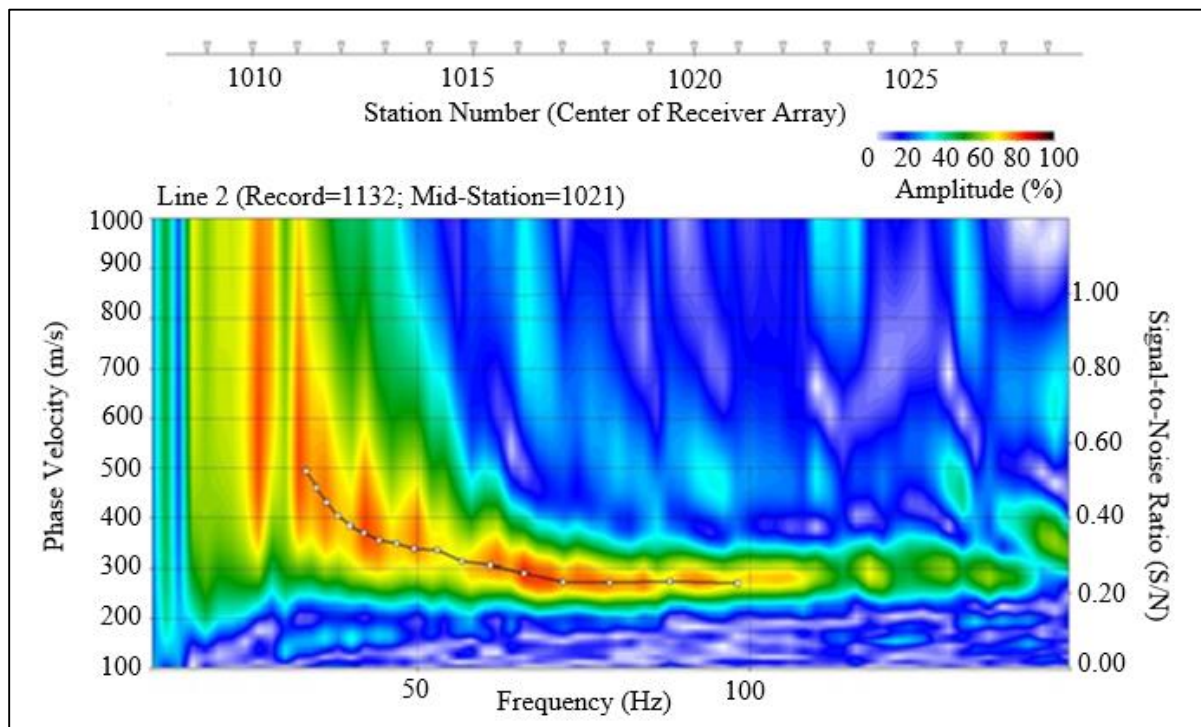
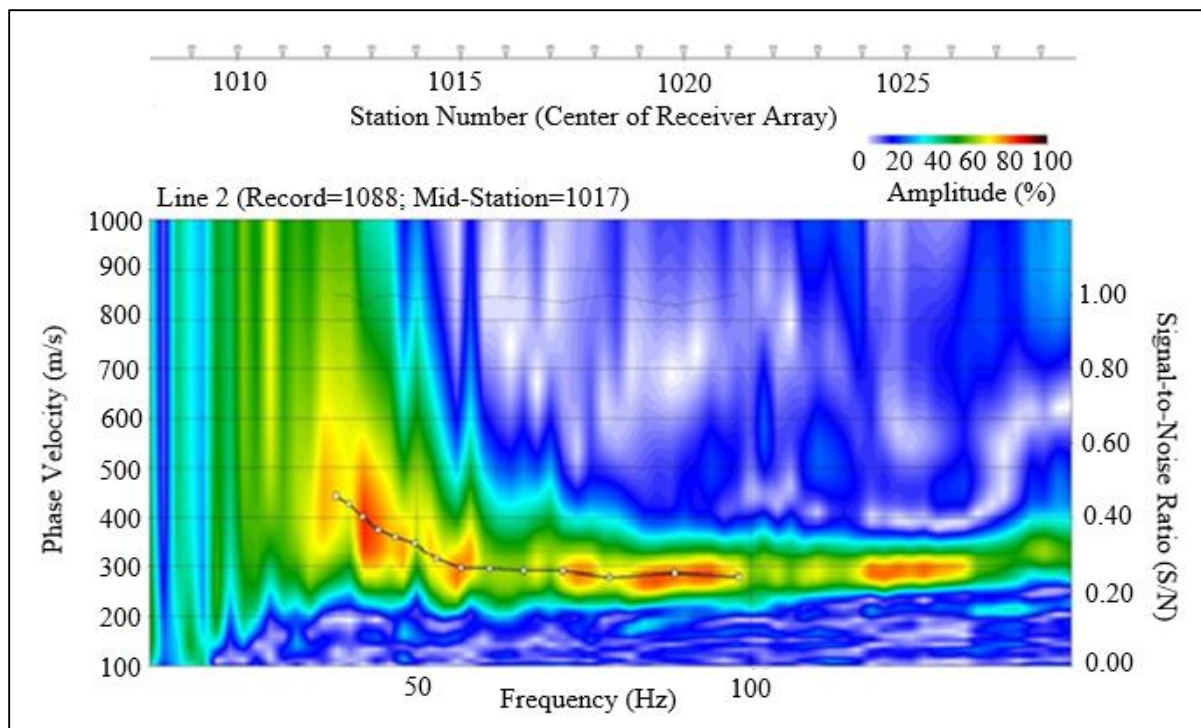
Surface Wave Dispersion Curves (Line 1)



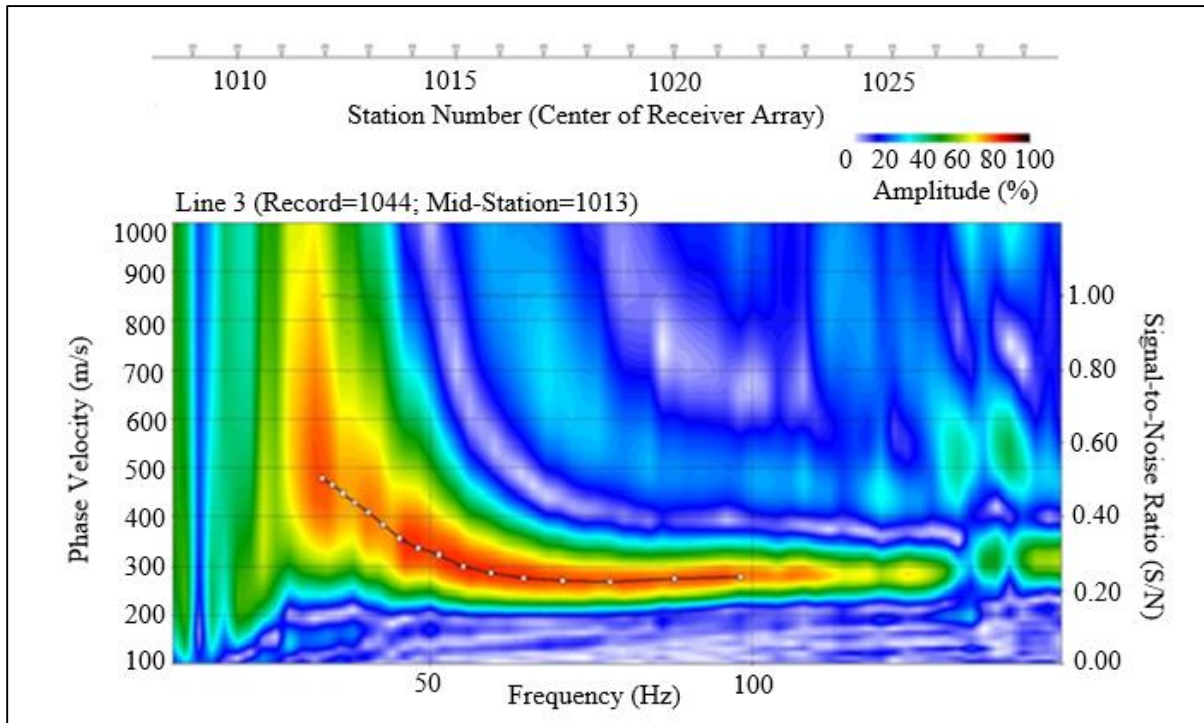
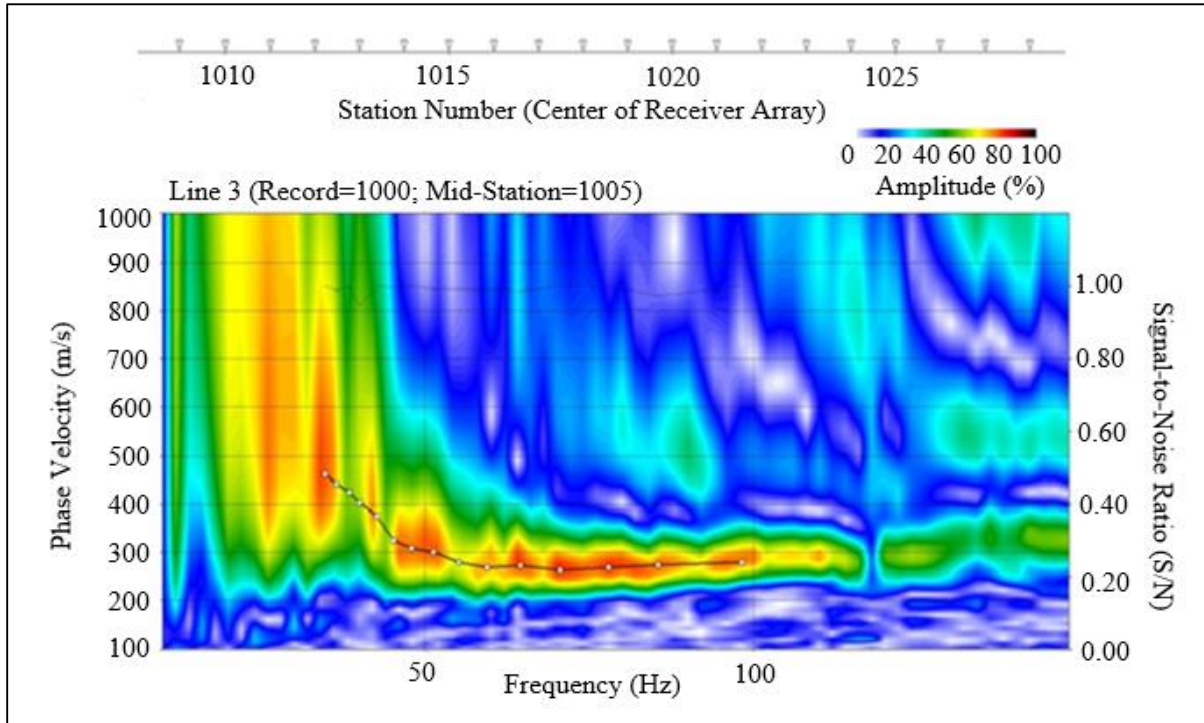


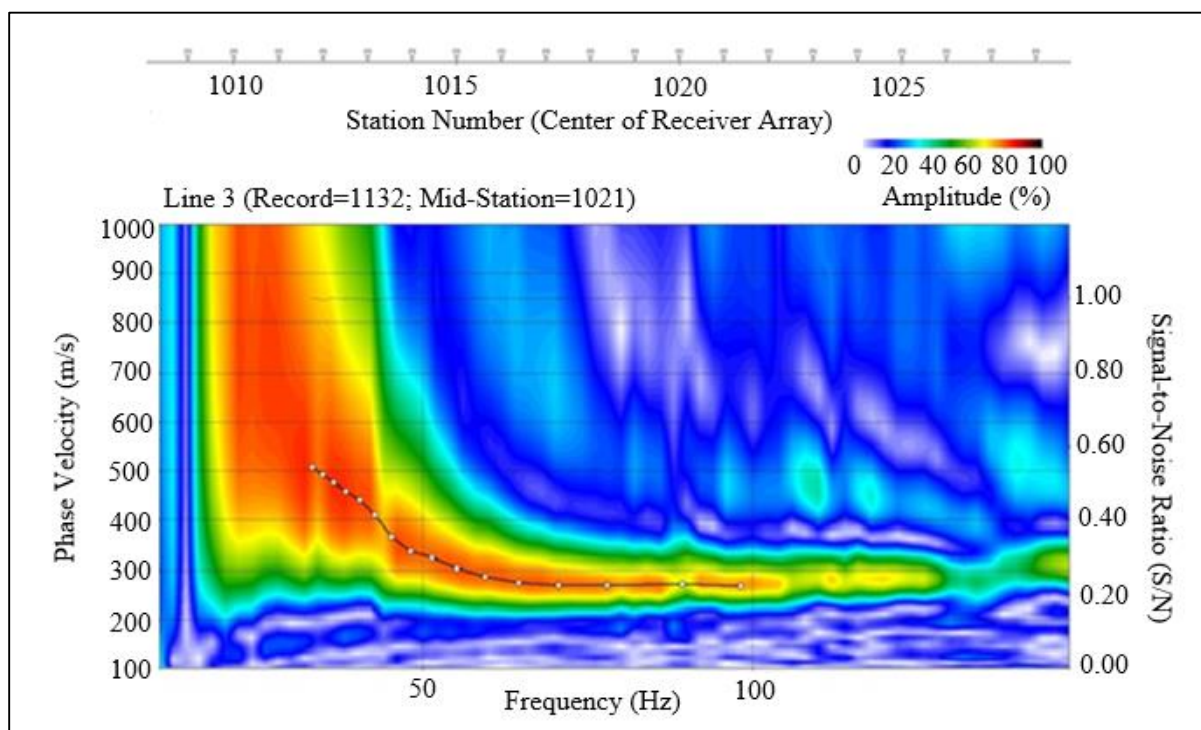
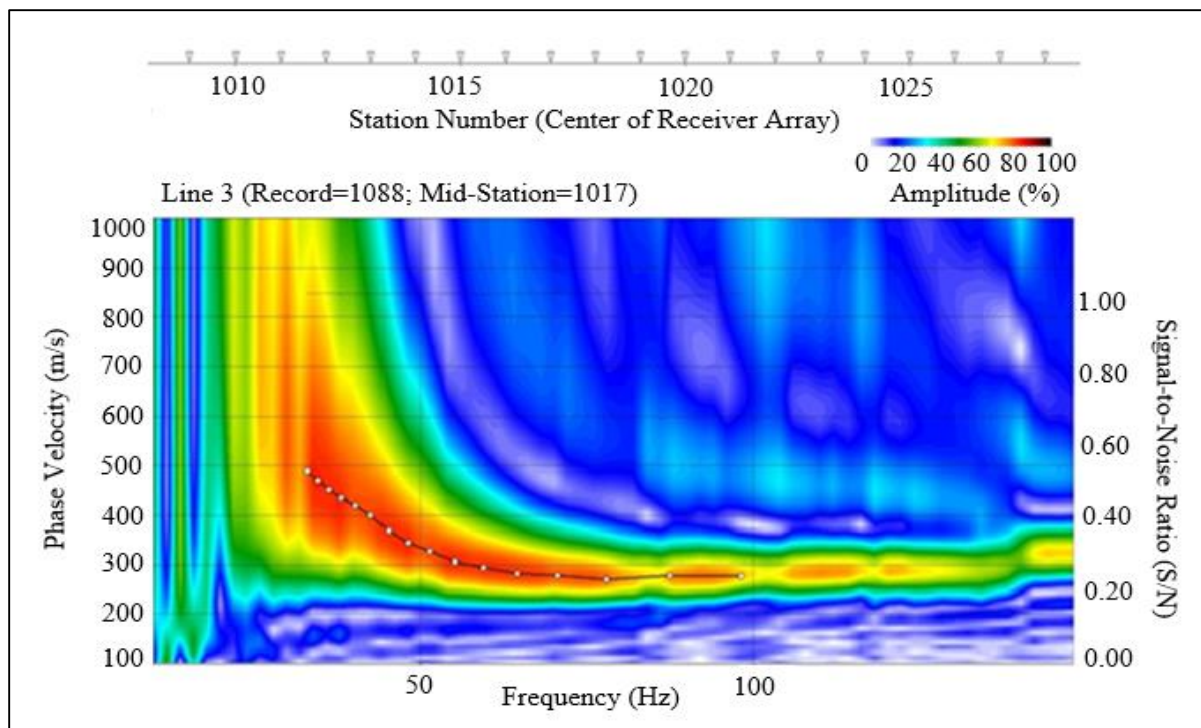
Surface Wave Dispersion Curves (Line 2)





Surface Wave Dispersion Curves (Line 3)

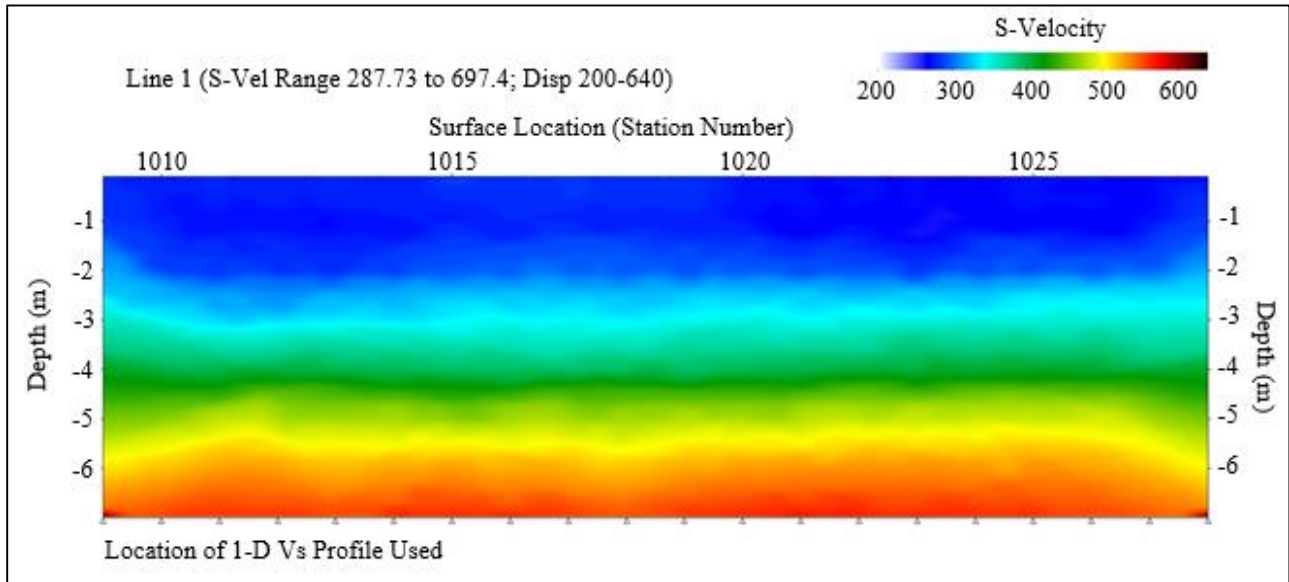




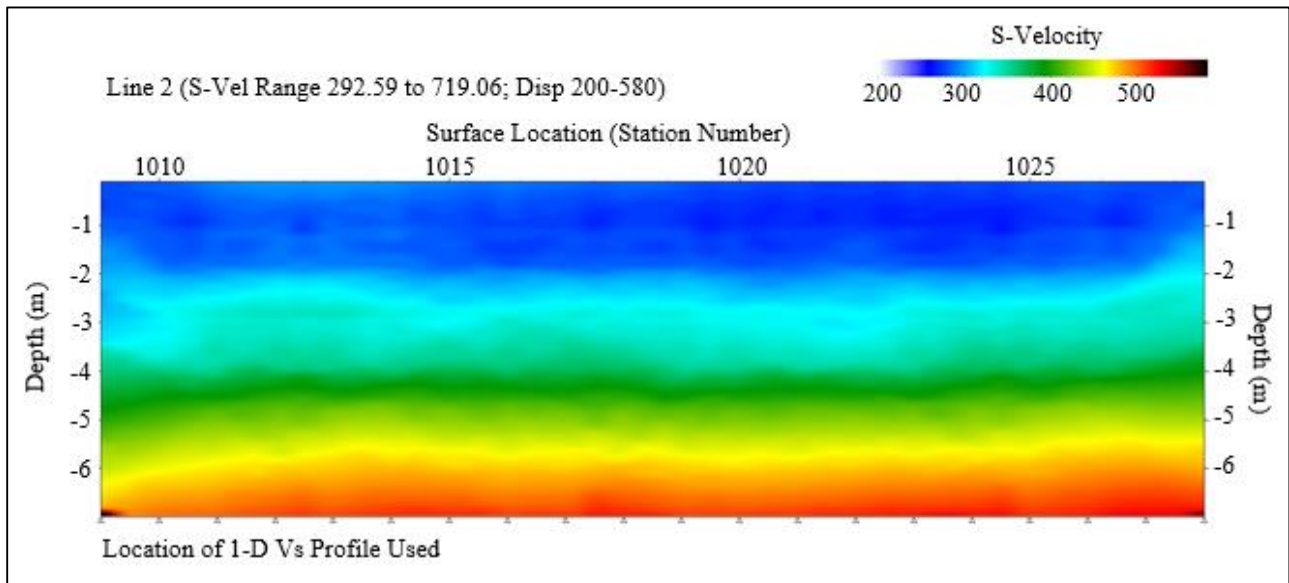
Appendix B

MASW Surface Wave 2D Vs Profiles

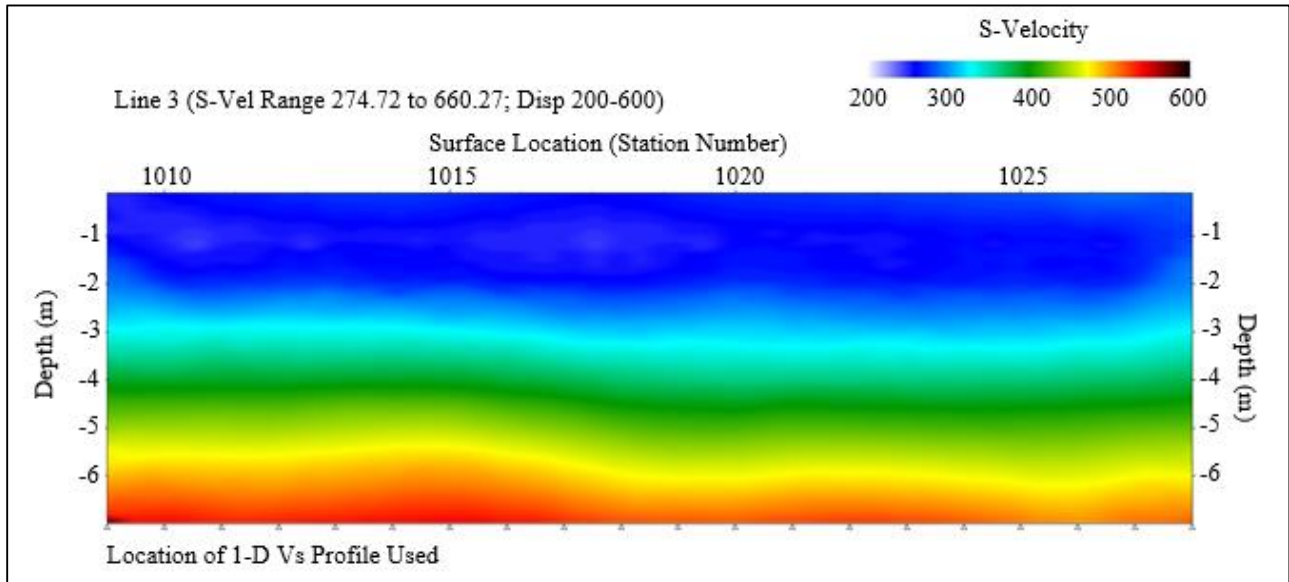
Surface Wave 2D Vs Profile (Line 1)



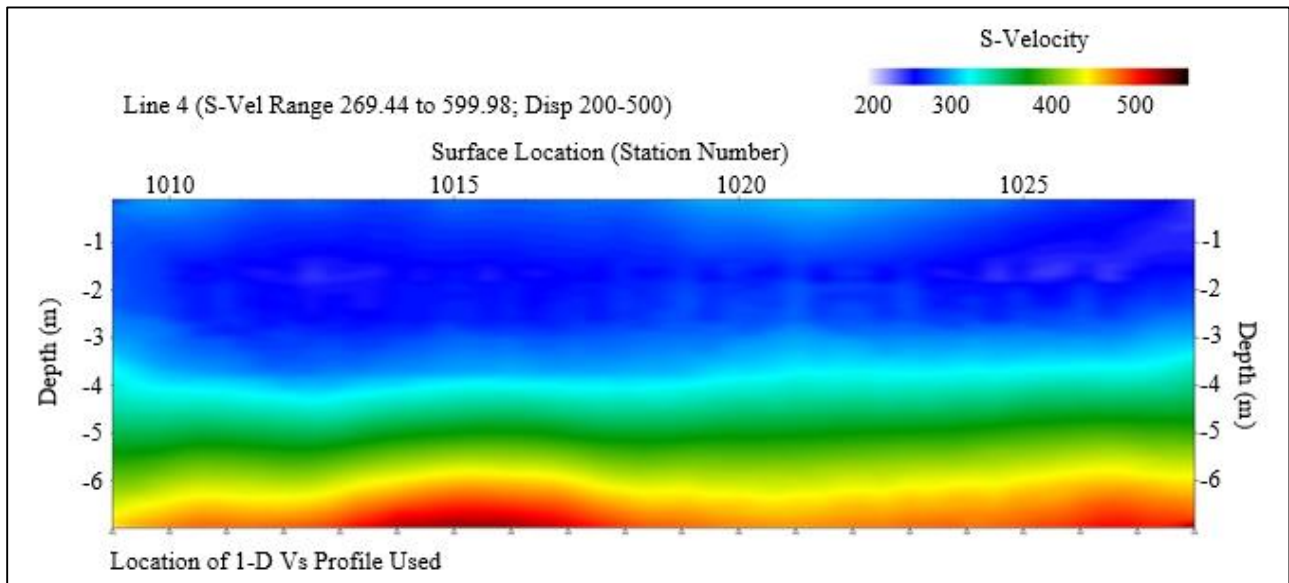
Surface Wave 2D Vs Profile (Line 2)



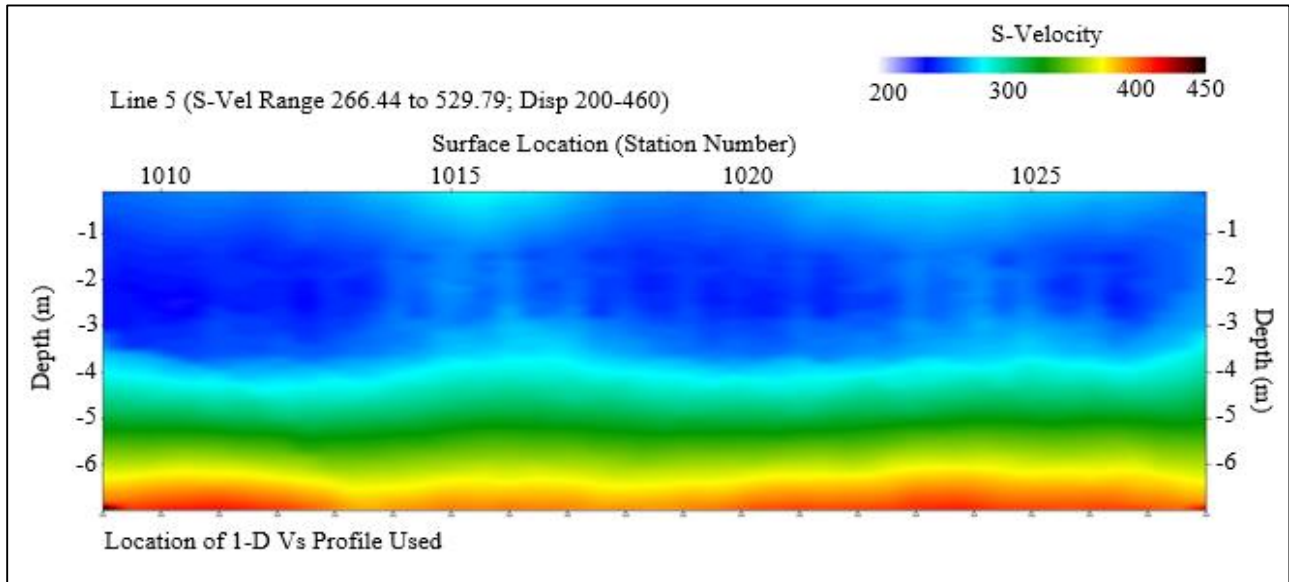
Surface Wave 2D Vs Profile (Line 3)



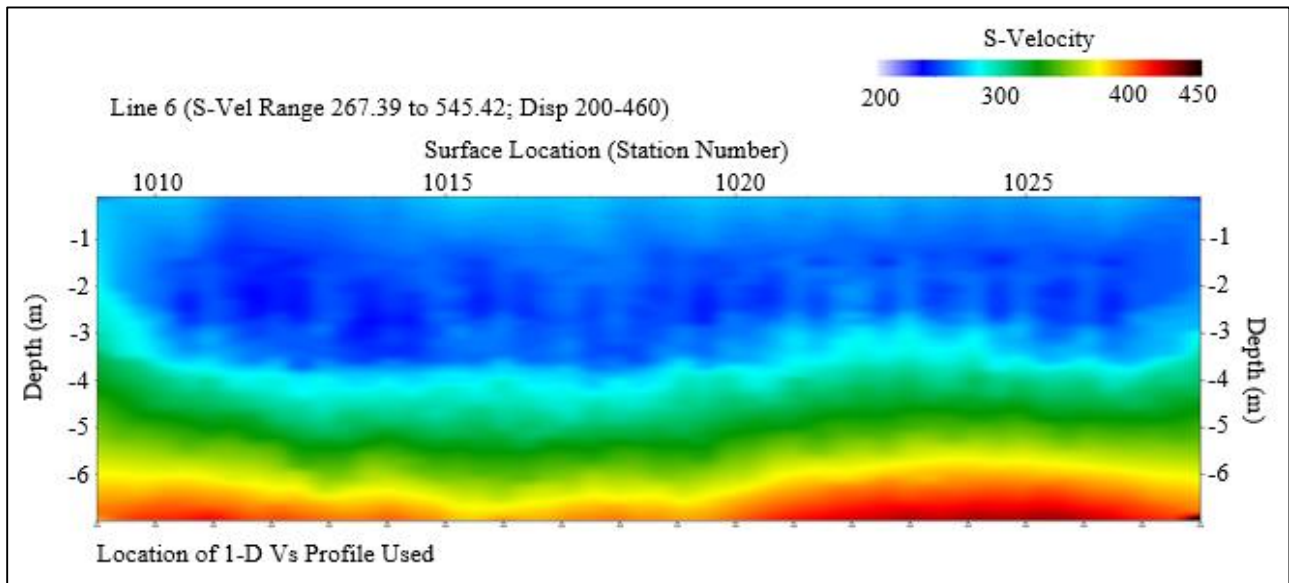
Surface Wave 2D Vs Profile (Line 4)



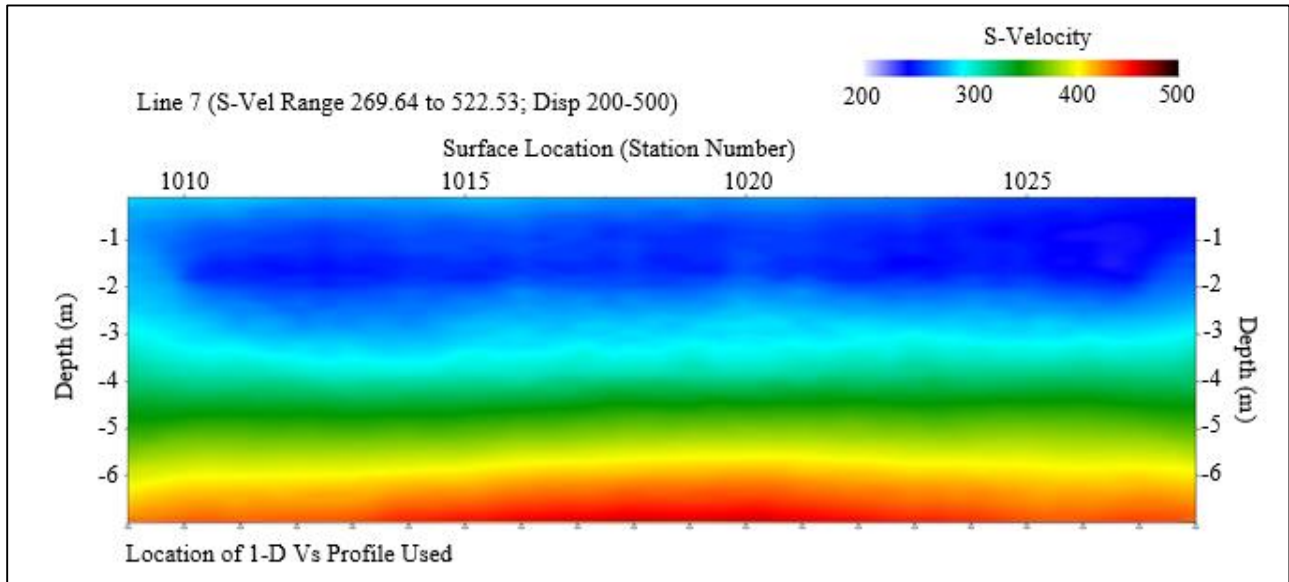
Surface Wave 2D Vs Profile (Line 5)



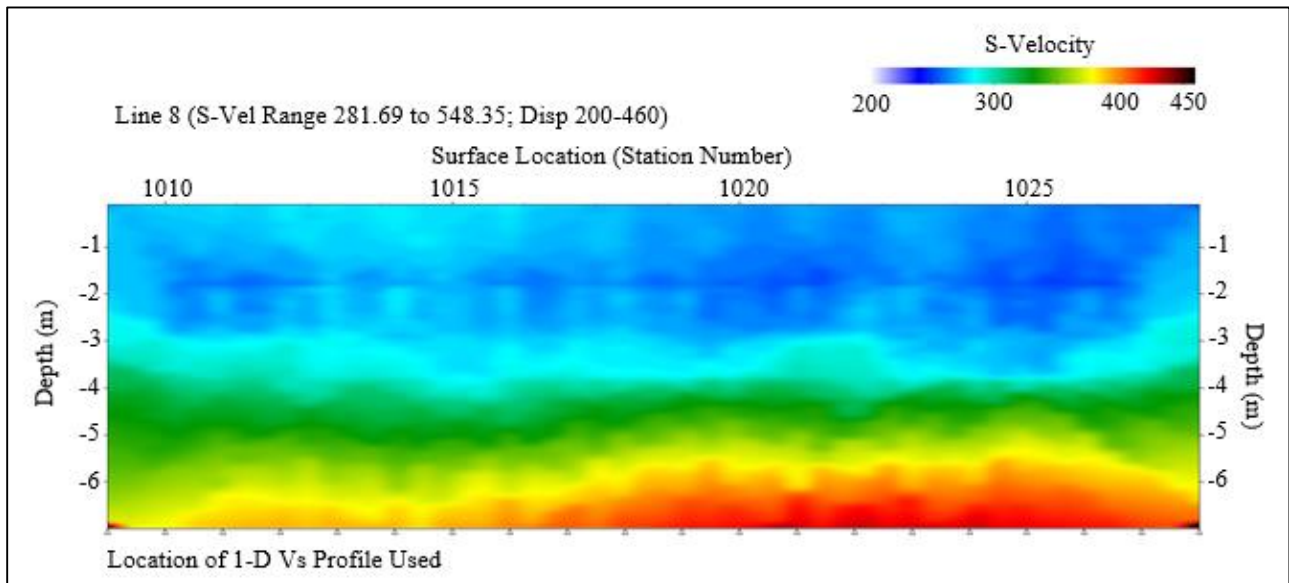
Surface Wave 2D Vs Profile (Line 6)



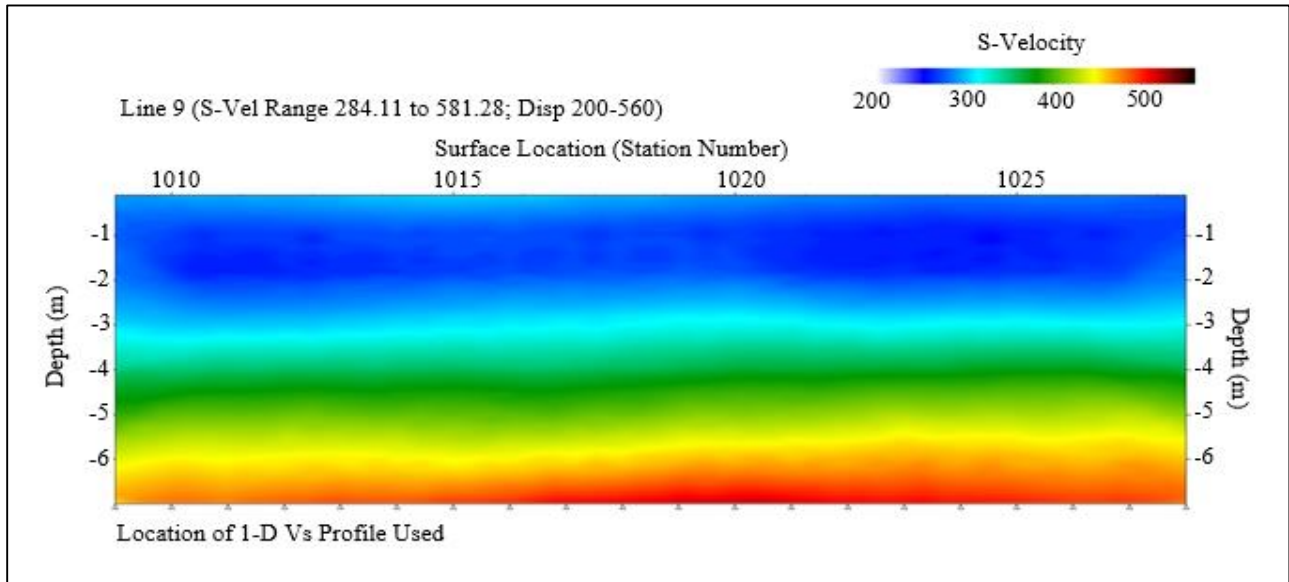
Surface Wave 2D Vs Profile (Line 7)



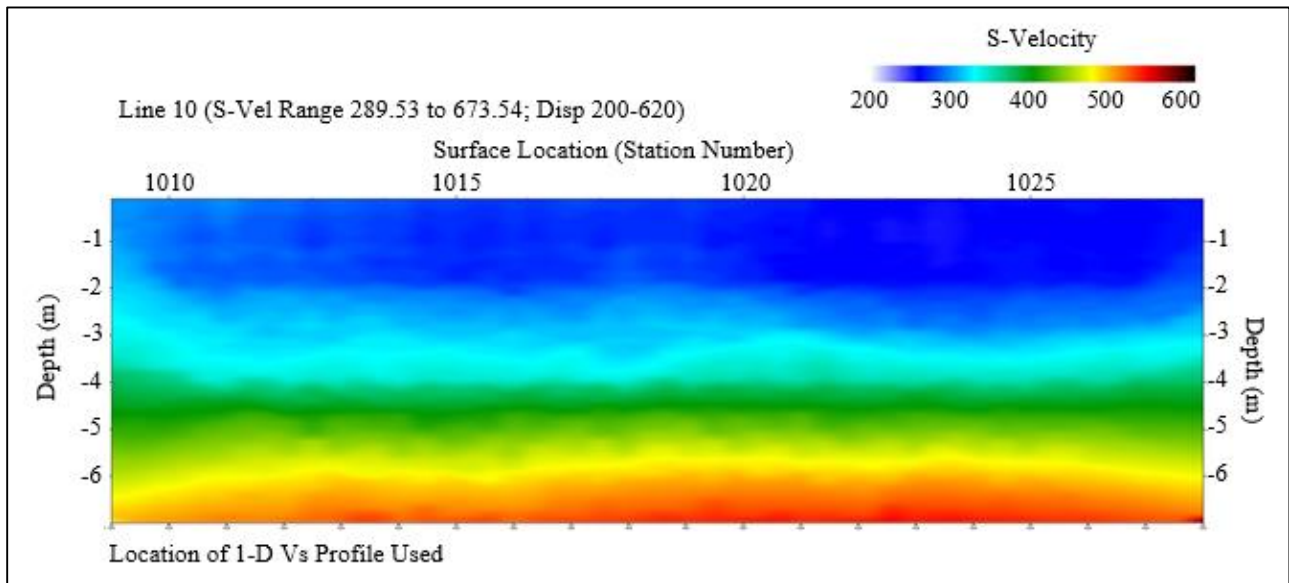
Surface Wave 2D Vs Profile (Line 8)



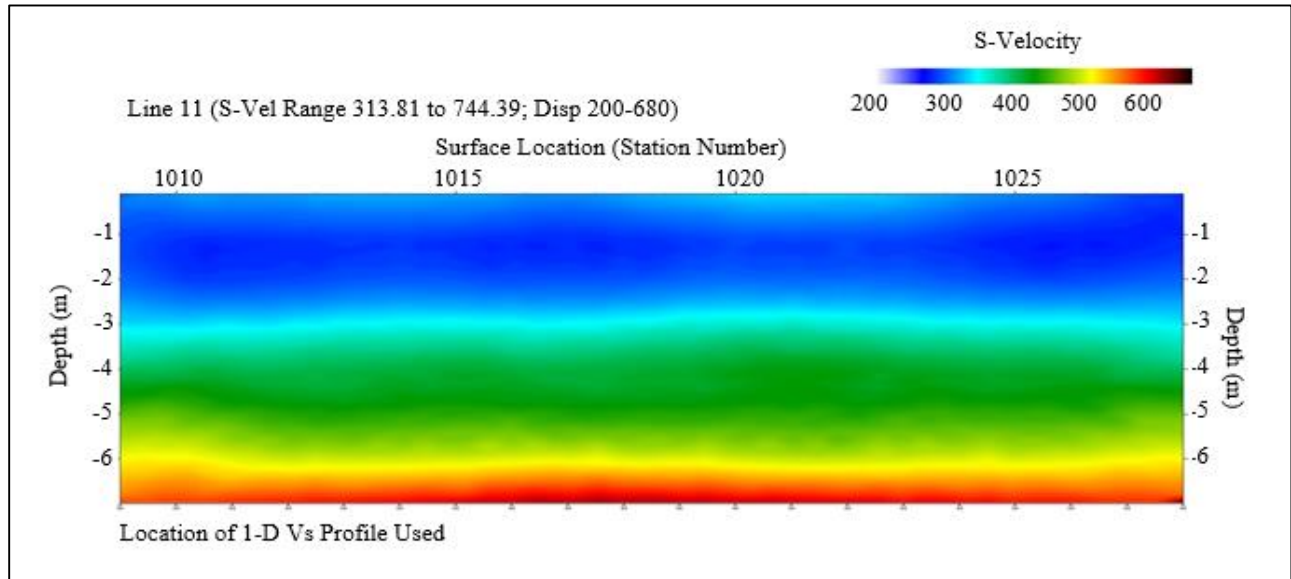
Surface Wave 2D Vs Profile (Line 9)



Surface Wave 2D Vs Profile (Line 10)



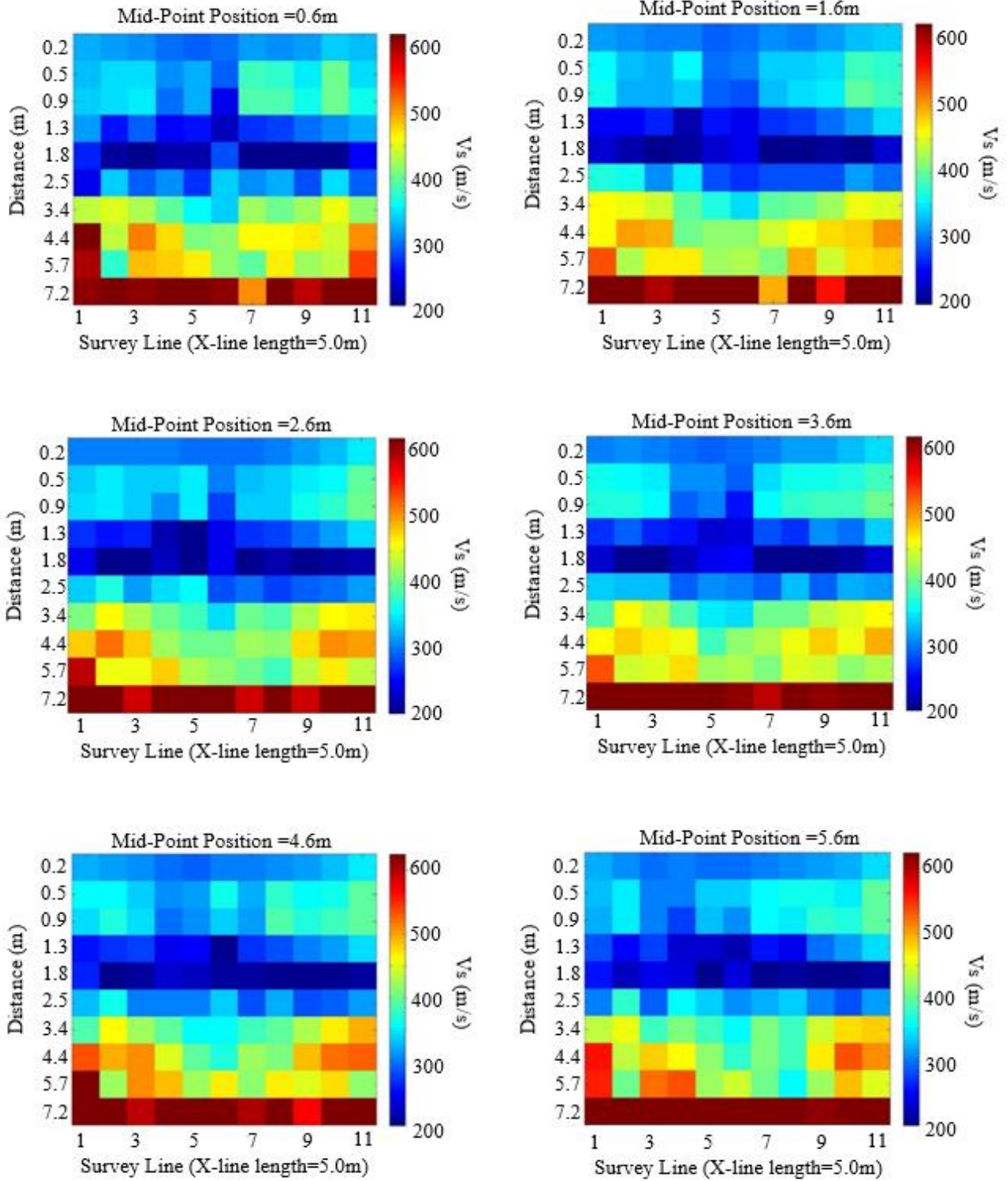
Surface Wave 2D Vs Profile (Line 11)

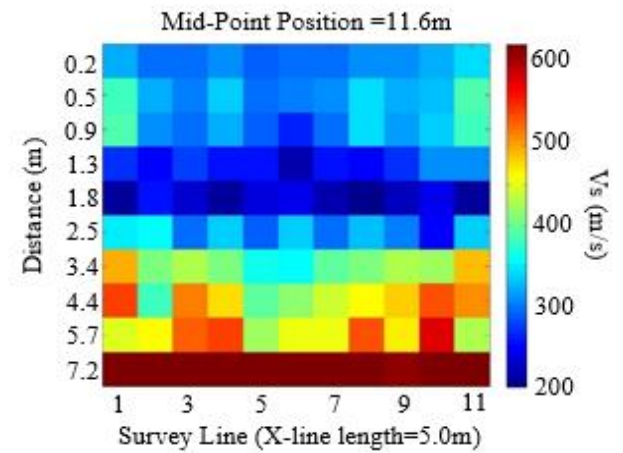
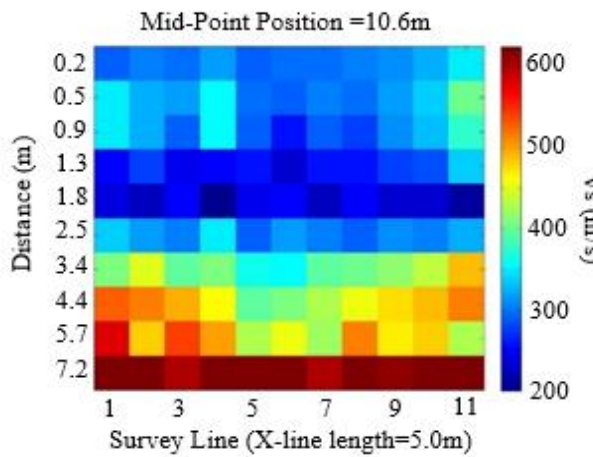
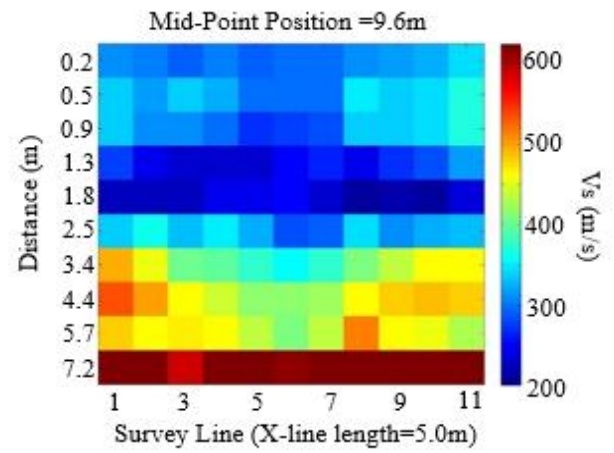
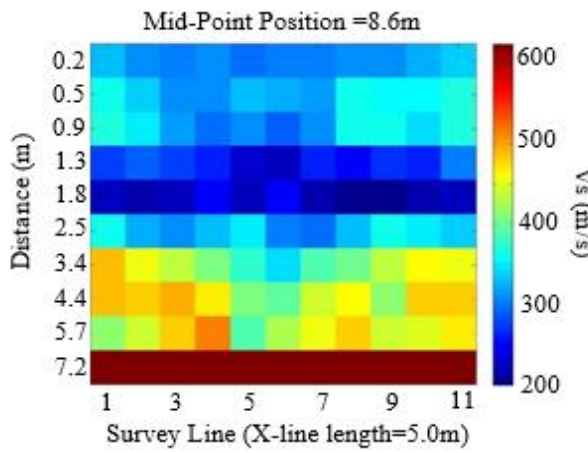
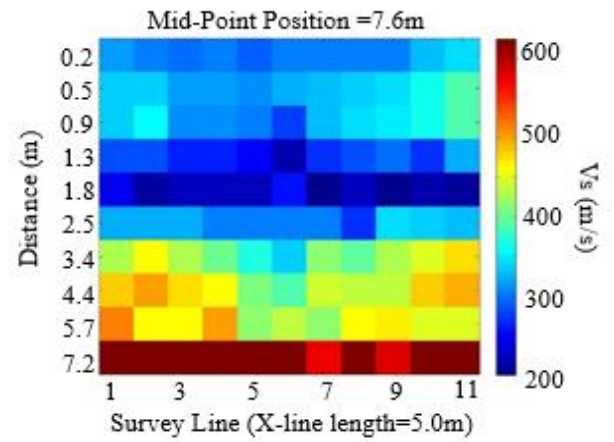
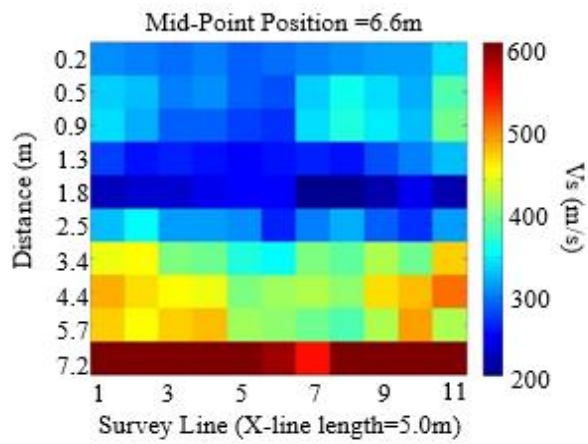


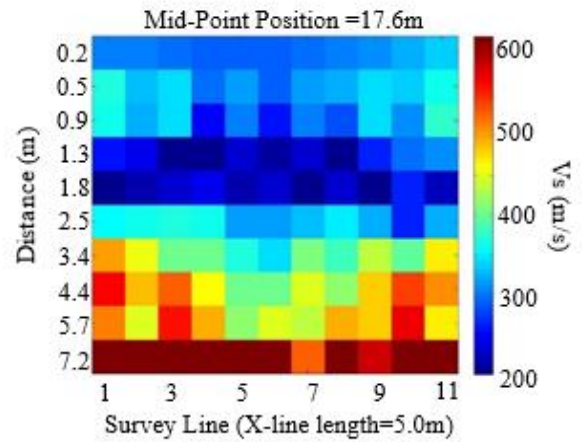
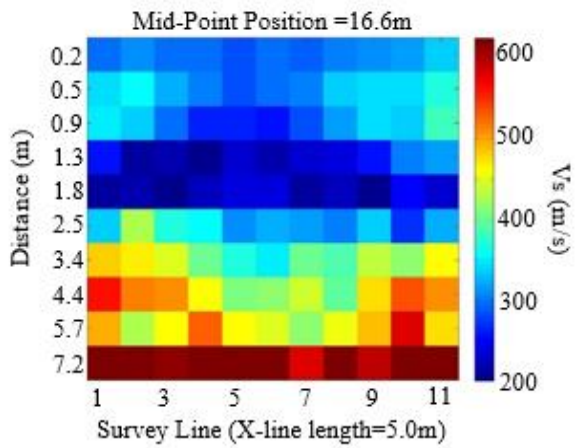
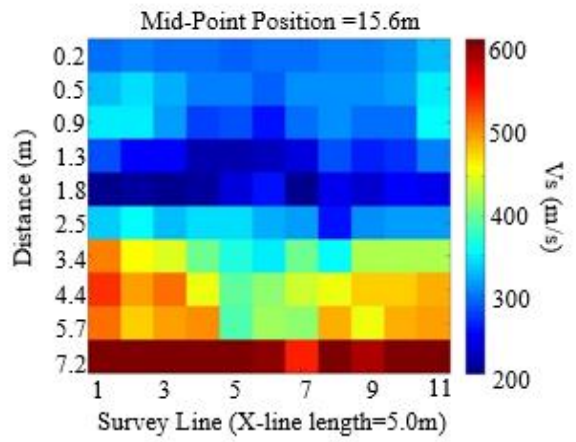
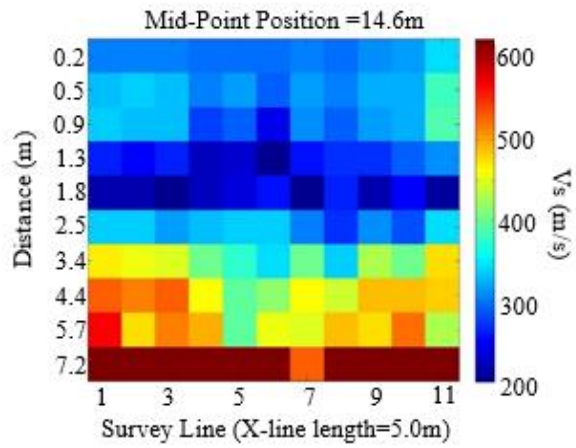
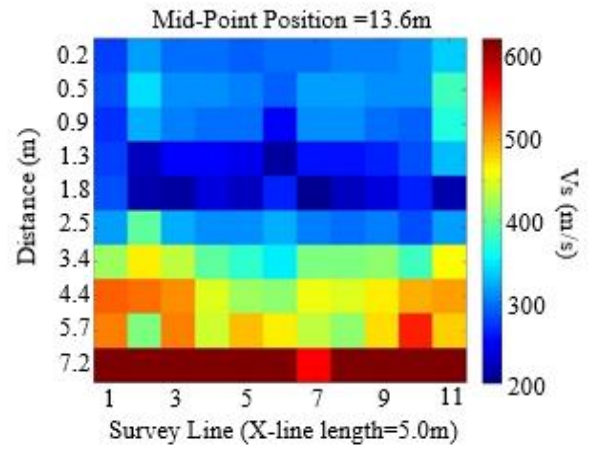
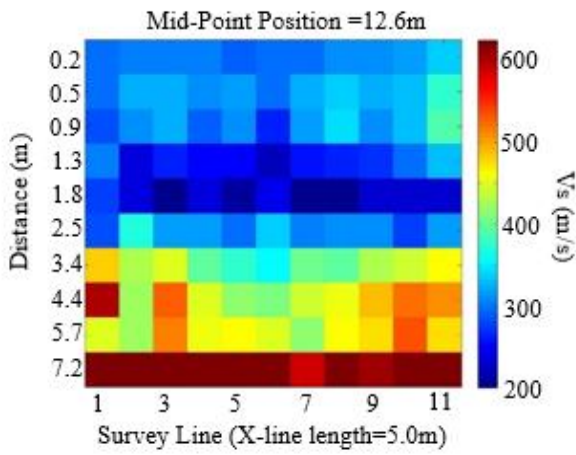
Appendix C

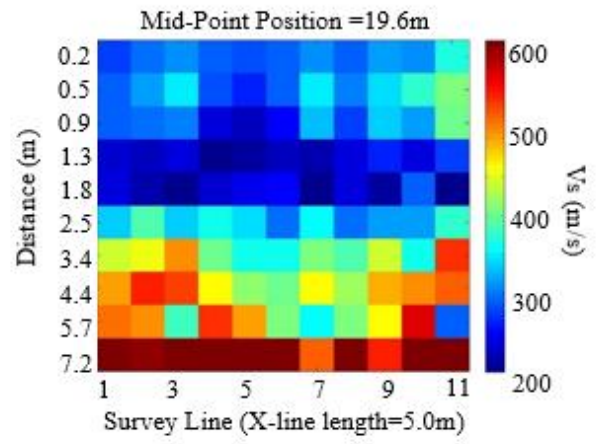
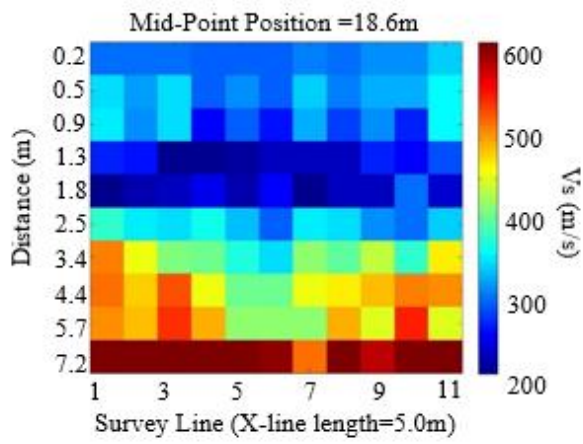
MASW Surface Wave Pseudo-3D Profiles

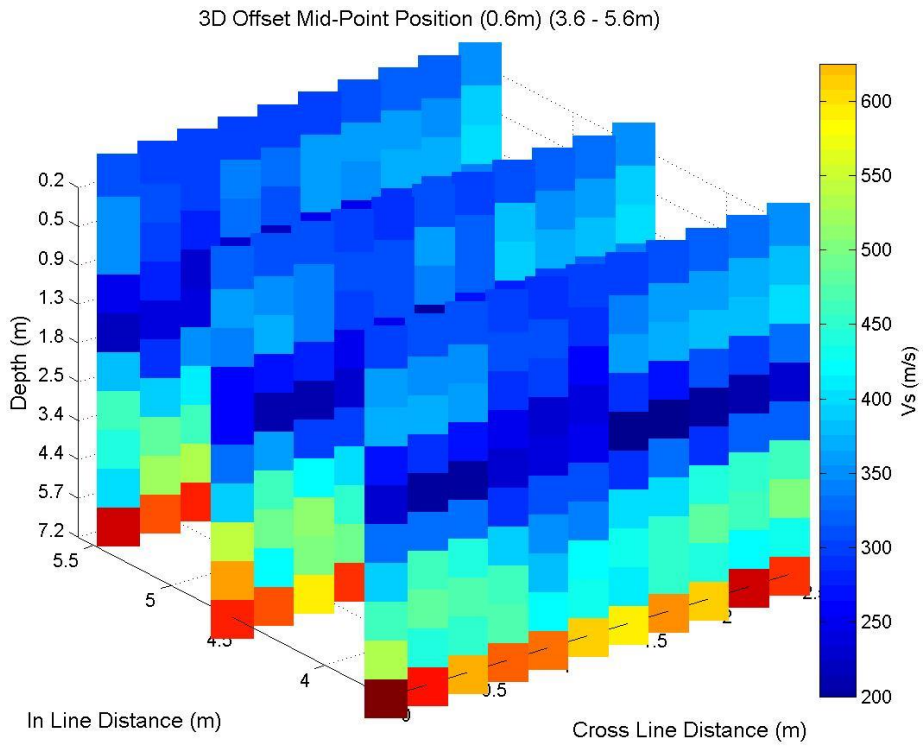
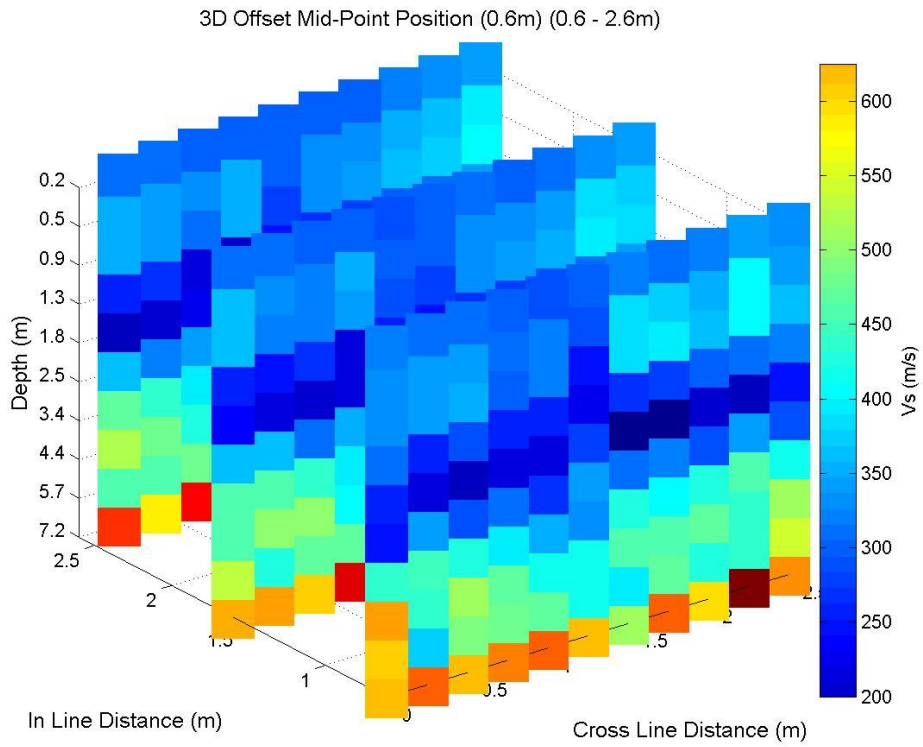
Cross Line (vertical) Vs Profiles

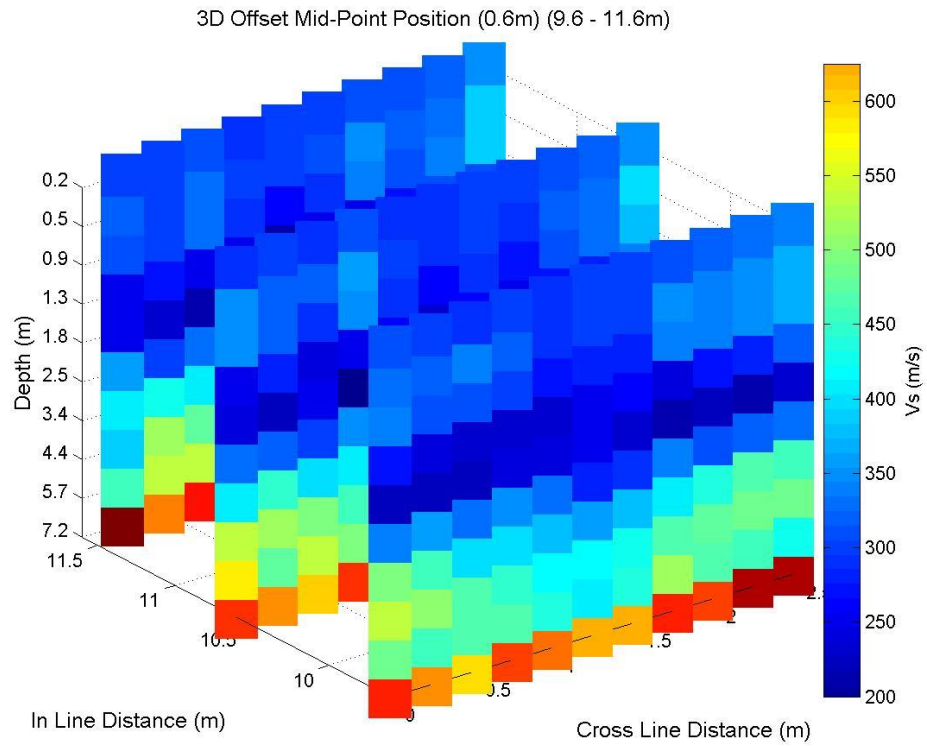
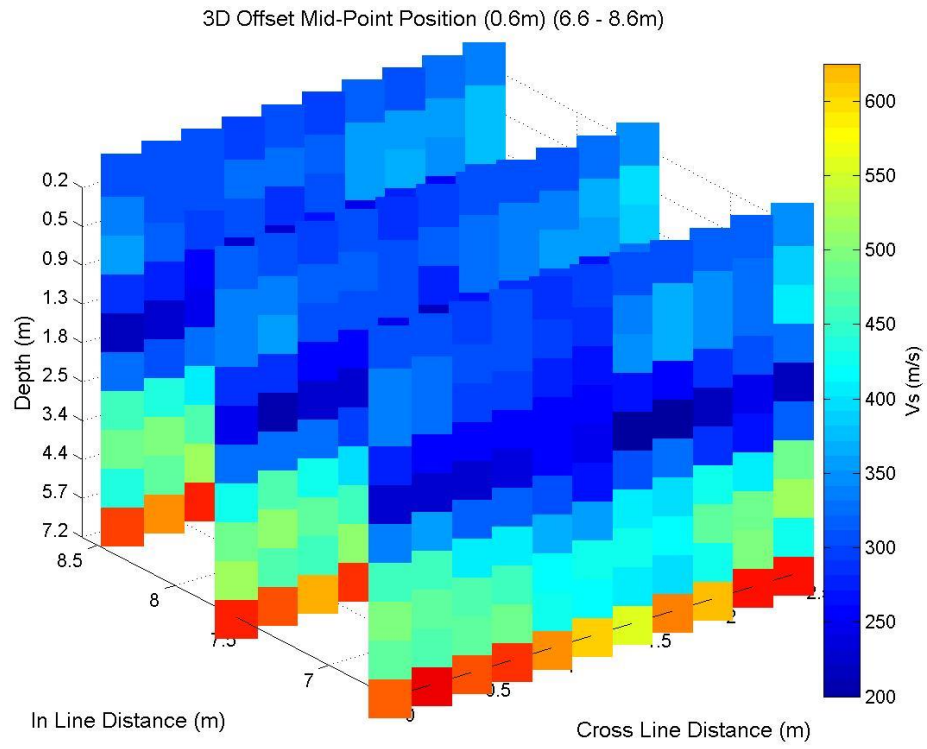


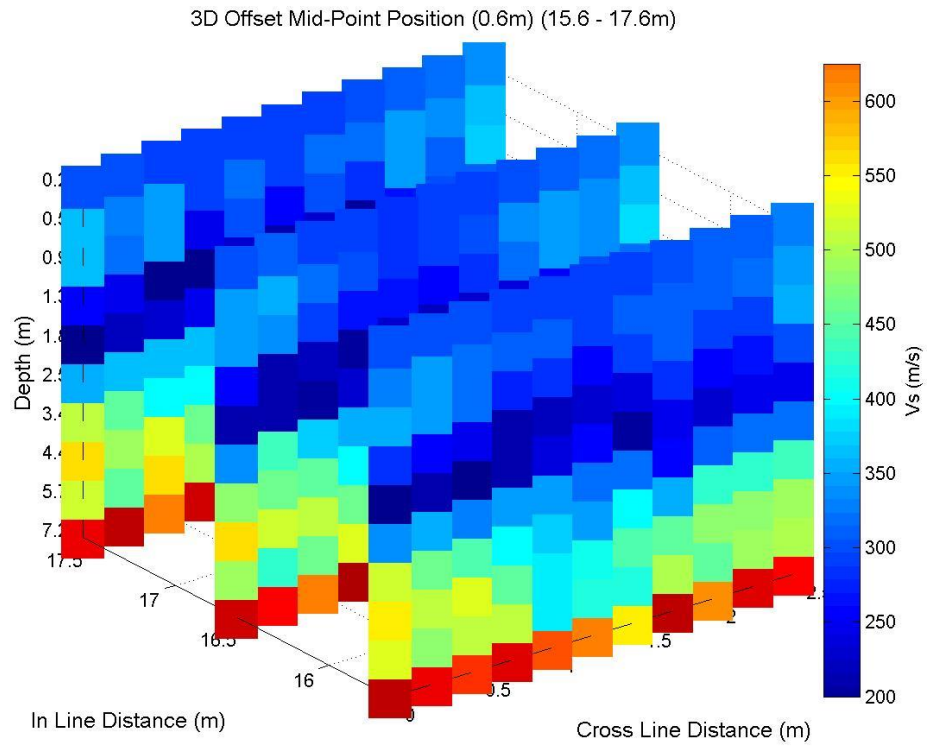
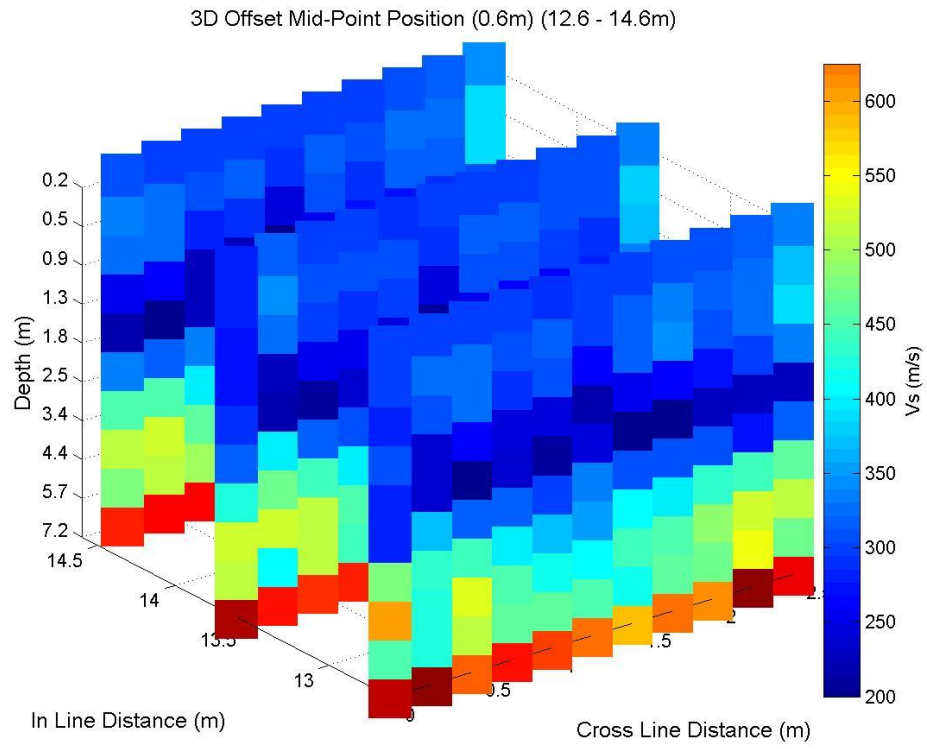


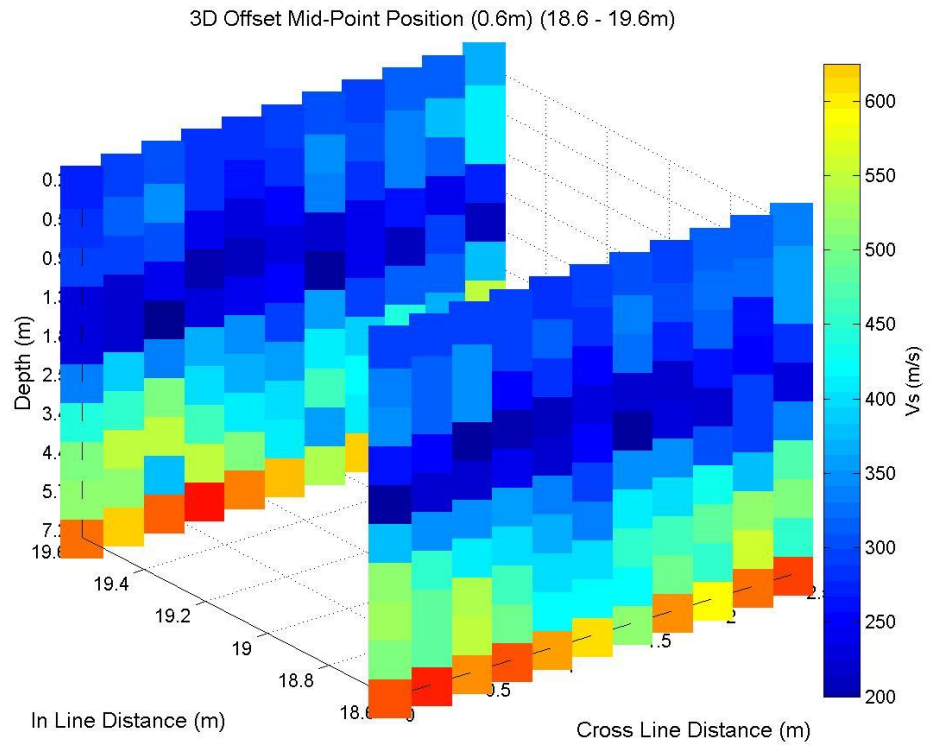




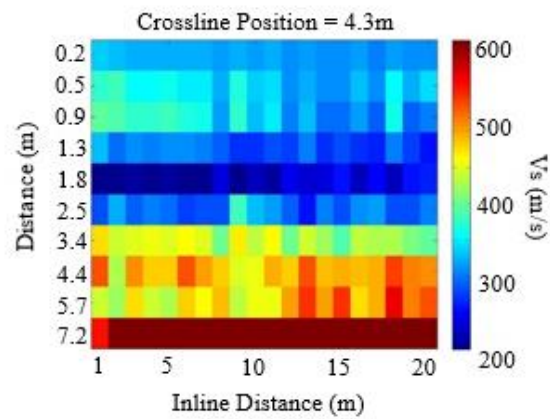
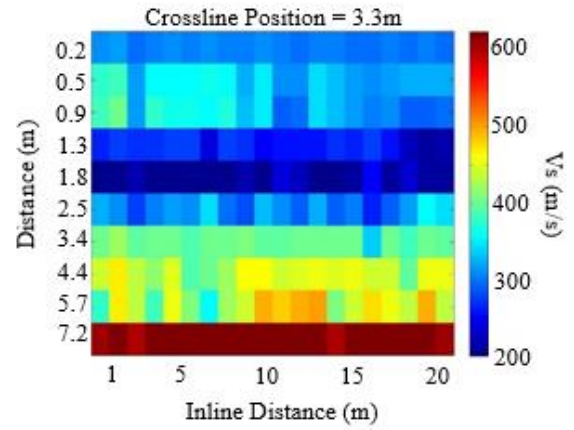
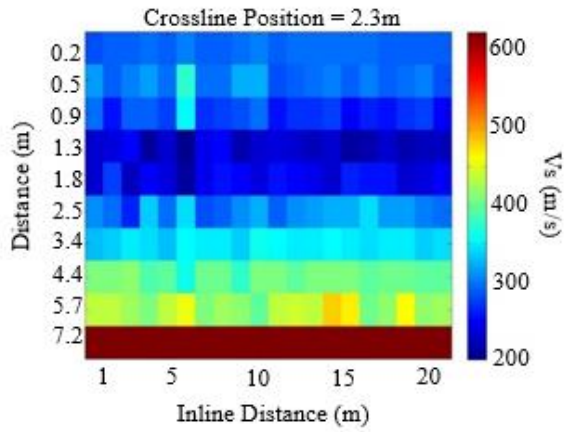
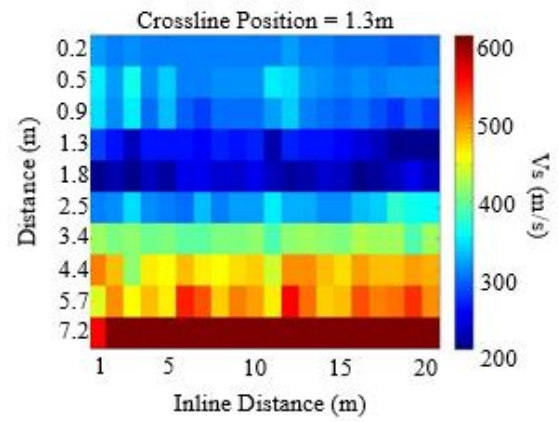
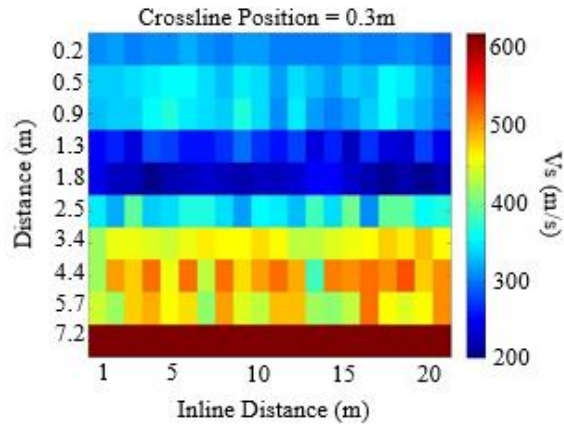


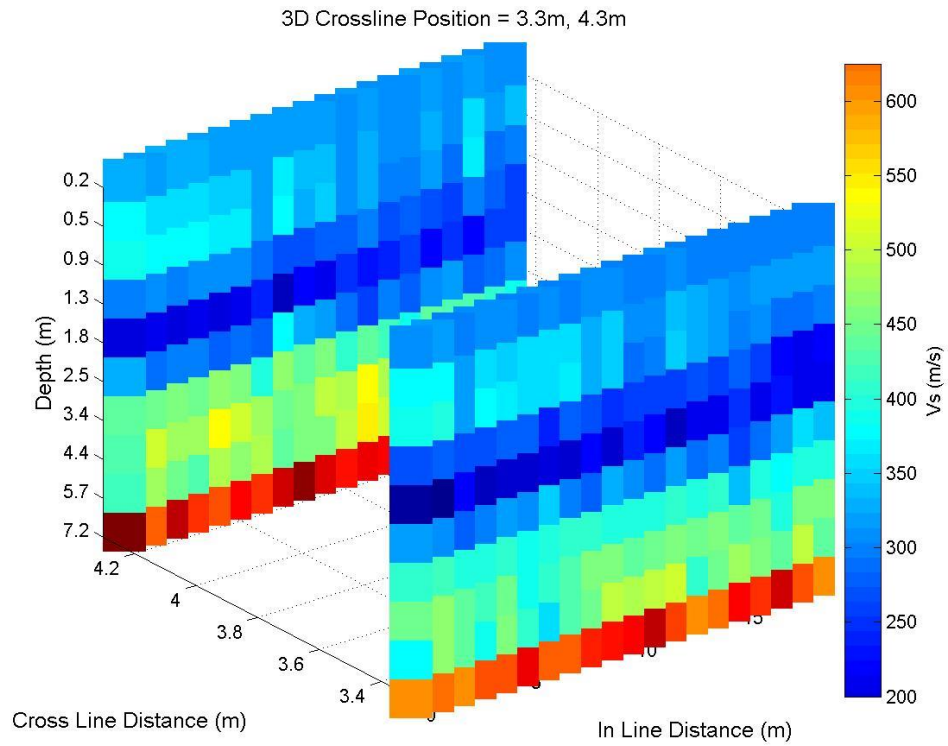
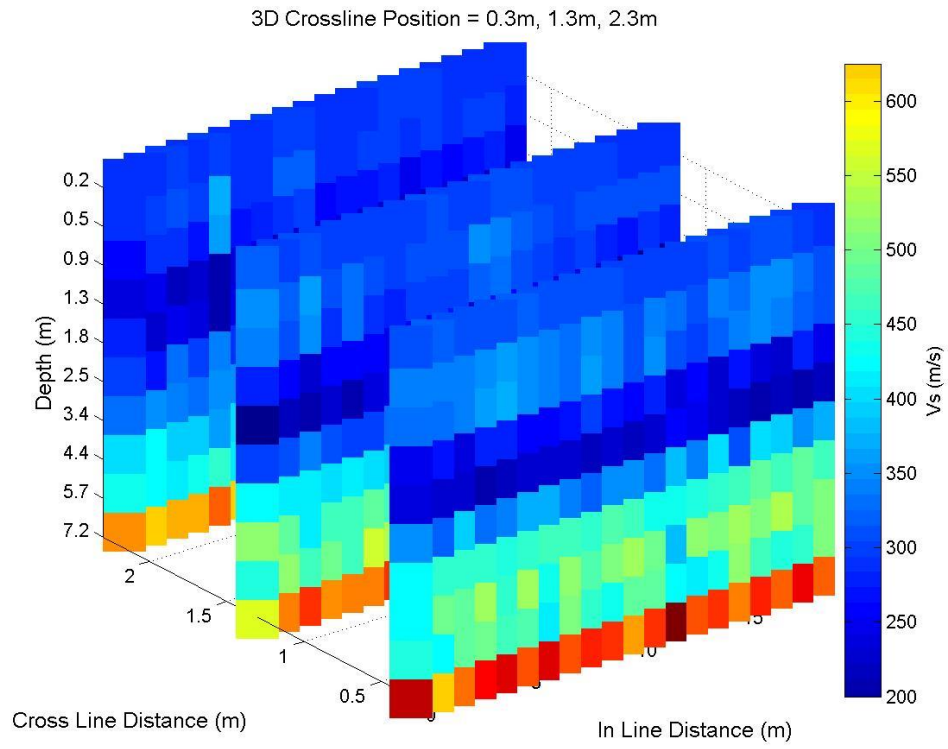




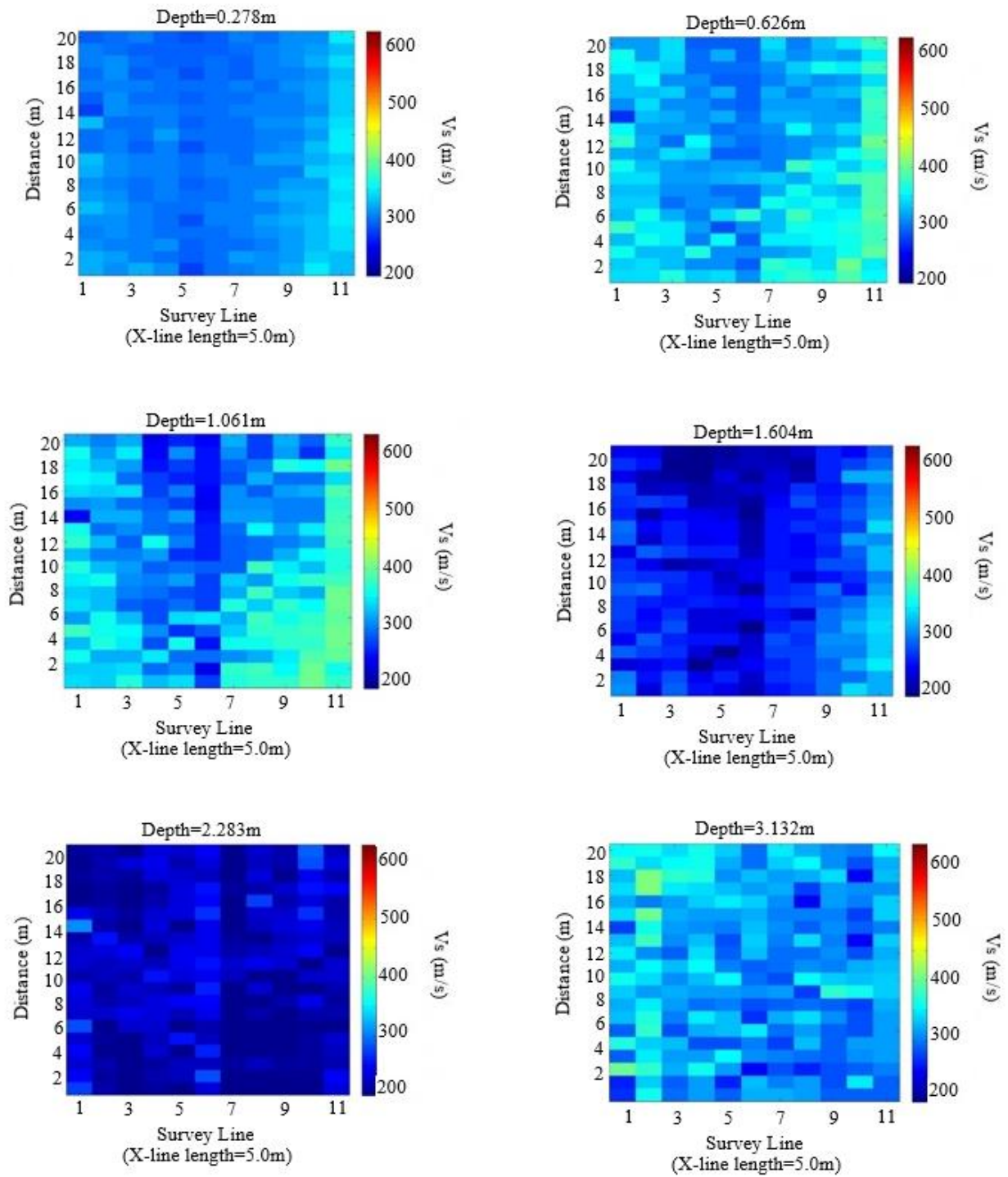


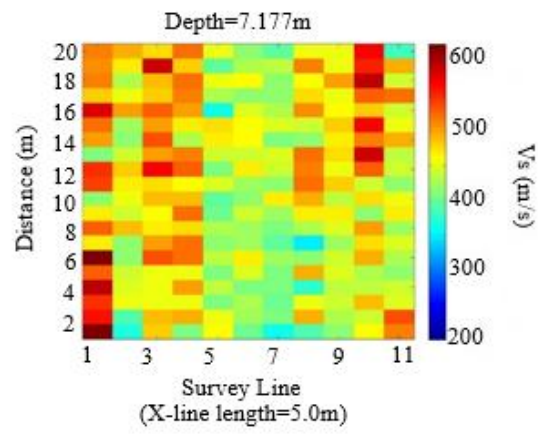
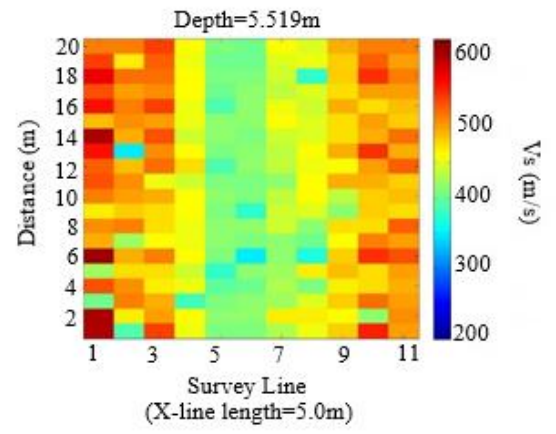
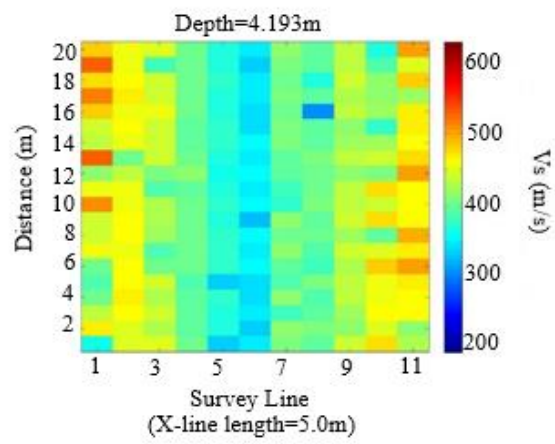
In Line (vertical) Vs Profiles



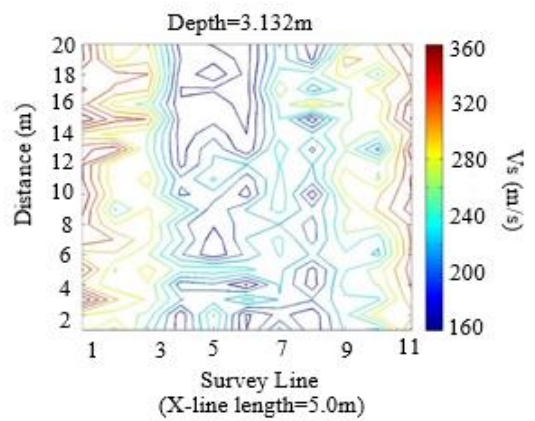
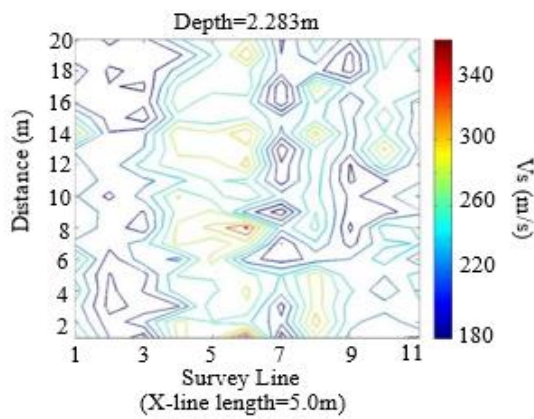
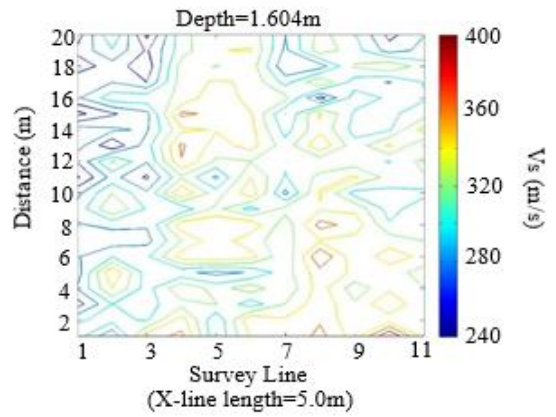
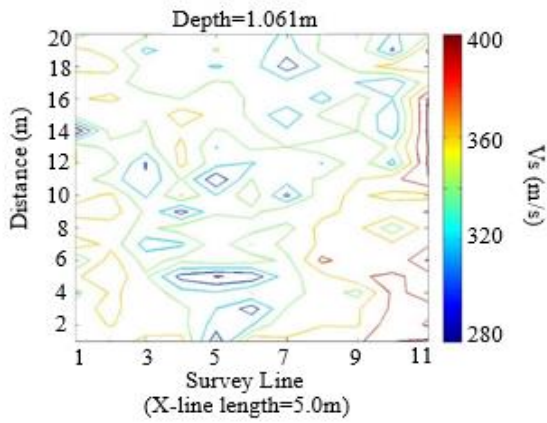
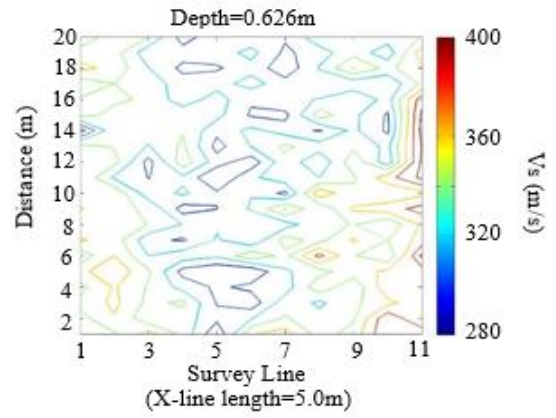
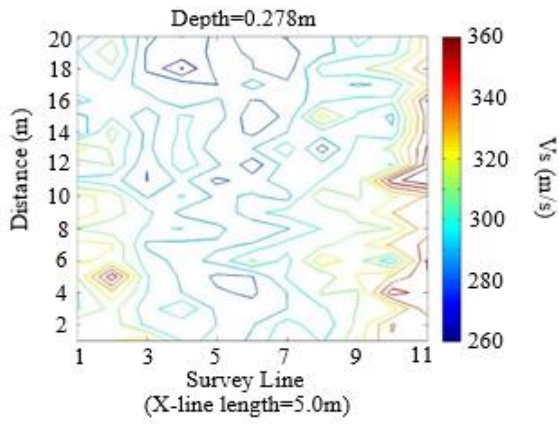


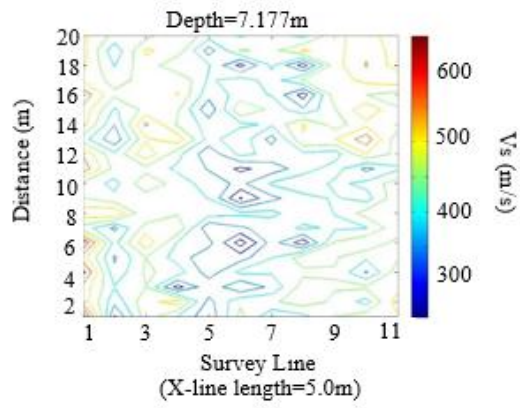
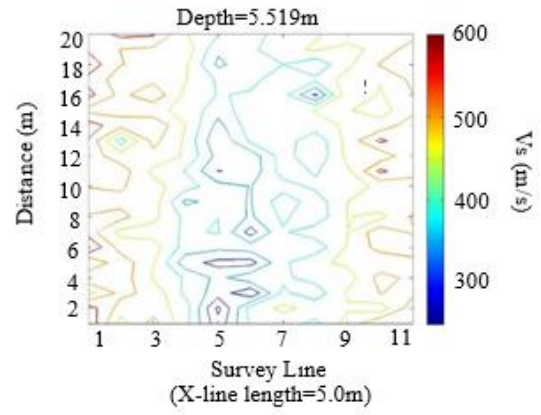
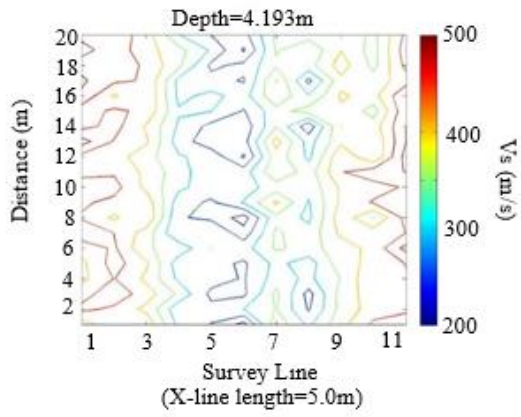
Depth (horizontal) Vs Profiles





Depth (horizontal) Contoured Vs Profiles

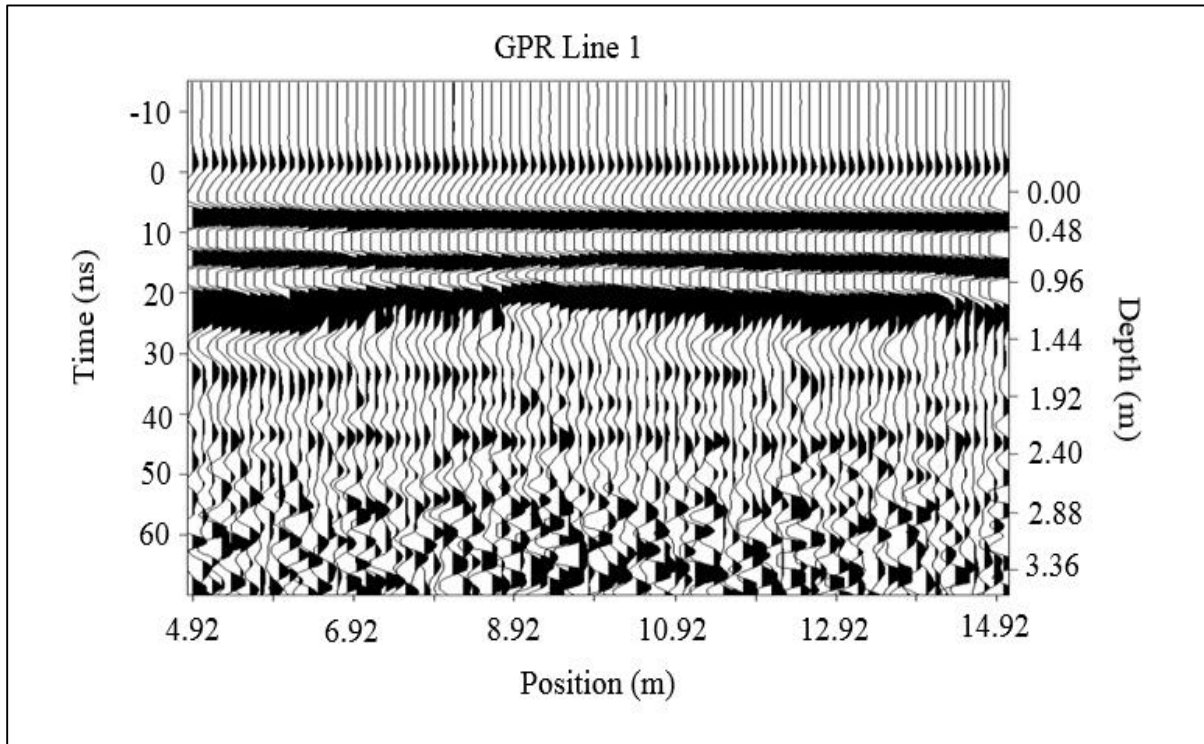




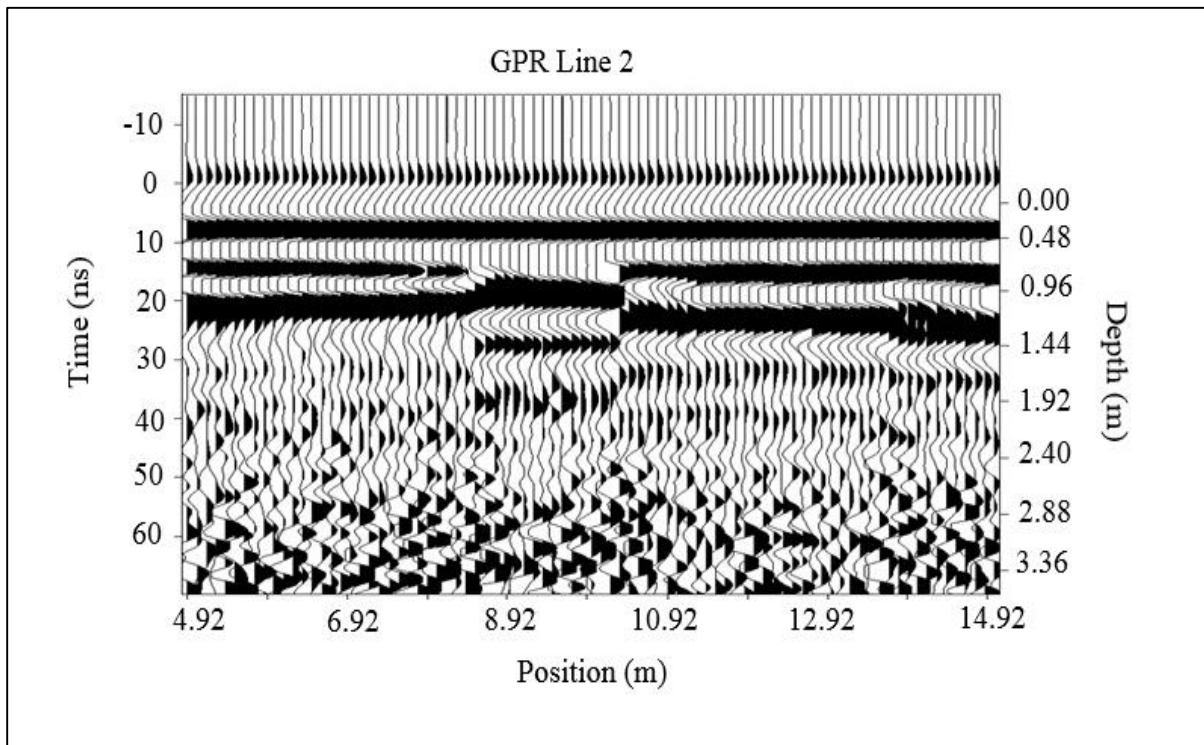
Appendix D

GPR and GPR/Surface Wave Combined Profiles

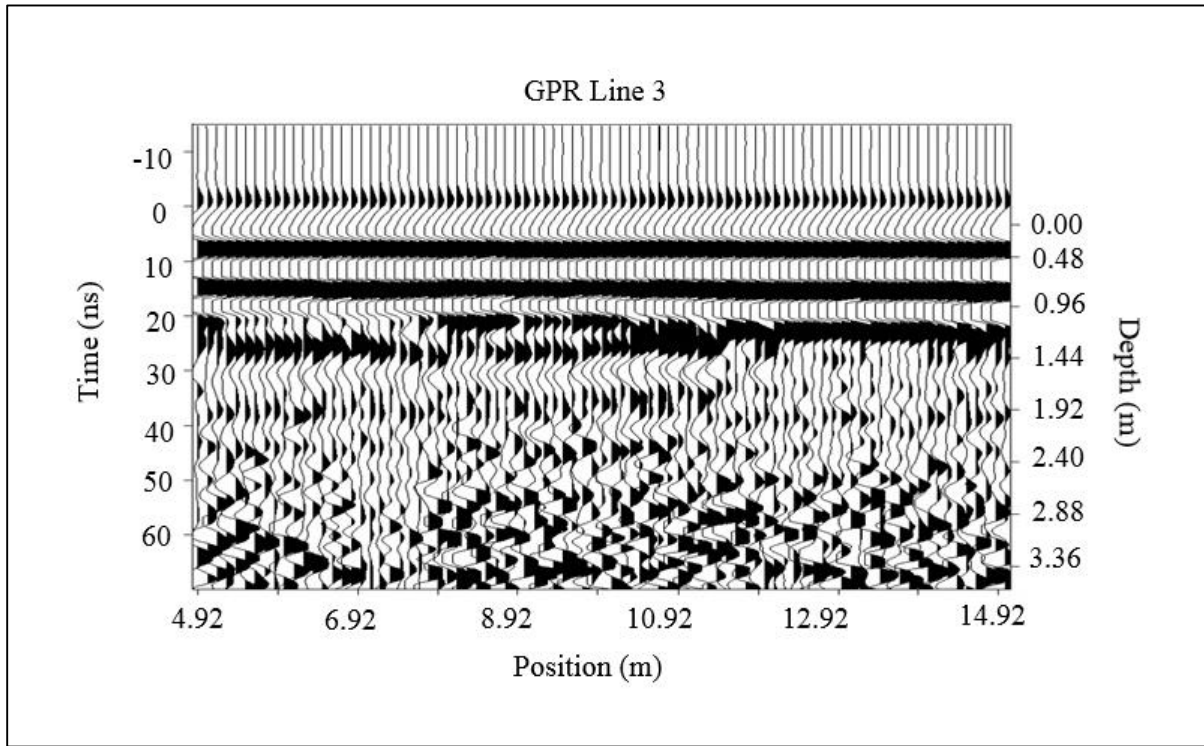
GPR Profile (Line 1)



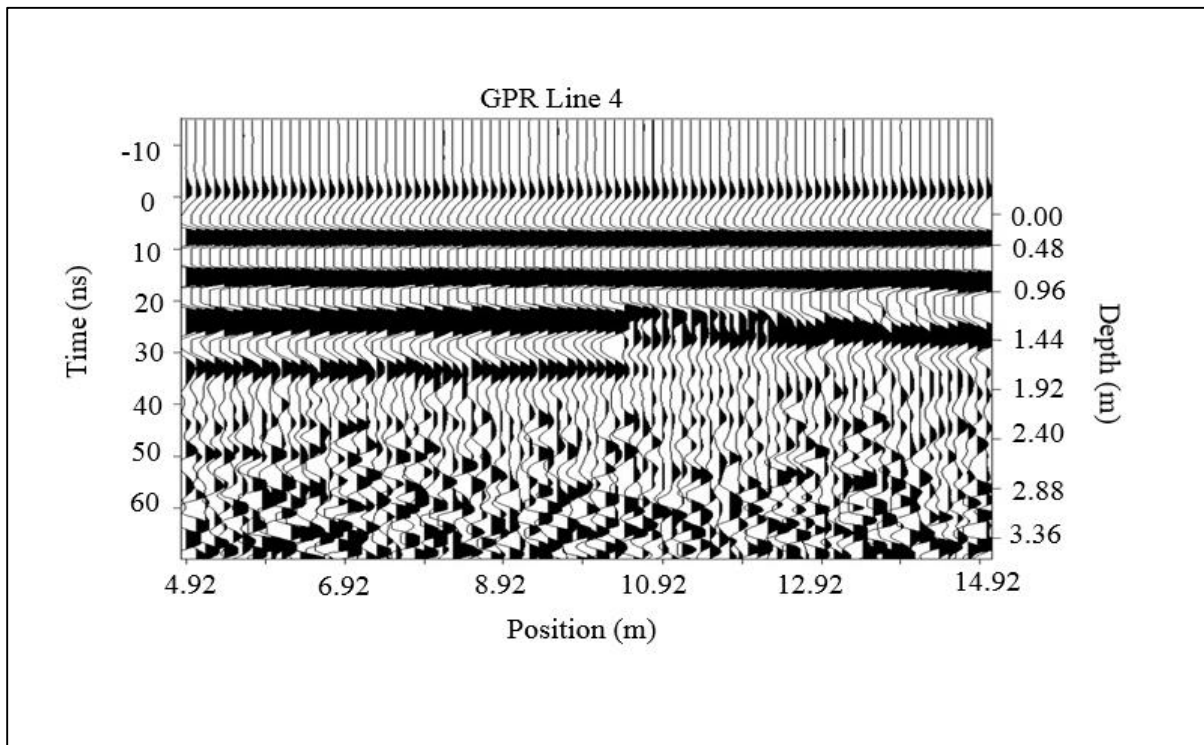
GPR Profile (Line 2)



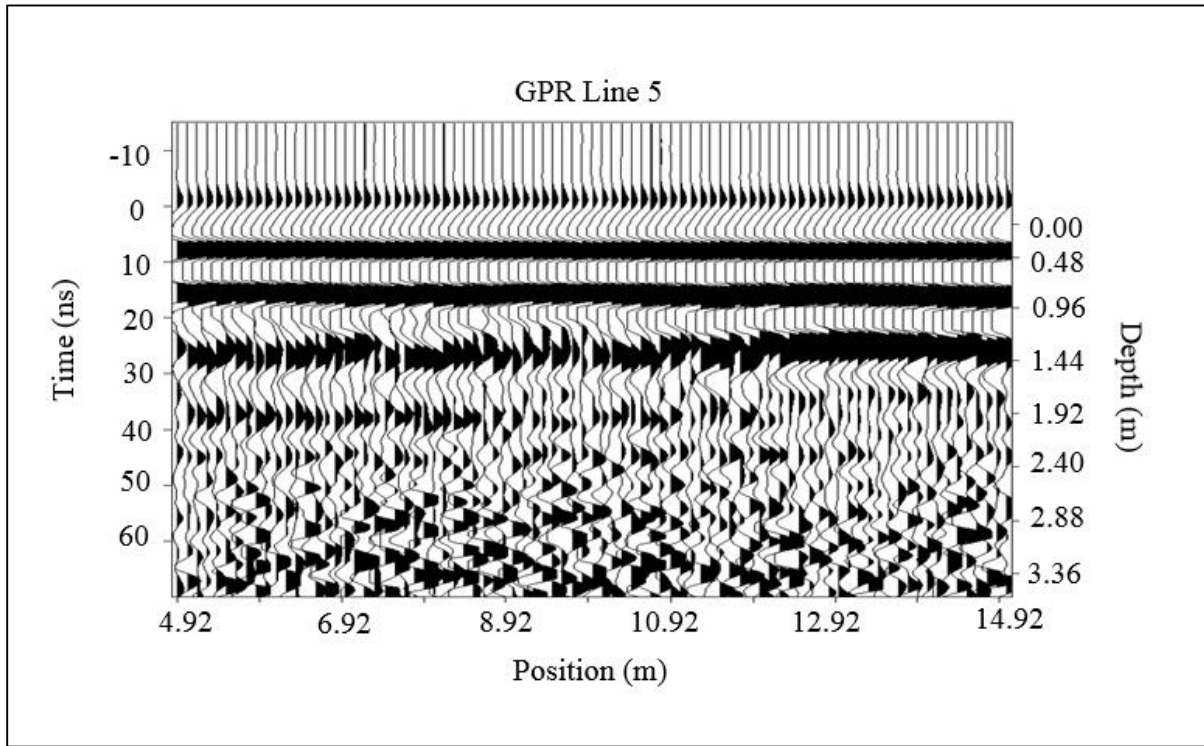
GPR Profile (Line 3)



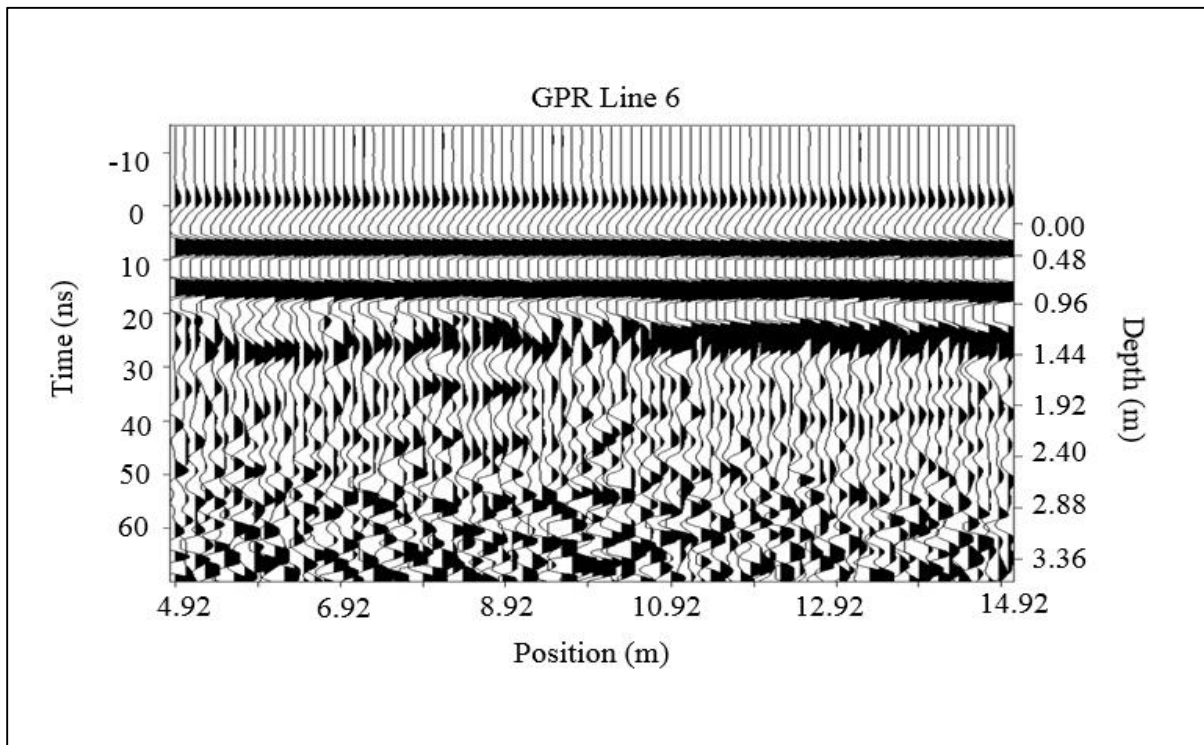
GPR Profile (Line 4)



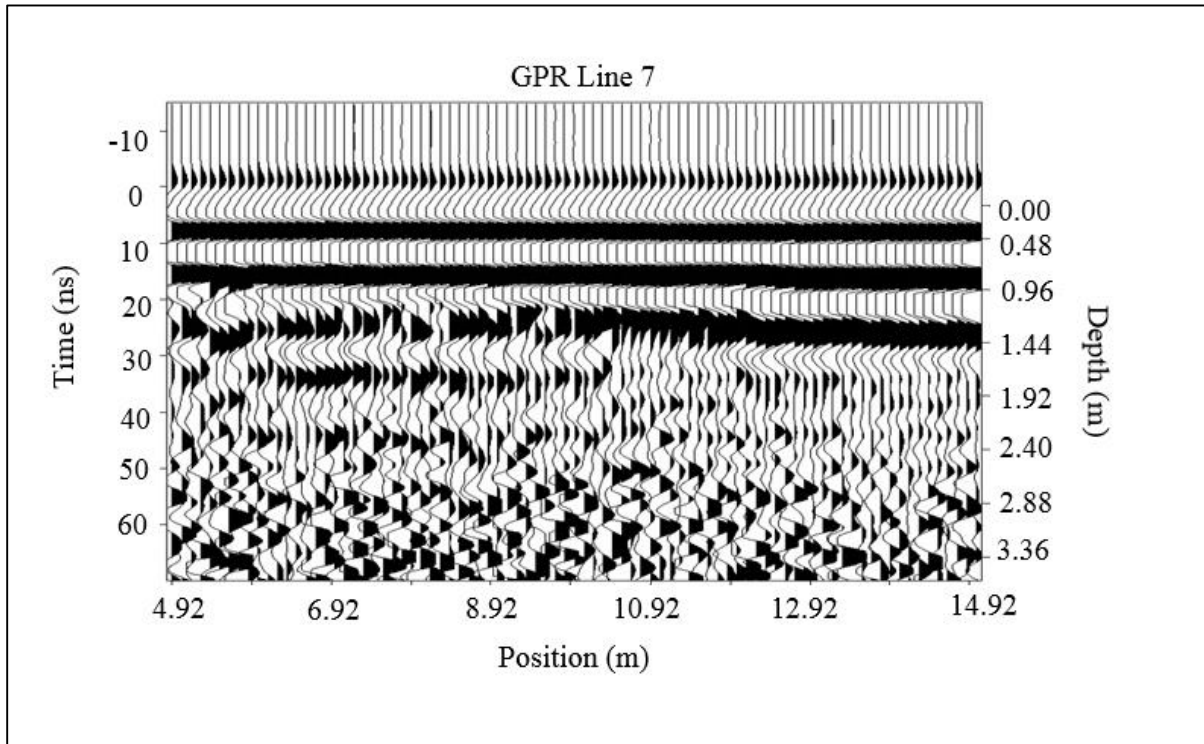
GPR Profile (Line 5)



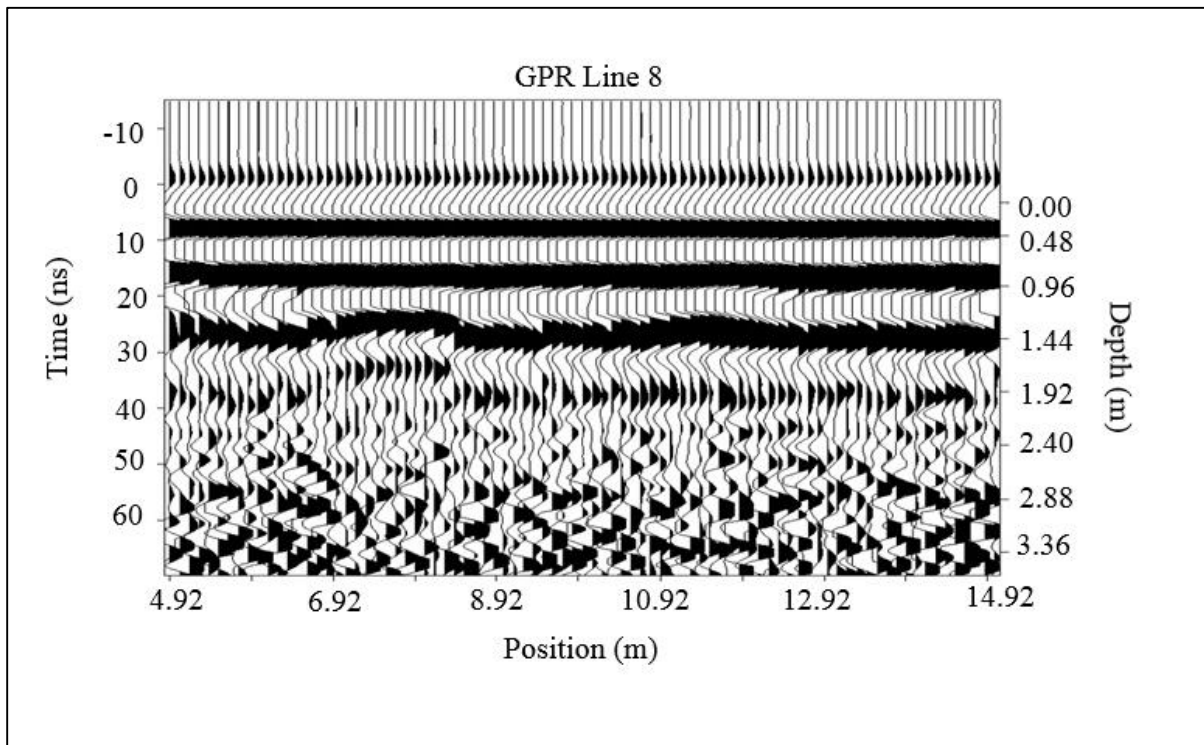
GPR Profile (Line 6)



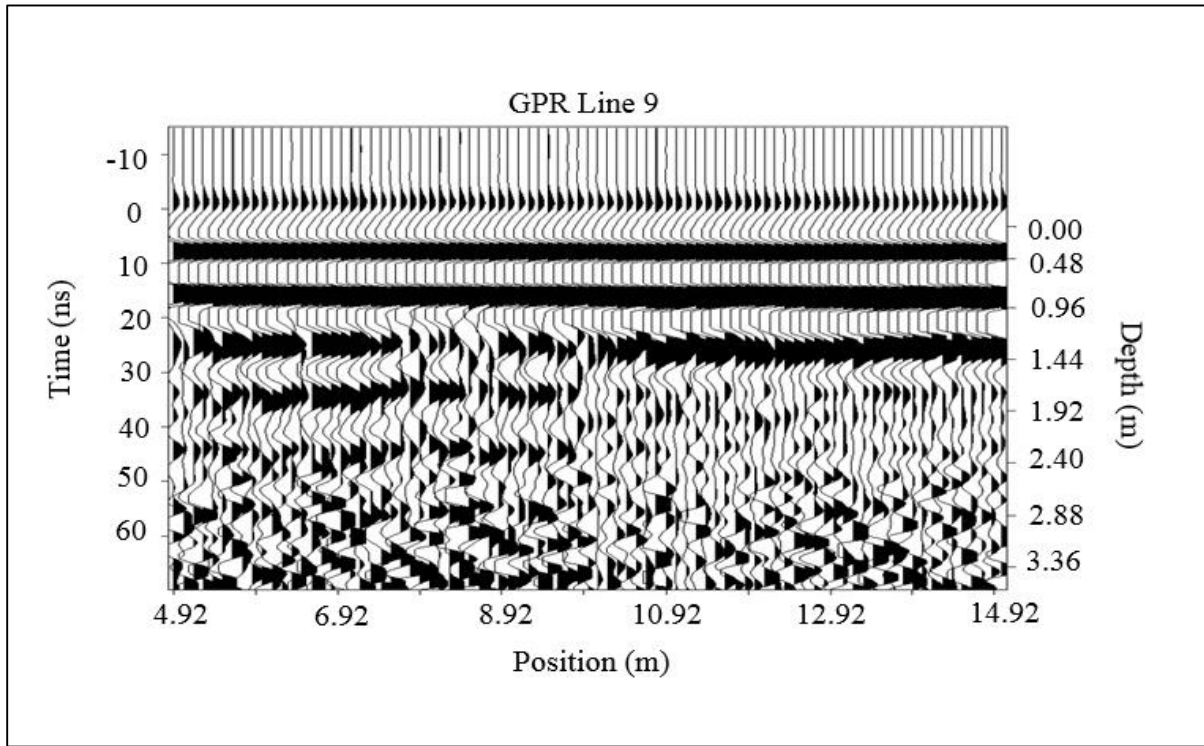
GPR Profile (Line 7)



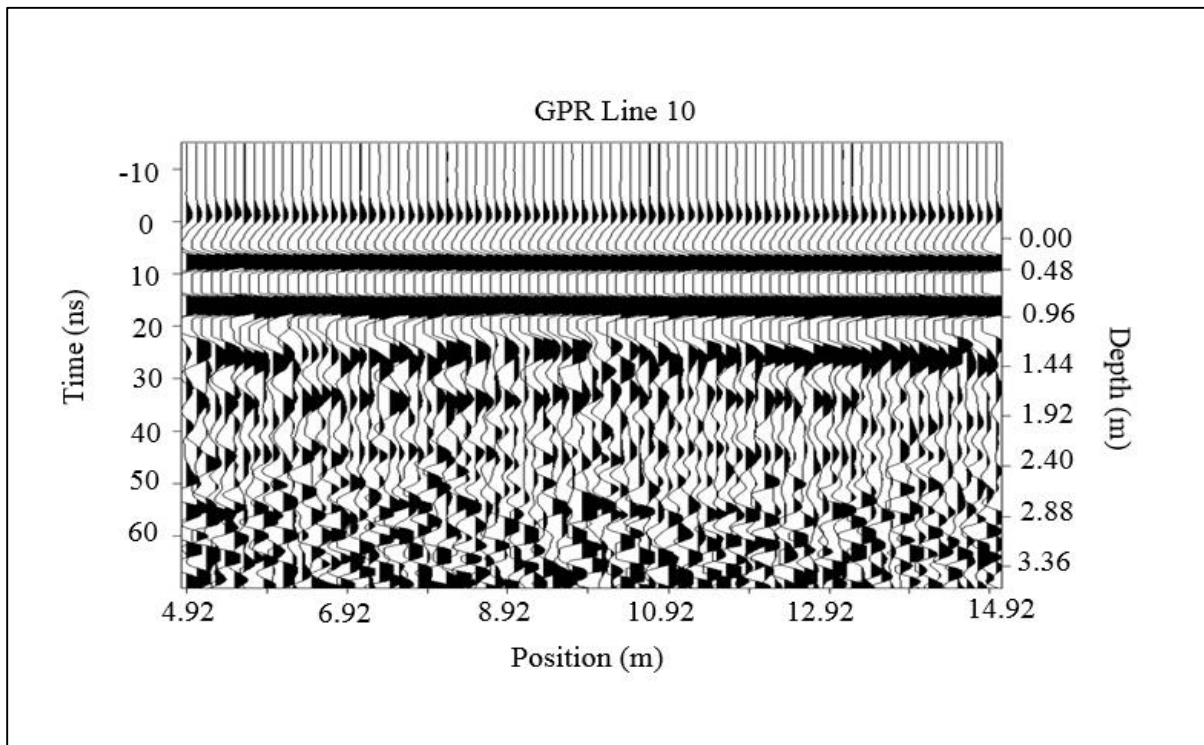
GPR Profile (Line 8)



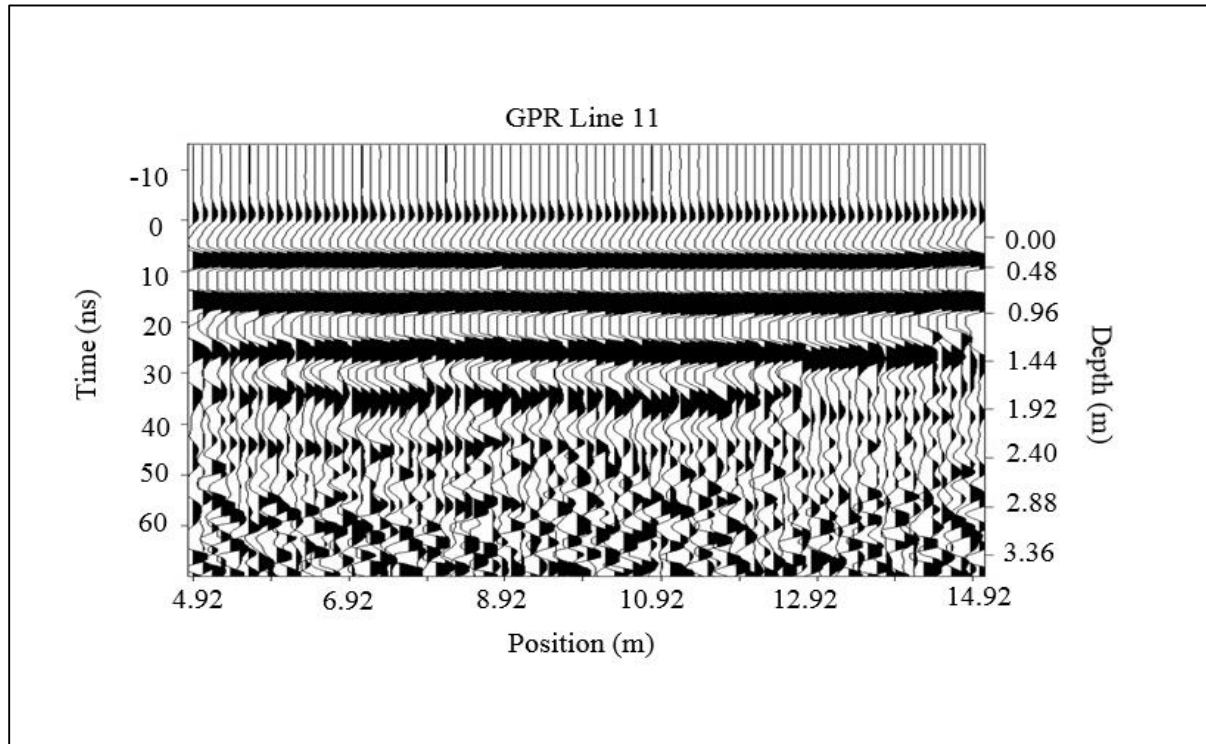
GPR Profile (Line 9)



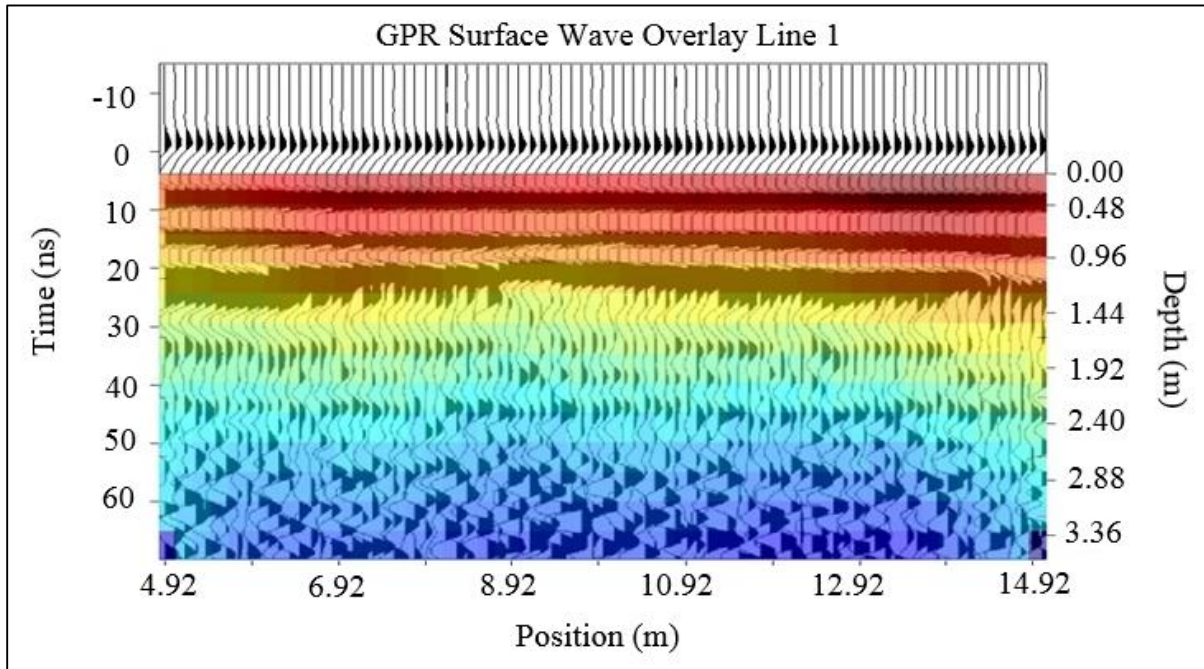
GPR Profile (Line 10)



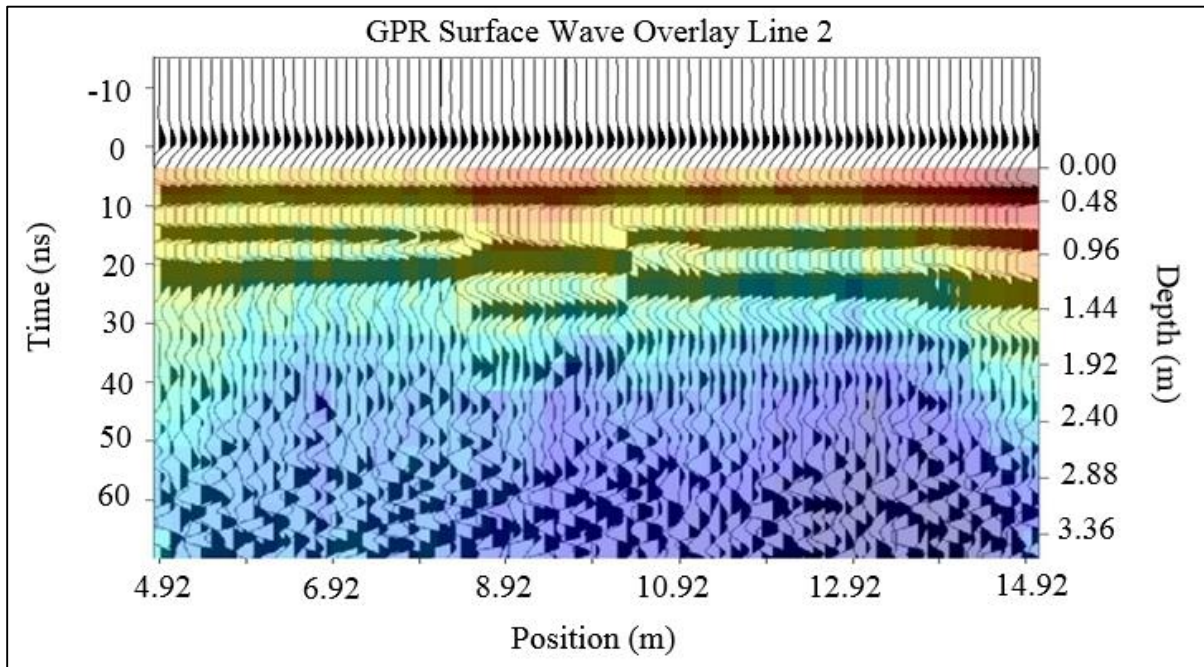
GPR Profile (Line 11)



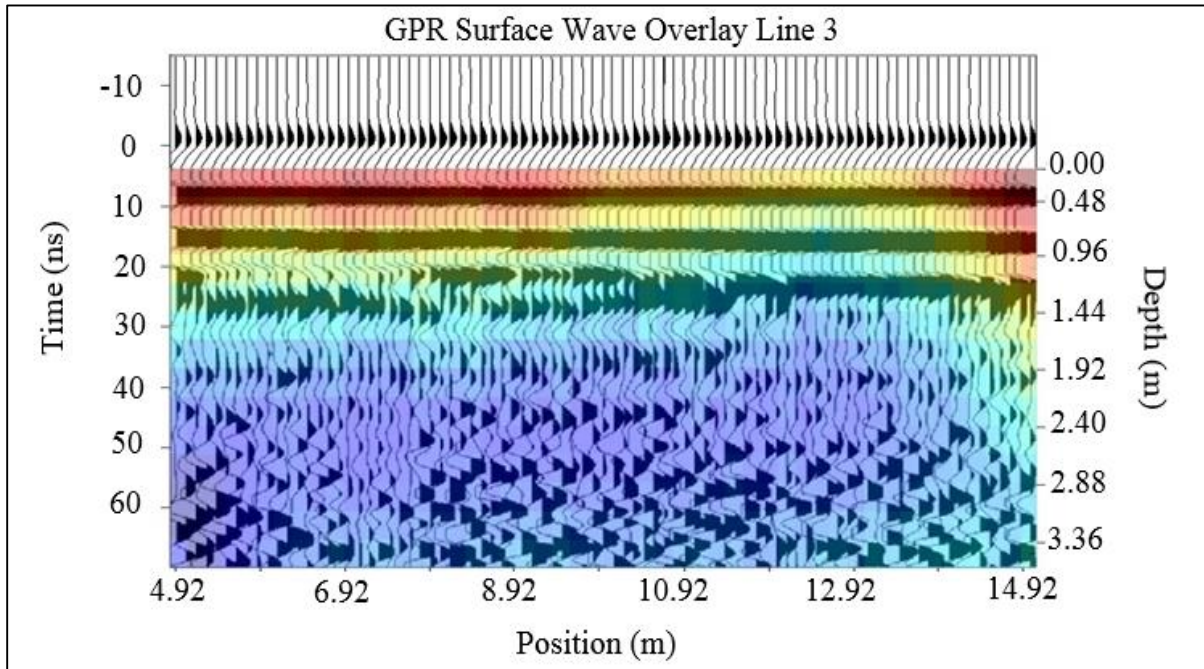
Overlaid Surface Wave and GPR Profile (Line 1)



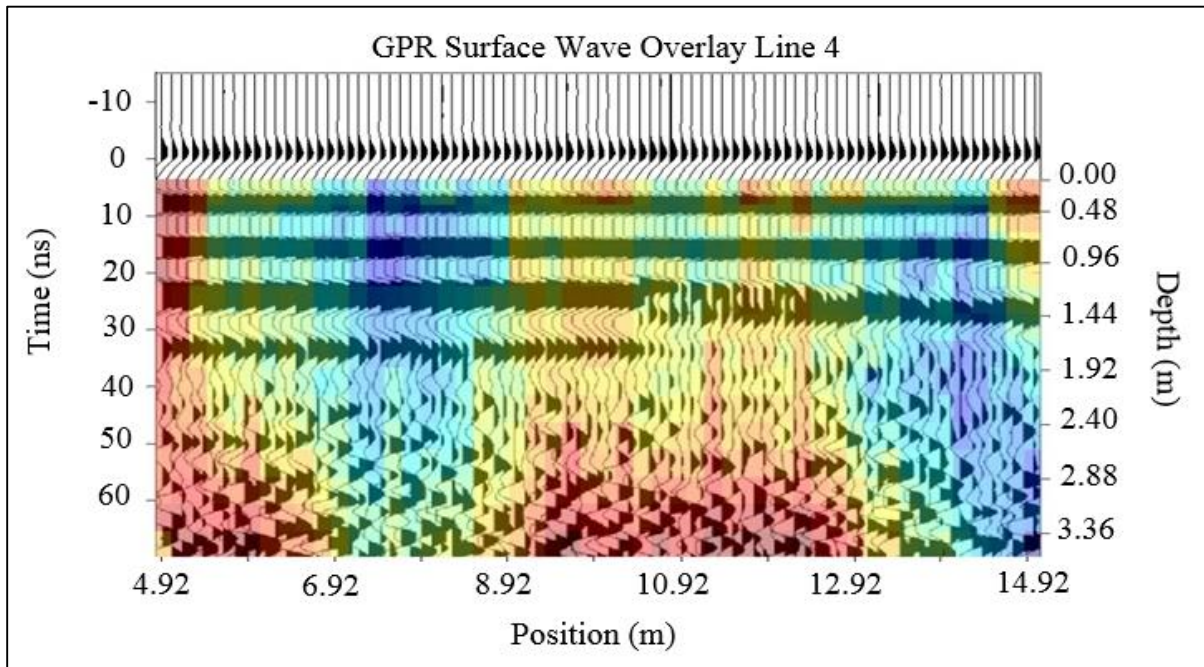
Overlaid Surface Wave and GPR Profile (Line 2)



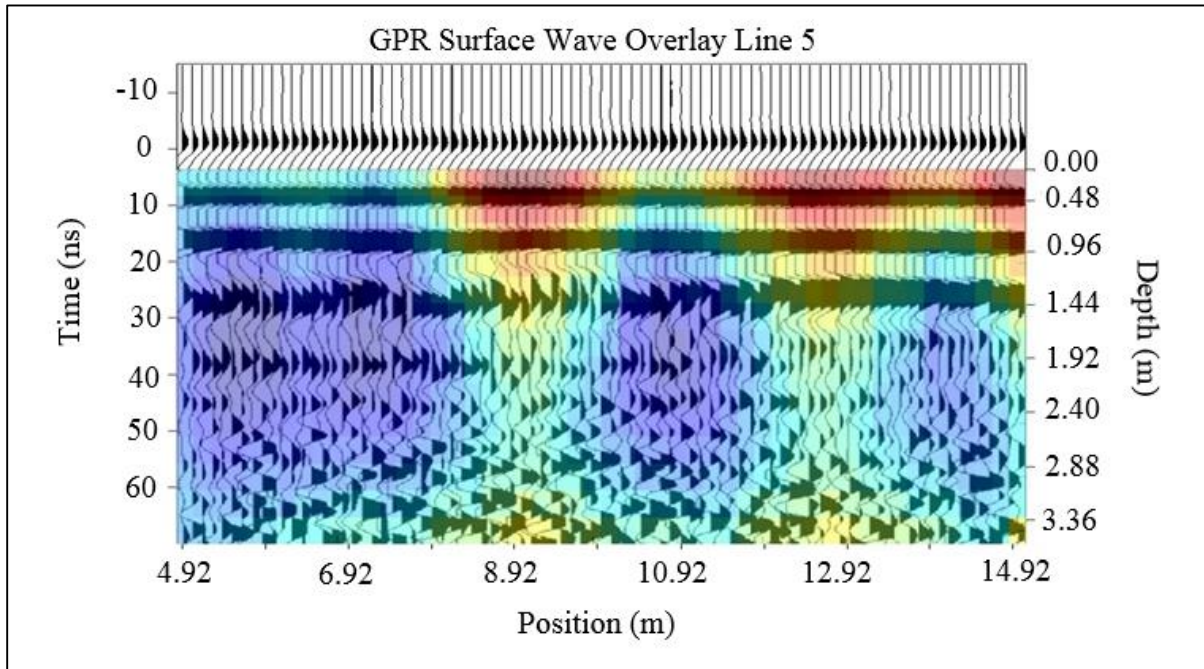
Overlaid Surface Wave and GPR Profile (Line 3)



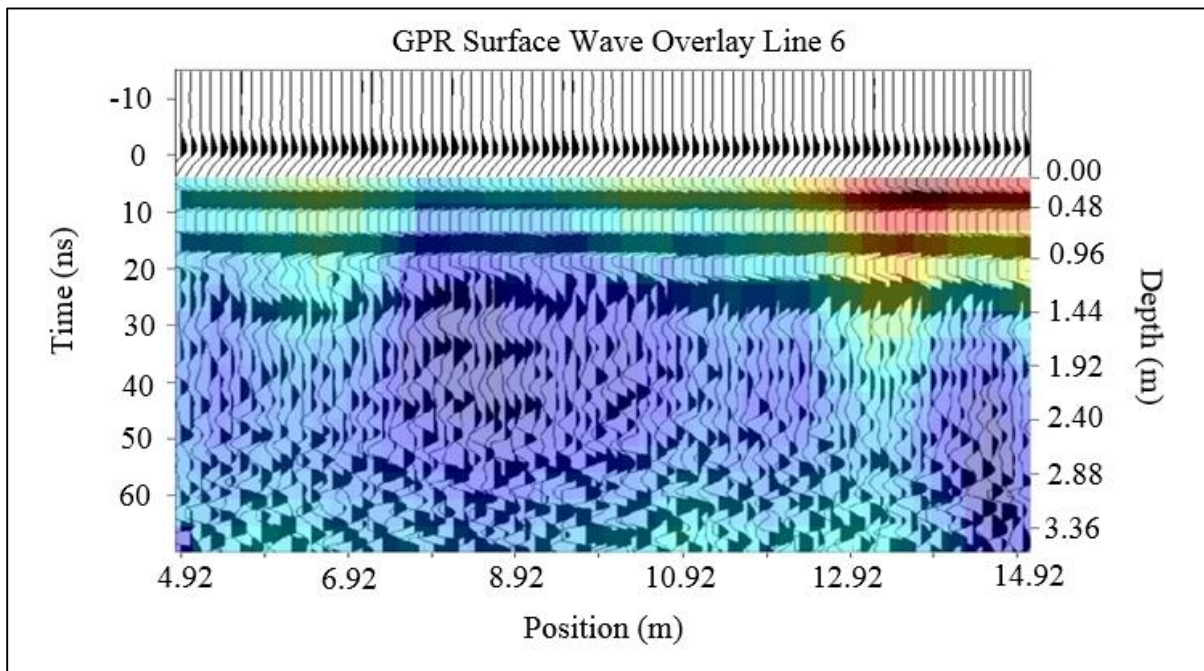
Overlaid Surface Wave and GPR Profile (Line 4)



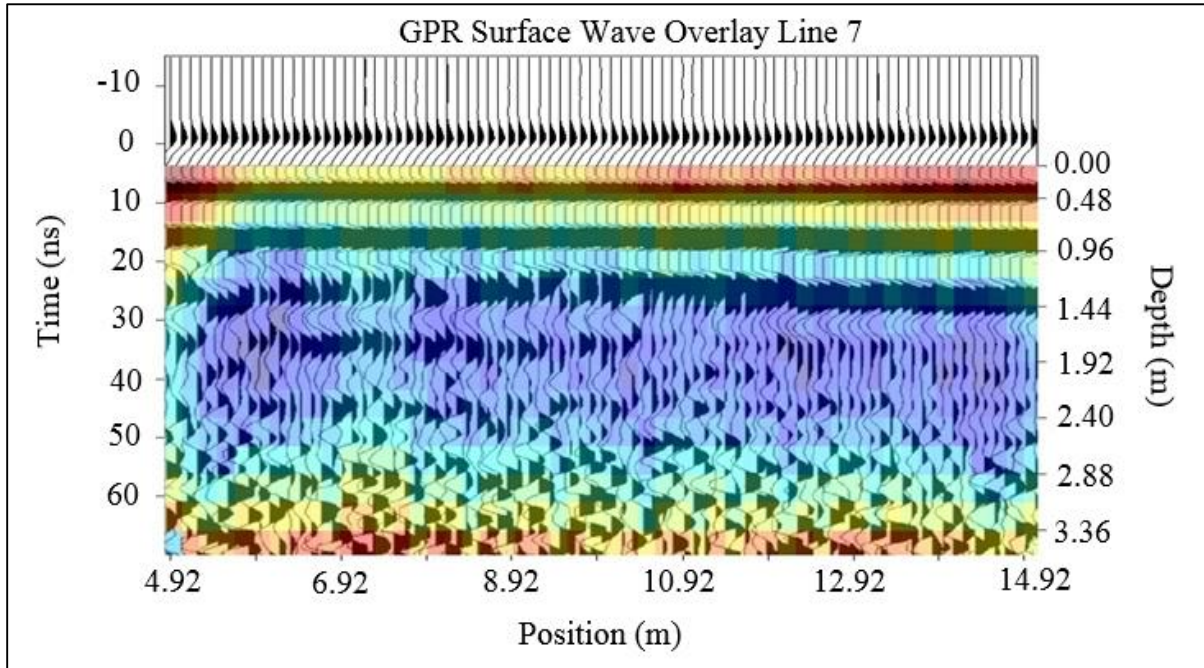
Overlaid Surface Wave and GPR Profile (Line 5)



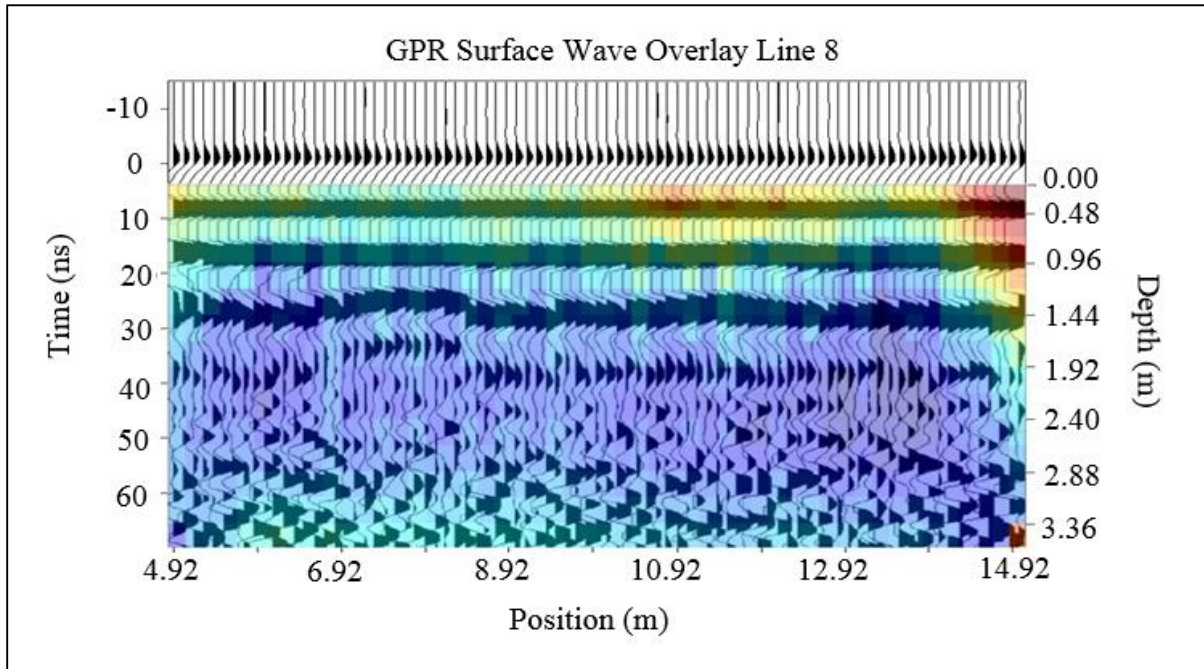
Overlaid Surface Wave and GPR Profile (Line 6)



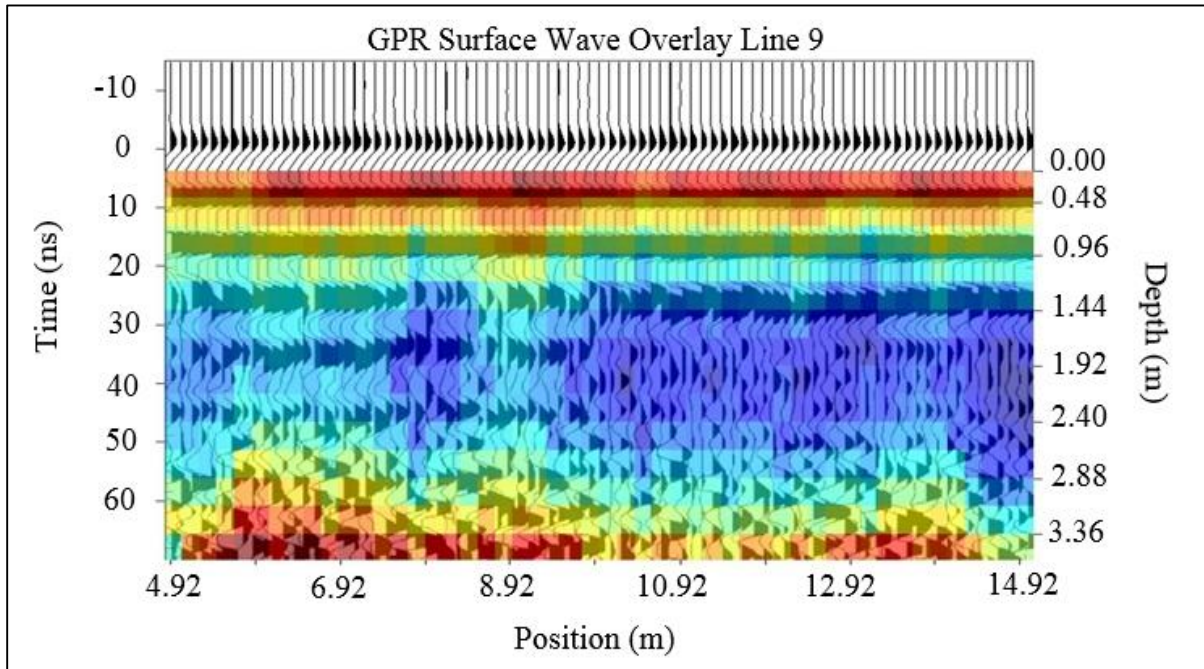
Overlaid Surface Wave and GPR Profile (Line 7)



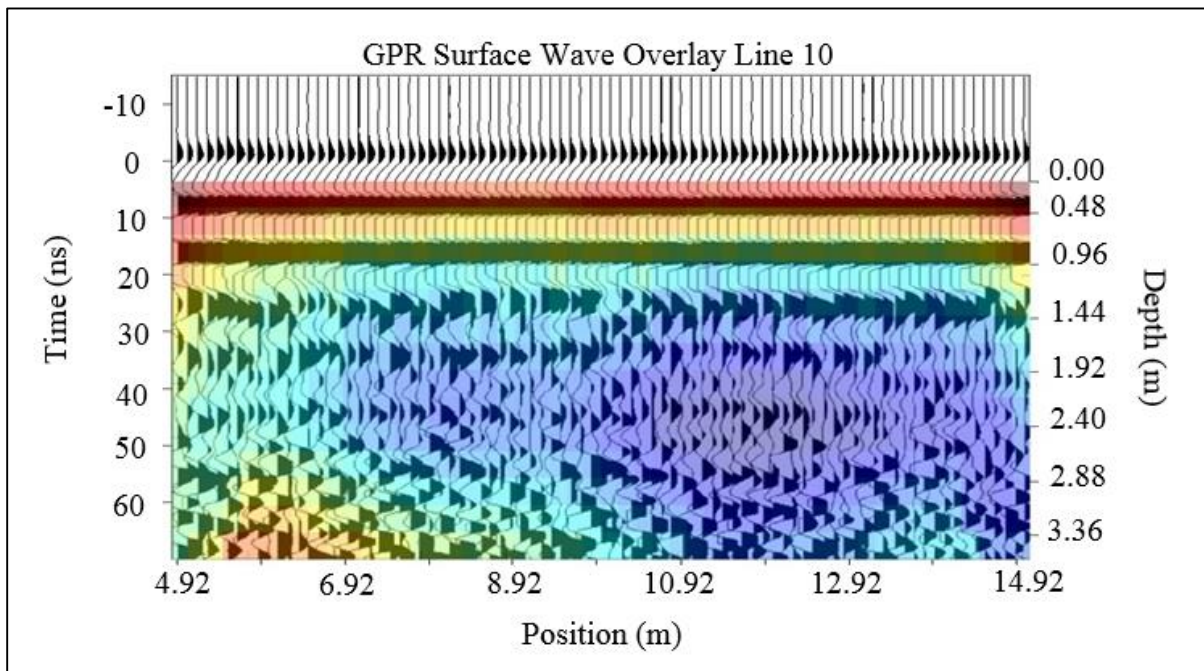
Overlaid Surface Wave and GPR Profile (Line 8)



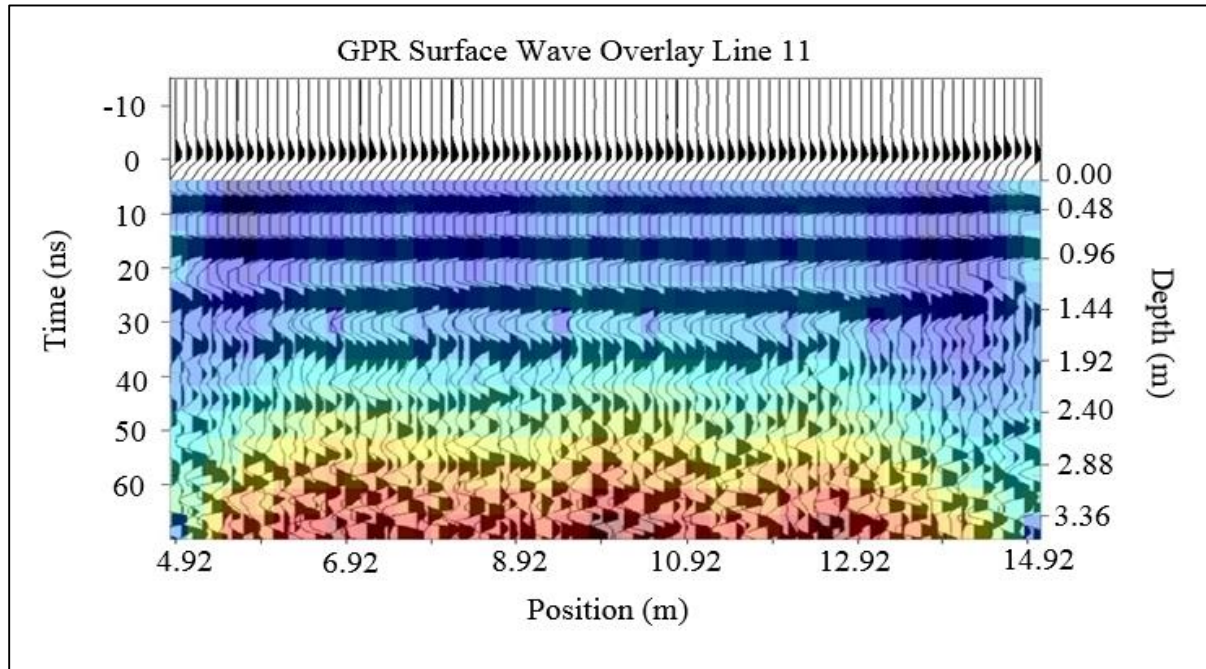
Overlaid Surface Wave and GPR Profile (Line 9)



Overlaid Surface Wave and GPR Profile (Line 10)



Overlaid Surface Wave and GPR Profile (Line 11)



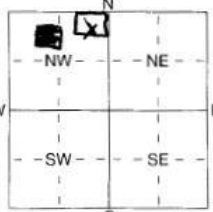
Appendix E

Driller Log

1 LOCATION OF WATER WELL: Fraction 1/4 NE 1/4 NW 1/4 Section Number 1 Township Number T 13 S Range Number R 17 EW
 County: Douglas

Distance and direction from nearest town or city street address of well if located within city?
1323 OHIO STREET LAWRENCE, KS.

2 WATER WELL OWNER: University of Kansas
 RR#, St. Address, Box # : 1323 OHIO ST. Board of Agriculture, Division of Water Resources
 City, State, ZIP Code : LAWRENCE, KS. Application Number:

3 LOCATE WELL'S LOCATION WITH AN "X" IN SECTION BOX:

 4 DEPTH OF COMPLETED WELL: 400 ft. ELEVATION:
 Depth(s) Groundwater Encountered 1 160-200 ft. 2 200-250 ft. 3 _____ ft.
 WELL'S STATIC WATER LEVEL _____ ft. below land surface measured on mo/day/yr
 Pump test data: Well water was _____ ft. after _____ hours pumping _____ gpm
 Est. Yield 20 gpm: Well water was _____ ft. after _____ hours pumping _____ gpm
 WELL WATER TO BE USED AS:
 1 Domestic 3 Feedlot 5 Public water supply 8 Air conditioning 11 Injection well
 2 Irrigation 4 Industrial 6 Oil field water supply 9 Dewatering 12 Other (Specify below)
 7 Domestic (lawn & garden) 10 Monitoring well _____
 Was a chemical/bacteriological sample submitted to Department? Yes _____ No X; If yes, mo/day/yr sample was submitted
 Water Well Disinfected? Yes _____ No X

5 TYPE OF BLANK CASING USED:
 1 Steel 3 RMP (SR) 5 Wrought iron 8 Concrete tile CASING JOINTS: Glued _____ Clamped _____
 2 PVC 4 ABS 6 Asbestos-Cement 9 Other (specify below) H.D. Polyethylene Welded Fusion
 7 Fiberglass Threaded _____
 Blank casing diameter 1 1/4 in. to _____ ft. Dia _____ in. to _____ ft. Dia _____ in. to _____ ft.
 Casing height above land surface 48 in. weight SPR 11 lbs./ft. Wall thickness or gauge No. _____
 TYPE OF SCREEN OR PERFORATION MATERIAL: None
 1 Steel 3 Stainless Steel 5 Fiberglass 7 PVC 10 Asbestos-Cement
 2 Brass 4 Galvanized Steel 6 Concrete tile 8 RMP (SR) 11 Other (Specify) _____
 9 ABS 12 None used (open hole)
 SCREEN OR PERFORATION OPENINGS ARE: None
 5 Gauzed wrapped 8 Saw cut 11 None (open hole)
 1 Continuous slot 3 Mill slot 6 Wire wrapped 9 Drilled holes
 2 Louvered shutter 4 Key punched 7 Torch cut 10 Other (specify) _____ ft.
 SCREEN-PERFORATED INTERVALS: From _____ ft. to _____ ft. From _____ ft. to _____ ft.
 GRAVEL PACK INTERVALS: From _____ ft. to _____ ft. From _____ ft. to _____ ft.

6 GROUT MATERIAL: Neat cement 2 Cement grout Bentonite 4 Other _____
 Grout Intervals: From 190 ft. to 200 ft., From 0 ft. to 190 ft., From 200 ft. to 400 ft.
 What is the nearest source of possible contamination: None
 1 Septic tank 4 Lateral lines 7 Pit privy 10 Livestock pens 14 Abandoned water well
 2 Sewer lines 5 Cess pool 8 Sewage lagoon 11 Fuel storage 15 Oil well/Gas well
 3 Watertight sewer lines 6 Seepage pit 9 Feedyard 12 Fertilizer storage 16 Other (specify below)
 13 Insecticide storage _____
 Direction from well? _____ How many feet? _____

FROM	TO	LITHOLOGIC LOG	FROM	TO	PLUGGING INTERVALS
0	28	Soil + Clay	0	190	High Solids Bentonite
28	96	Shale			
96	107	Limestone	190	200	Neat Cement
107	250	Sandstone			
250	270	Limestone	200	400	High Solids Bentonite
270	276	Shale			
276	280	Limestone			
280	289	Shale			
289	310	Limestone			
310	340	Shale			
340	391	Limestone			
391	400	Shale			

7 CONTRACTOR'S OR LANDOWNER'S CERTIFICATION: This water well was (1) constructed, (2) reconstructed, or (3) plugged under my jurisdiction and was completed on (mo/day/year) Aug. 30 2004 and this record is true to the best of my knowledge and belief. Kansas Water Well Contractor's Licence No 561 This Water Well Record was completed on (mo/day/yr) Sept 14 2004 under the business name of EVANS Energy Dev. Inc. by (signature) [Signature]

INSTRUCTIONS: Use typewriter or ball point pen. PLEASE PRESS FIRMLY and PRINT clearly. Please fill in blanks, underline or circle the correct answers. Send top three copies to Kansas Department of Health and Environment, Bureau of Water, Geology Section, 1000 SW Jackson St., Suite 420, Topeka, Kansas 66612-1367. Telephone 785-296-5522. Send one to WATER WELL OWNER and retain one for your records. Fee of \$5.00 for each constructed well.